Spring 2017

Deformation processes at the leading edge of the sevier fold and thrust belt, southwest Utah

William Joseph Michael Chandonia

Department:

DEFORMATION PROCESSES AT THE LEADING EDGE OF THE SEVIER FOLD AND THRUST BELT, SOUTHWEST UTAH

by

WILLIAM JOSEPH MICHAEL CHANDONIA

A THESIS

Presented to the Faculty of the Graduate School of the

MISSOURI UNIVERSITY OF SCIENCE AND TECHNOLOGY

In Partial Fulfillment of the Requirements for the Degree

MASTER OF SCIENCE IN GEOLOGY AND GEOPHYSICS

2017

Approved by

John P. Hogan, Advisor
Andreas Eckert
Wan Yang

ABSTRACT

Deformation processes leading to formation and abandonment of "triangle zones" along the leading edge of the Sevier fold and thrust belt are investigated near Kanarraville, Utah through construction of a detailed geologic map and cross-section along Spring Creek. Here the eastern limb of the Kanarra fold, a Sevier structure, is well exposed along the Hurricane Cliffs due to uplift and erosion of the footwall of the Hurricane Fault. The east-verging Kanarra fold changes from upright to overturned within Spring Creek. Within the fold limb, parasitic folds, minor thrust faults, and duplex structures result in local tectonic overthickening of units and demonstrate overall east-directed tectonic transport. Results from construction of the geologic cross-section indicate the Kanarra fold is a fault propagation fold forming above a blind thrust ramp – the "Kanarra thrust". In addition, the Taylor Creek thrust system, a system of west-directed thrust faults (backthrusts) as previously mapped along strike to the south, is inferred to be folded and overturned within the line of section. A combination of east-directed fault-related folding, the presence of a west-directed major backthrust, and the beginnings of tectonic overthickening, represent basic structural elements of a nascent "triangle zone". This triangle zone appears to have been abandoned prior to becoming fully developed. Merging of the Kanarra thrust and the folded Taylor Creek backthrust creates an effective west-dipping ramp that circumvented development of the triangle zone by enabling the Kanarra thrust to continue to cut up section through the Navajo Sandstone (Jn). These results suggest triangle zones may be less likely to fully develop in association with fault-propagation folds in comparison to fault bend folds.

ACKNOWLEDGMENTS

I would like to thank my advisor and mentor Dr. John P. Hogan for all his expertise and guidance. He has always pushed and believed in me from the beginning of my graduate school career. I cannot express enough thanks to him for his motivation and support. I offer my sincere appreciation to my research committee members - Dr. Andreas Eckert for his insight, continuous encouragement, and for creating a friendly, collaborative work environment, and to Dr. Wan Yang for his inspiration and extensive knowledge as a petroleum geologist whose advice and expertise I could not have done without.

I would also like to thank Dr. Jason Kaiser and Dr. Johnny MacLean of Southern Utah University for their hospitality and assistance, which helped make this project possible.

My completion of this degree could not have been accomplished without the unwavering love, support and patience from my family and loved ones, thank you. I would also like to acknowledge all my colleagues for their recommendations and support.

I am deeply grateful to Missouri University of Science and Technology for their financial support from the Chancellor's Fellowship which allowed me to move here and funded my education.

Last, but not least, I recognize the use of the Move Software Suite granted by Midland Valley's Academic Software Initiative, and I especially thank the Missouri S&T IT Help Desk, who worked with me to acquire Midland Valley's Move™ software.

TABLE OF CONTENTS

Page

LIST OF ILLUSTRATIONS

Page

LIST OF TABLES

Page

1. INTRODUCTION

Triangle zones are a common structure at the leading edge of fold and thrust belts worldwide, including the Canadian Cordillera, the Andes, and the Sulaiman Range (Baby et al., 1992; Banks and Warburton, 1986; Dahlstrom, 1970; Jones, 1982; Ramos, 1989; Vann et al., 1986). They are a type of duplex structure where an upper detachment (i.e., roof thrust) is passively uplifted and separated from the lower detachment (i.e., floor thrust) by thickening of the duplex stack – a process referred to as "tectonic wedging" (Banks and Warburton, 1986; Boyer and Elliott, 1982; Charlesworth and Gagnon, 1985; Jones, 1982; Jones, 1996; Price, 1986; Tanner et al., 2010). Triangle zones and other thrust systems form structural traps due to folding during the growth of thrust faults (Suppe, 1983; Suppe and Medwedeff, 1990). As regions of prolific hydrocarbon traps, frontal margin thrust system processes, including triangle zone initiation and growth, remain the focus of exploration geology research.

In southwest Utah, the leading edge of the Sevier fold and thrust belt is well exposed along the Hurricane Cliffs - the footwall of the Basin and Range Hurricane Fault. East-west drainages across the Hurricane Cliffs, such as Spring Creek, afford an excellent opportunity to investigate deformation processes at the leading edge of the fold and thrust belt (Averitt, 1962; Threet, 1963; Kurie, 1966; Biek and Hayden, 2013). Preliminary mapping between June 16 and July 7, 2016 near Kanarraville along the Spring Creek drainage and environs, documents the presence of a fault propagation fold (the Kanarra fold), and a major folded backthrust, the Taylor Creek fault zone. Within the fold limb, parasitic folds, minor thrust faults, and duplex structures result in local tectonic overthickening of units and demonstrate overall east-directed tectonic transport. A

combination of east-directed fault-related folding, the presence of a west-directed major backthrust, and the beginnings of tectonic overthickening, represent basic structural elements of a nascent “triangle zone”. However, this triangle zone appears to have been abandoned prior to full development. Previous workers in the Canadian Cordillera have suggested the presence of abandoned triangle zones without elaborating on the process leading to abandonment (Jones 1996; Jamison 1996; Soule and Spratt 1996; Charlesworth and Gagnon 1985). Triangle zones are areas of high hydrocarbon potential, but due to their complexity, the initiation and abandonment of these structural traps remains poorly understood.

The question of 1) how “nascent” triangle zones are initiated and 2) the processes that lead to triangle zone abandonment before fully developing is the subject of this study. To investigate these processes, the area in and around Spring Creek near Kanarraville UT was mapped at 1:10000 scale and the map was digitized. A geologic cross-section, constructed following standard guidelines (Dahlstrom, 1969; Jamison, 1987; Suppe and Medwedeff, 1990; Woodward et al. 1989), along Spring Creek is presented. The results of this structural investigation suggest that merging of a newly named thrust, the Kanarra thrust, and folding of the previously recognized Taylor Creek backthrust (Kurie, 1966; Biek, 2007) created an effective west-dipping ramp which circumvented development of the triangle zone by enabling the Kanarra thrust to continue to cut up section through the Navajo Formation. These results suggest that triangle zones maybe less likely to fully develop in association with fault-propagation folds in comparison to fault bend folds.

1.1. REGIONAL GEOLOGIC SETTING

The Sevier Orogeny was a compressional event driven by subduction of the Farallon plate along the length of western North America (DeCelles and Coogan, 2006). Subduction of this plate and consequent collision with offshore island chains (suspect terranes) produced west-to-east deformation over a thousand km inland from eastward-directed compressive forces (Price, 1986). This compressive plate interaction caused thin-skinned deformation of the sedimentary cover and is characterized by the development of the Sevier fold and thrust belt (Figure 1.1), which spans much of the North American West. The fold and thrust belt includes the triangle zone type area of the southern Alberta Rockies, and is well-studied in central Utah (Chester, 1996; DeCelles and Mitra, 1995; DeCelles and Coogan, 2006; Royse, 1993). The youngest evidence of thrust faulting is 40 Ma, but one of the oldest thrusts, the Canyon Range thrust, initiated in the Late Jurassic around 145 Ma. Thrusting lasted between the Late Jurassic to the Eocene (Biek, 2007; DeCelles and Coogan, 2006; Lawton et al., 1997; Willis, 1999). Flexure of the crust due to loading from stacks of thrusted rock in the hinterland formed a back-bulge basin throughout much of Utah in the Middle to Late Jurassic. This may be the earliest known influence of Farallon subduction in the area. (Willis, 1999). Major thrusts have been traced into southwest Utah from the central Utah ranges, including the Wah Wah, Blue Mountain, and Iron Springs thrusts (Goldstrand, 1994, Willis 1999).

1.2. LOCAL GEOLOGY

In southwestern Utah, the Sevier Orogeny is characterized by the presence of several folds and thrusts (Figure 1.2). The thrusts include the Wah Wah, Blue Mountain, and Iron Springs thrusts. These thrusts are in-sequence, with the Wah Wah being the

oldest and at the highest structural level (Goldstrand, 1994). Older Sevier structures are locally overprinted by Basin and Range extension. For example, the Kanarra fold appears to curve and die out past Cedar City, but folded strata near Parowan are likely a dismembered portion of the Kanarra fold from displacement along the Hurricane Fault (Threet, 1963).

Uplift and erosion associated with the Basin and Range Hurricane Fault has exposed the transition zone between Sevier deformation and the Colorado Plateau near the leading edge of the Sevier fold and thrust belt within the Hurricane Cliffs (Biek, 2007). Compressional features associated with Sevier deformation include the Taylor Creek thrust fault system and the Pintura, Virgin, and Kanarra anticlines (Kanarra fold here). The Virgin anticline and Kanarra fold are collinear and may be closely related (Biek, 2007). The folds are interpreted to be frontal structures which absorbed the last stages of deformation along the eastern-most faults (Willis, 1999).

The Kanarra fold crops out between Cedar City and Zion National Park, near the leading edge of the thrust belt (DeCelles and Coogan 2006; Threet 1963; Willis 1999). The fold predates the Hurricane Fault and is a result of west to east compression (Averitt, 1962; Biek, 2007). At Zion, the fold is broad and upright, but overturns along strike north towards Cedar City (Biek, 2007; Biek and Hayden, 2013) this transition occurs within Spring Creek (this study). First mapped by Kurie (1966), and later by Biek (2007), the Taylor Creek thrust fault system may be the last major Sevier-related structure before the transition to the Colorado Plateau.

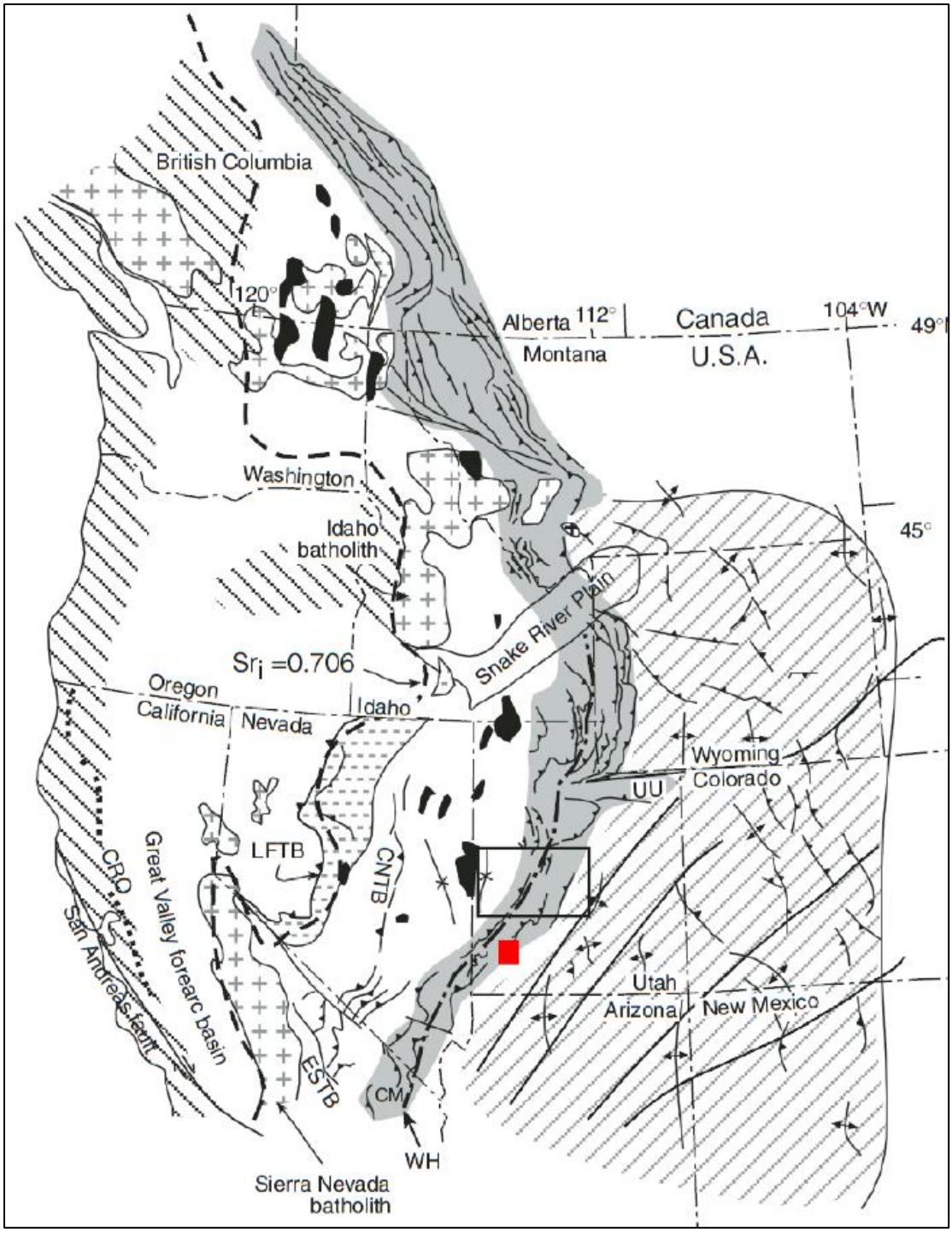

Figure 1.1. Regional map showing extent of Sevier fold and thrust belt. Field area is in the red square. From DeCelles and Coogan (2006).

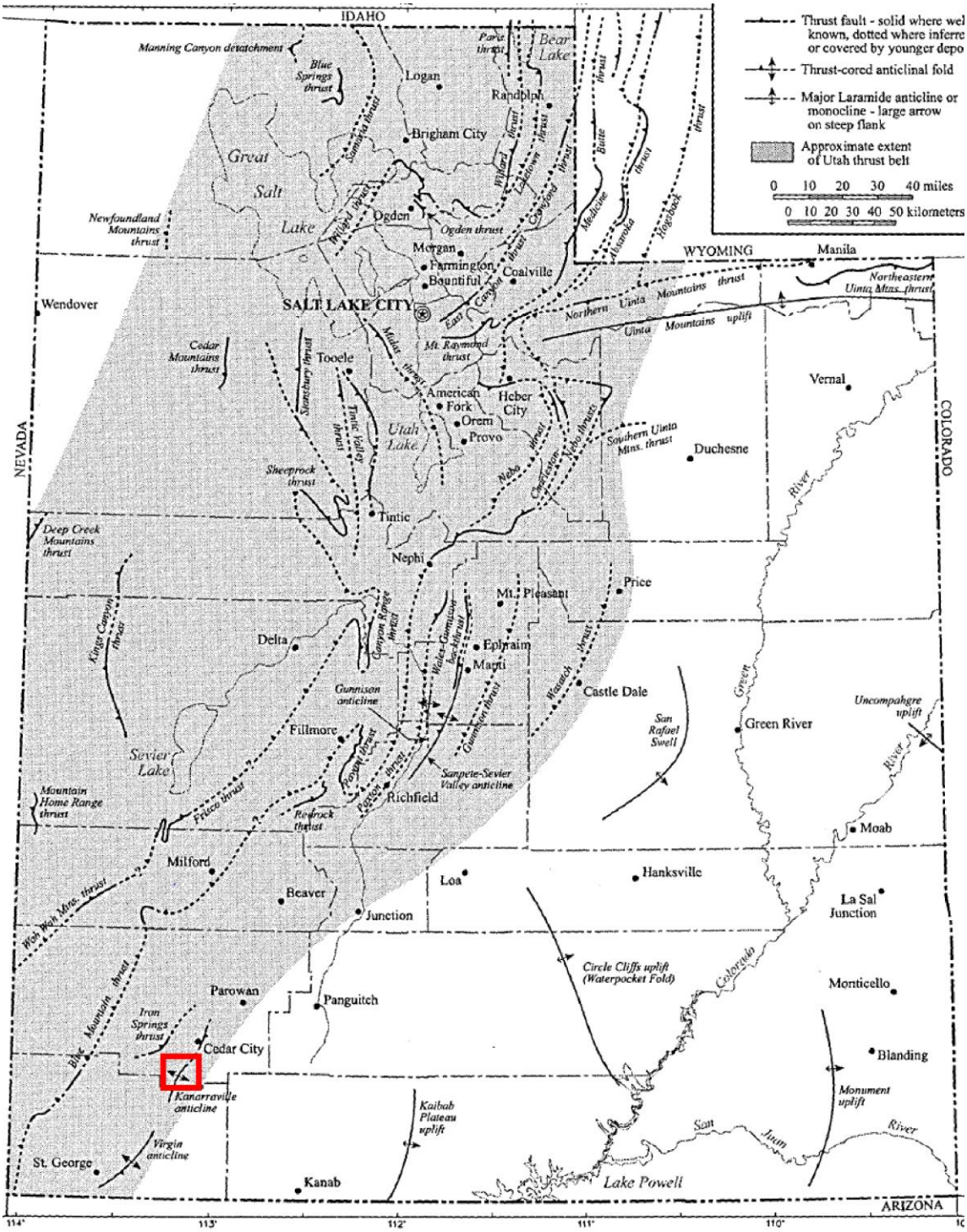

Figure 1.2. Regional map showing extent of Sevier fold and thrust belt in gray. Note the major southwestern faults. Field area is in the red square. From Willis (1999).

2. METHODOLODY

Mapping was conducted during the summer of 2016 from June 16 to July 7 following standard mapping procedures. The map was constructed from topographic base maps cropped along three traverses (see Appendix D, Figure D.1) at 1:10000 scale. These were later compiled and digitized at the same scale with the Move™ software suite. Field work focused on defining the location of stratigraphic and structural contacts based on the lithology and attitudes of stratigraphic units. Traverses were followed across strike up canyons that provide topographic relief and resistant units were followed on along strike traverses. The map is produced partly from modifications of unpublished mapping of Hogan (pers. comm.) and from consultation of a previously published 1:24000 scale map (Biek and Hayden, 2013). In addition to stratigraphic control, mapping was constrained by topping indicators including cross bedding and ripple marks. Locations were determined using a combination of GPS, field checking based on topography, and contacts were visually checked using Google Earth™.

3. MAP AND CROSS-SECTION

3.1. OVERVIEW

The geologic map of the Spring Creek area shows uplifted Paleozoic to Mesozoic strata (Figure 3.1) exposed in the footwall of the Hurricane Fault (Figure 3.2). The Hurricane Fault is a steep, west-dipping normal fault associated with Basin and Range extension. It is approximately Quaternary-age (approximately 1 Ma to 850 ka) with 1100-1500 m of total throw (Biek, 2007; Lund et al., 2007). Its location is inferred by a prominent topographic scarp about 566 m high that trends about 035 across the western edge of the map area and is readily visible in a Digital Elevation Model with the mapped geology projected onto the erosional surface (Figure 3.3). The trace of the fault is concealed by recent alluvium and colluvium from dissection and erosion of the footwall block, which rises from the valley floor at 1812 m to high peaks such as “the Saucer” at 2378 m elevation in the map area.

Within the footwall block, Upper Permian to Lower Jurassic strata crop out in narrow, approximately linear belts with an overall strike of 190 (010 where upright, Figure 3.2). A geologic cross-section along the southern edge of the Spring Creek drainage has a trend of 109 and is nearly perpendicular to the strike of the major units (Figure 3.4). Here, dips are approximately 34° E, and moving from west to east across the map (Figure 3.2) and in the cross-section (Figure 3.4) become steep (63° E) to overturned (81° W). Further east, strata become upright again, then abruptly approach horizontal where the Jurassic Navajo Sandstone (Jn) and Jurassic Carmel Formation (Jcu) cap the high peaks. The changing dips of these strata are attributed to the Kanarra fold - an

upright to overturned fold that developed between 83 to 71 Ma during the Sevier Orogeny (Biek 2007).

Upper Permian to Lower Jurassic strata exposed in the footwall block represent a gradual transition from shallow marine to continental eolian deposition. The Kanarra fold is cored by the Permian Kaibab Formation (Harrisburg (Pkh) and Fossil Mountain (Pkf) Members) and Triassic Timpoweap Member (TRmt) of the Moenkopi Formation. The Upper Permian Kaibab and Lower Triassic Timpoweap Member (TRmt) limestones were deposited in a shallow epicontinental sea during a major global transgression (Biek and Hayden, 2013; Hintze, 1988). An unconformity separates the Permian and Triassic intervals (Figure 3.1). The Lower Triassic interval is distinguished by a pattern of cyclic sedimentation (transgression and regression) between marginal marine to continental clastics and shallow marine carbonates that comprise the Moenkopi Formation (Dubiel, 1994). The Upper Triassic Chinle Formations rests unconformably on the Lower Triassic Moenkopi Formation (Figure 3.1) The entire Middle Triassic is absent. Continental clastics, both fluvial and lacustrine, dominate sedimentation in the Upper Triassic. The Chinle Formation is represented by the Shinarump Conglomerate Member (TRcs) and the Petrified Forest Member (TRcu) (see Appendix A). The transition from Upper Triassic to Lower Jurassic is represented by the Moenave Formation (JTRm) which spans this boundary (Figure 3.1). The Moenave Formation (JTRm) consists of fluvial clastics of the Dinosaur Canyon Member (JTRm) (see Appendix A) which rest unconformably on the Chinle Formation (Dubiel, 1989). A transition from fluvial to eolian deposition is observed in the fluvial and eolian Jurassic Kayenta Formation (Jku) to the chiefly eolian Jurassic Navajo Sandstone (Jn) (Blakey 1994; Biek and Hayden, 2013).

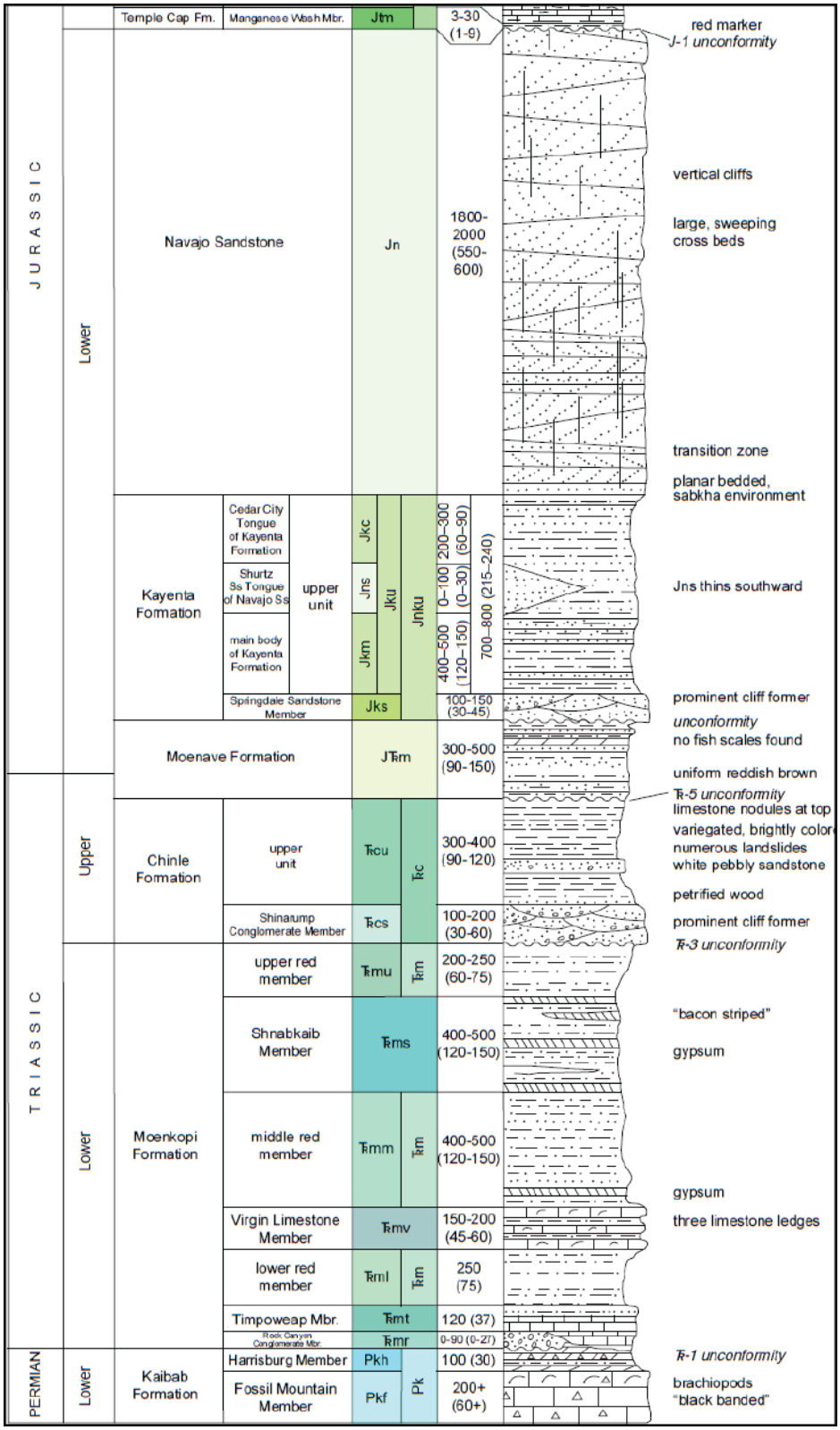

Figure 3.1. Stratigraphic column. Stratigraphy of the area including lithologic column and thickness ranges. Modified from Biek and Hayden (2013).

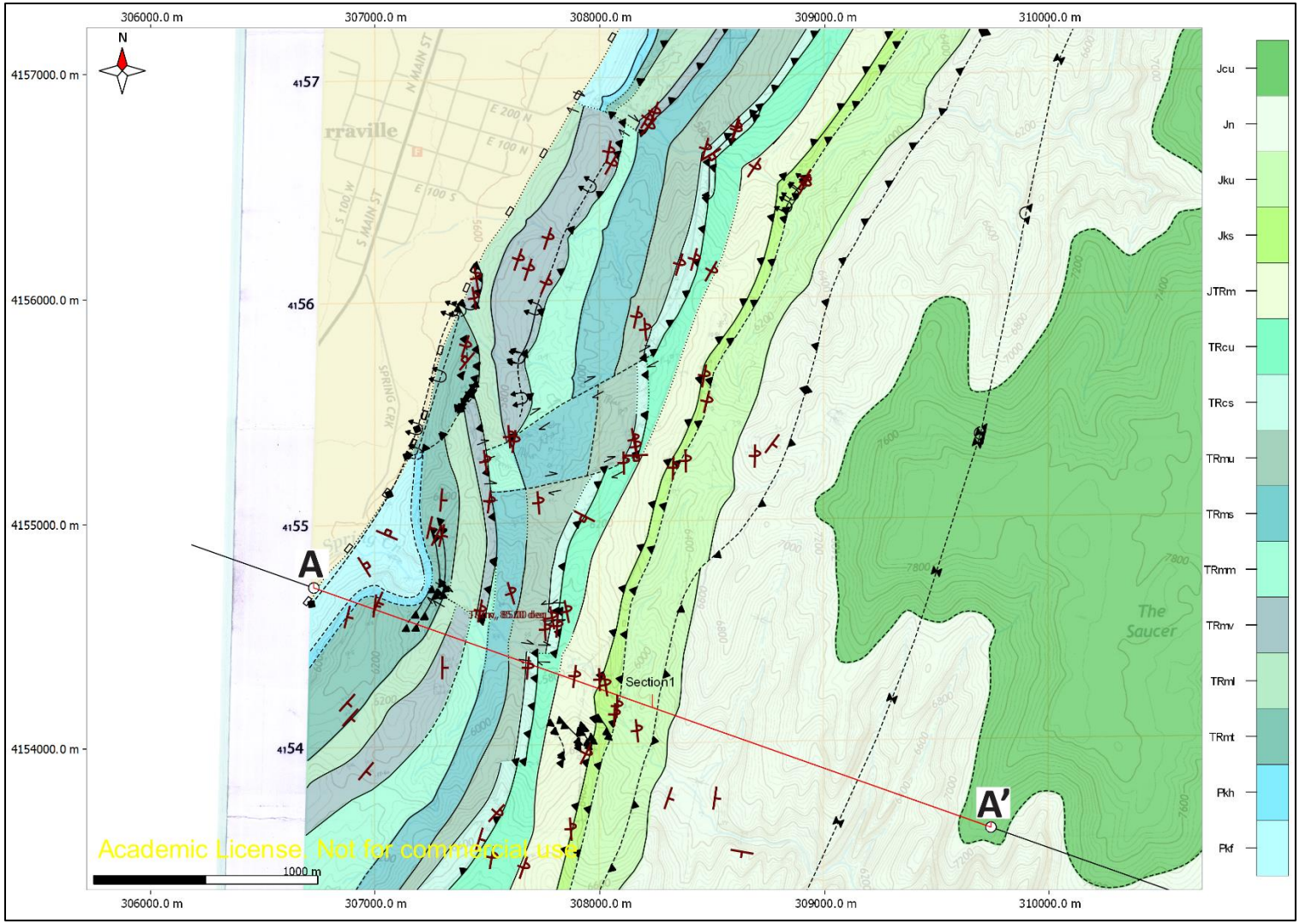

Figure 3.2. Geologic map. Paleozoic and Mesozoic units of the Hurricane Cliffs, exposed from uplift along the Hurricane Fault.

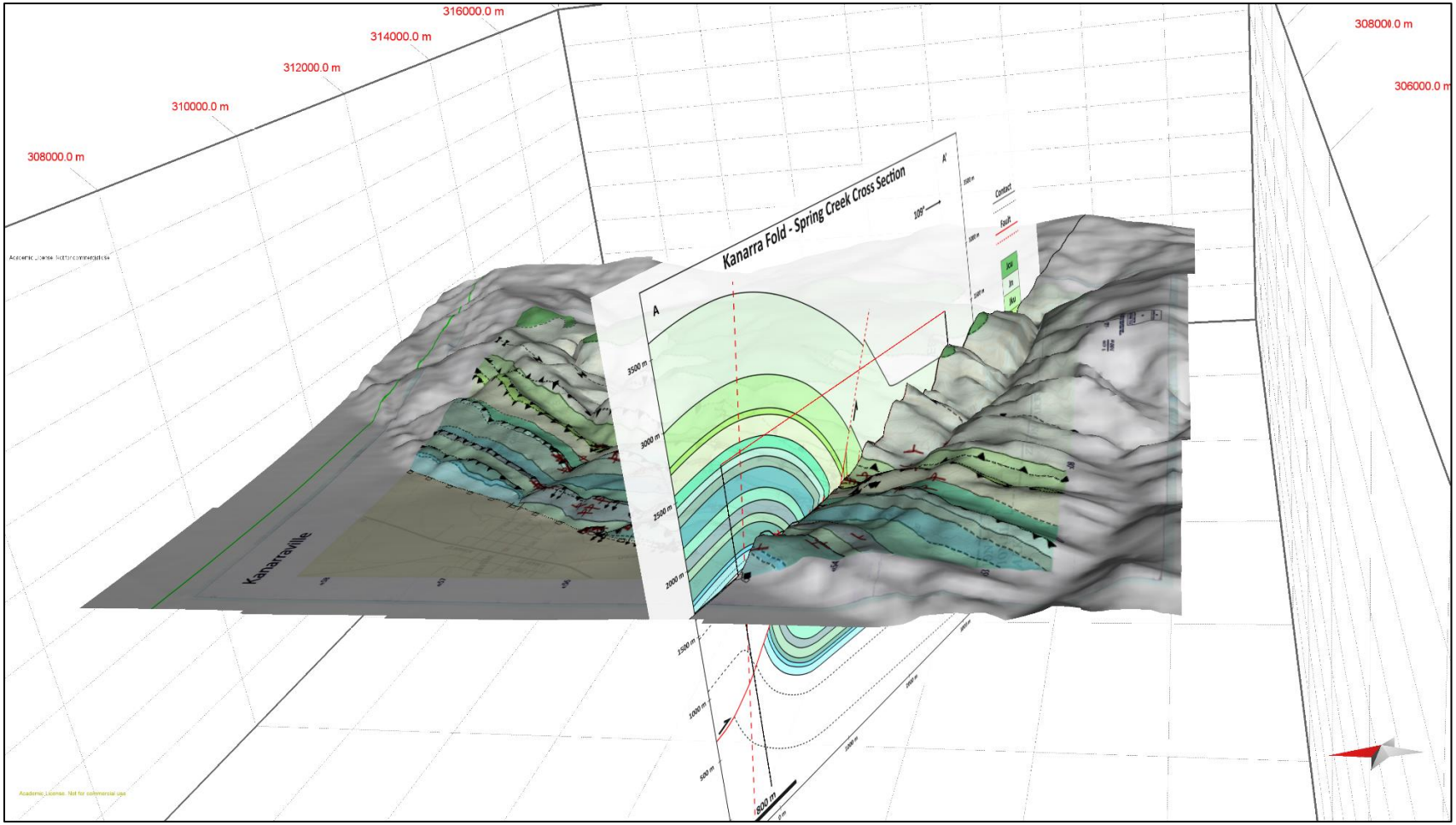

Figure 3.3. 3D DEM of the field area. 3D Digital Elevation Model (DEM) depicting the topography of the Hurricane Cliffs. Note location of cross-section A-A' in red.

3.2. STRUCTURE AND STRATIGRAPHY

3.2.1. Folded Units. From west to east, the major fold structures consist of the Kanarra fold and its accompanying syncline. Some Permian units are present in the cross-section but do not outcrop in the mapping area (Toroweap Formation (Pt), Queantoweap Sandstone (Pq), Pakoon Dolomite (Ppk) Members; Hintze, 1988). Units affected by folding crop out on the east limb of the fold and include Upper Permian through Lower Jurassic strata. Presumably, the western limb of the Kanarra fold is in the downthrown hanging wall of the Hurricane Fault, which was subsequently buried by over 1000 m of Quaternary sediments (Averitt, 1962). Minor folds are observed in the Fossil Mountain (Pkf), Timpoweap, Virgin Limestone (TRmv), and Springdale (Jks) Members (Figure 3.4).

The following descriptions of rock units in the map area are based on field observations and descriptions by Biek and Hayden (2013). Detailed rock descriptions are presented in Appendix A. The Permian Fossil Mountain Member (Pkf) is a highly competent limestone unit with massive bedding that forms tall cliffs. Based on structural mapping (summer 2016), it is 111 m thick (roughly twice the published thickness, Figure 3.1). The abnormal thickness of this unit may be due to local tectonic overthickening from duplexes and backthrusts observed in the field (Figure 3.5). The upper contact with the Harrisburg Member (Pkh) is gradational and difficult to delineate.

The Permian Harrisburg Member (Pkh) is a slope forming mudstone and limestone unit. It is approximately 30 m thick (62 m from mapping, Figure 3.2). Little structural information was acquired from this unit due to the difficulty in accessing and placing the contacts. It forms a gradational upper contact with the Lower Triassic Timpoweap Member (TRmt).

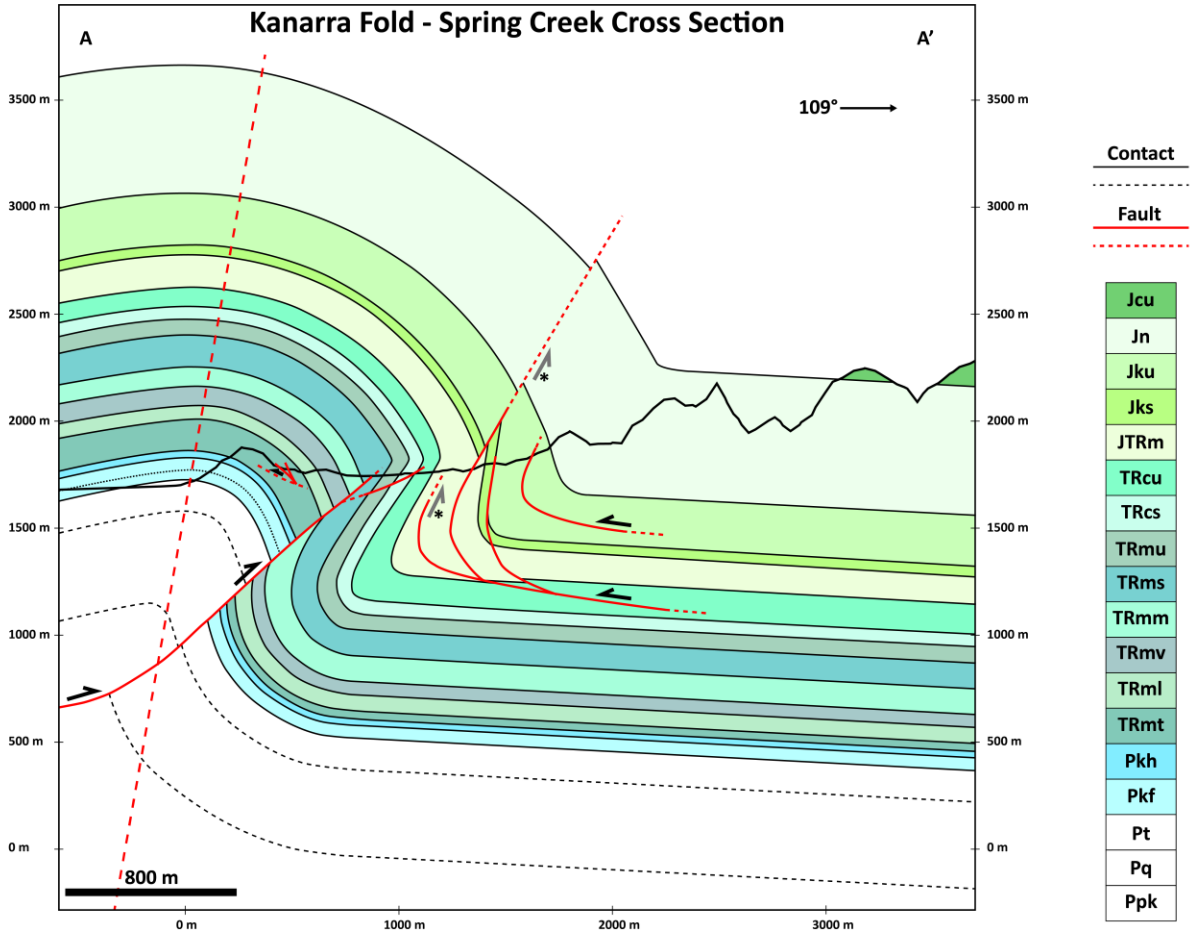

Figure 3.4. Geologic Cross-Section. This cross-section of the map area portrays a complexly deformed fault propagation fold and a structural architecture reminiscent of a triangle zone (Jones, 1982). Locked backthrusts are starred and gray.

The Timpoweap Member (TRmt) is a competent ridge-forming limestone unit which weathers to a yellow-brown color and commonly contains thinner, shaley yellow beds. It has been thickened considerably (from 37 m to 156 m). Several backthrusts and complex folding were observed in this unit (Figure 3.2). Along the line of section, it forms an antiformal hogback, gently dipping 35°east at the base. Approaching the anticline axis towards the west, dips shallow (near 25° E). The Triassic Timpoweap Member (TRmt) is in sharp contact with the overlying Triassic Lower Red Member (TRml), identified by the color change from yellow limestone to incompetent red mudstone.

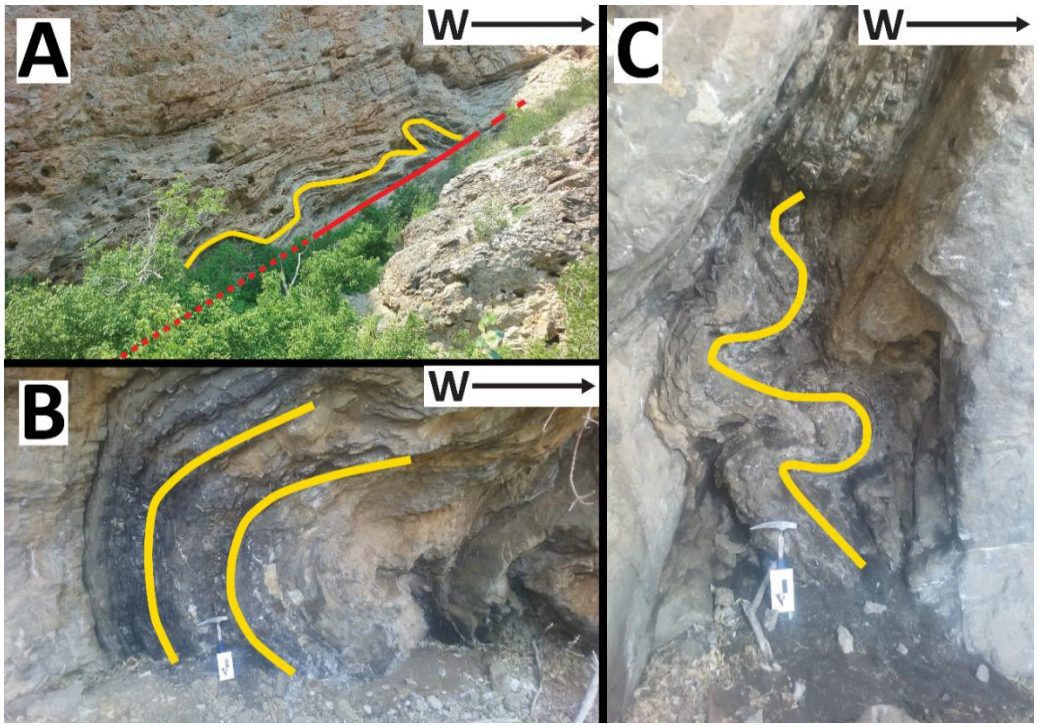

Figure 3.5. Examples of overthickening in the Kaibab Formation (Pkf, Pkh). The competent limestone units in the anticline core are deformed by small (1.5 to 10 m in length) minor faults and parasitic folds that may be involved in overthickening. A) Backthrust and fold series. B, C) Folding near the base of the fault.

The Triassic Lower Red Member (TRml) is a slope former consisting primarily of red mudstone and gypsum. Typically, the Triassic Lower Red Member (TRml) is 75 m thick. Within the cross-section, the Triassic Lower Red Member (TRml) is slightly thinner than usual (Figure 3.4, Table 4.1). It is partially faulted out in some locations by both minor thrust sheets (e.g., just north of Spring Creek) and by the Hurricane Fault (Figure 3.2). The contact with the overlying Triassic Virgin Limestone Member (TRmv) is represented by a sharp change in color and lithology to gray limestone ledges.

In Spring Creek, the Triassic Virgin Limestone Member (TRmv) forms a set of prominent, thin (1.5 to 3 m), gray ridges interbedded with yellow to brown mudstone. It is approximately 60 m thick. Ripple marks are common in this unit and provide topping indicators. Chattermarks, related to faulting, are present throughout the unit, especially on float. South of Spring Creek, along the section line, it is the last upright unit (dipping 65° E). North of Spring Creek, it is overturned (85° W) and appears to have faulted out much of the Middle Red Member (TRmm). The upper contact with the overlying Triassic Middle Red Member (TRmm) is commonly interpreted as a fault contact throughout the field area (Figure 3.2).

The slope forming Triassic Middle Red Member (TRmm) is easily distinguished by thick (approximately 3 to 4 m), double gypsum layers at the base and some minor gypsum stringers encased in red mudstone. It is approximately 120 m thick (Figure 3.1, Table 4.1). Folding of the “double” gypsum layers is observed throughout the field area (Figure 3.6). The unit is commonly faulted out by the Triassic Virgin Limestone Member (TRmv) (Figure 3.2).

The Triassic Middle Red Member (TRmm) shares a gradational upper contact with the overlying Triassic Shnabkaib Member (TRms). The location of the upper contact is defined by the first appearance of a thick (typically > 2 m) gypsum layer. The Shnabkaib Member (TRms) is distinguished by thick (typically > 2 m) gypsum beds interbedded with red mudstone, and has a "bacon stripe" appearance. It is approximately 120 m thick (Figure 3.1, Table 4.1). Folding of the gypsum is observed throughout the field area (Figure 3.6; Figure 3.7). The upper contact with the overlying Triassic Upper Red Member (TRmu) is gradational and is primarily recognized by a change in color and lithology to deep red siltstones and sandstones.

The Triassic Upper Red Member (TRmu) is a slope former punctuated by ledges from interbedded sandstone bodies. These ledges vary greatly in thickness from almost 1 m to 8 m and pinch-out laterally along strike. Its thickness is approximately 75 m. Throughout the field area, this unit is consistently overturned, with average dips around 47° W. The sharp upper contact with the overlying Triassic Shinarump Conglomerate Member (TRcs) is marked by a thick, commonly yellow sandstone and conglomerate ridge.

The ridge forming Shinarump Conglomerate Member (TRcs) of the Upper Triassic Chinle Formation is marked by prominent, cross bedded, yellow, coarse sandstone and conglomerate. Its thickness is approximately 60 m. Abundant cross beds regularly indicate overturning (42° W along the line of section, Figure 3.4), except towards Zion National Park to the south where the unit becomes upright (Figure 3.2). Slickensides are widespread and commonly contain slickenlines. This unit consistently cuts into the Triassic Petrified Forest Member (TRcu) and the upper contact is interpreted

to be a thrust fault that persists along strike. This sharp contact is recognized by a distinct change in color and lithology to gray-green and purple mudstone.

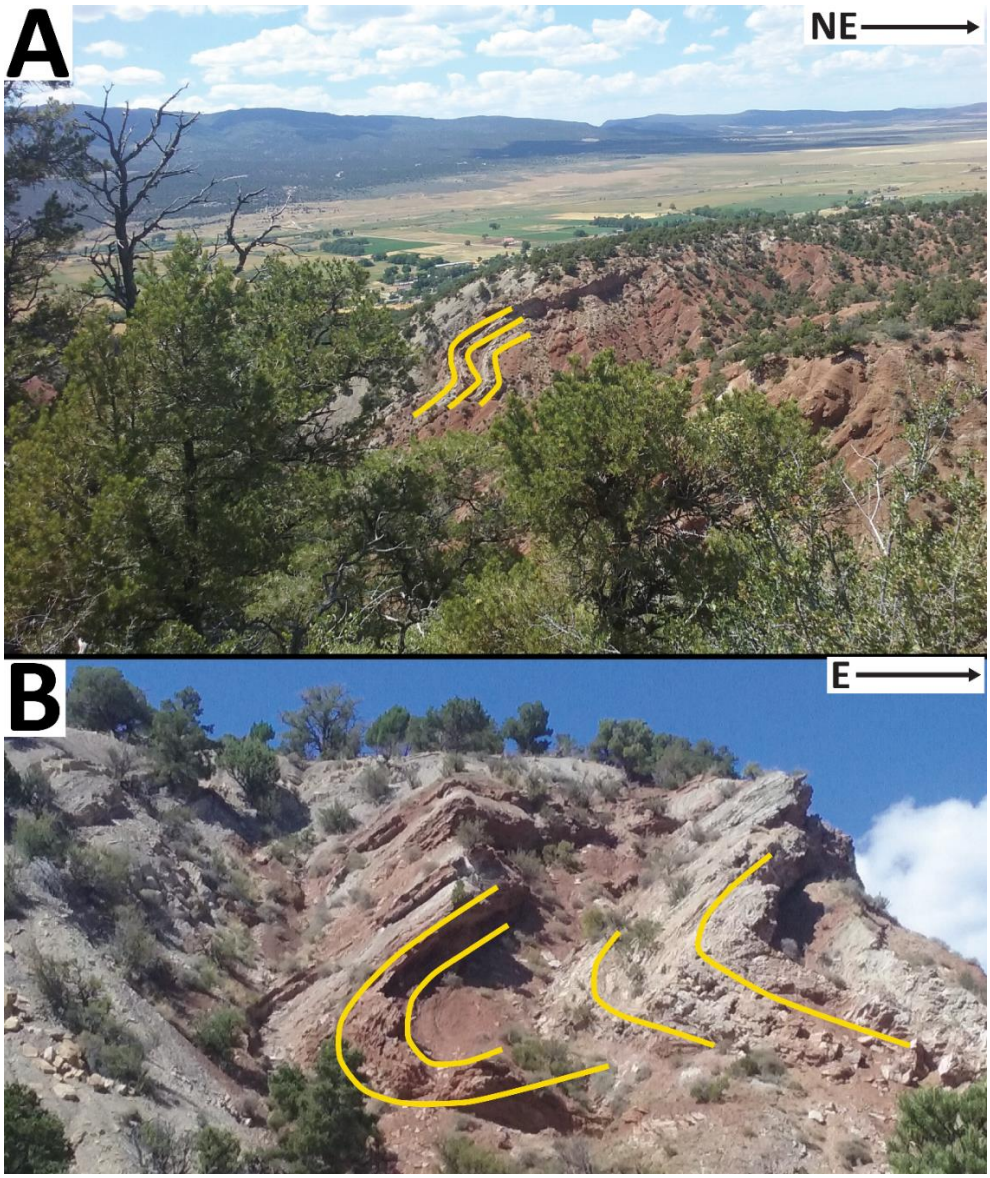

Figure 3.6. Parasitic folding of gypsum in the Triassic Middle Red Member (TRmm). A) Folding of the Middle Red gypsum double layer as seen from a distance. B) Closer (~10 m away) view of folding of the Middle Red gypsum double layer. Note the thickness variation and discordances between layers shown by the contacts. The gray limestone to the left forms a recumbent anticline (Davis et al., 2012), and suggests the presence of a nearby fault.

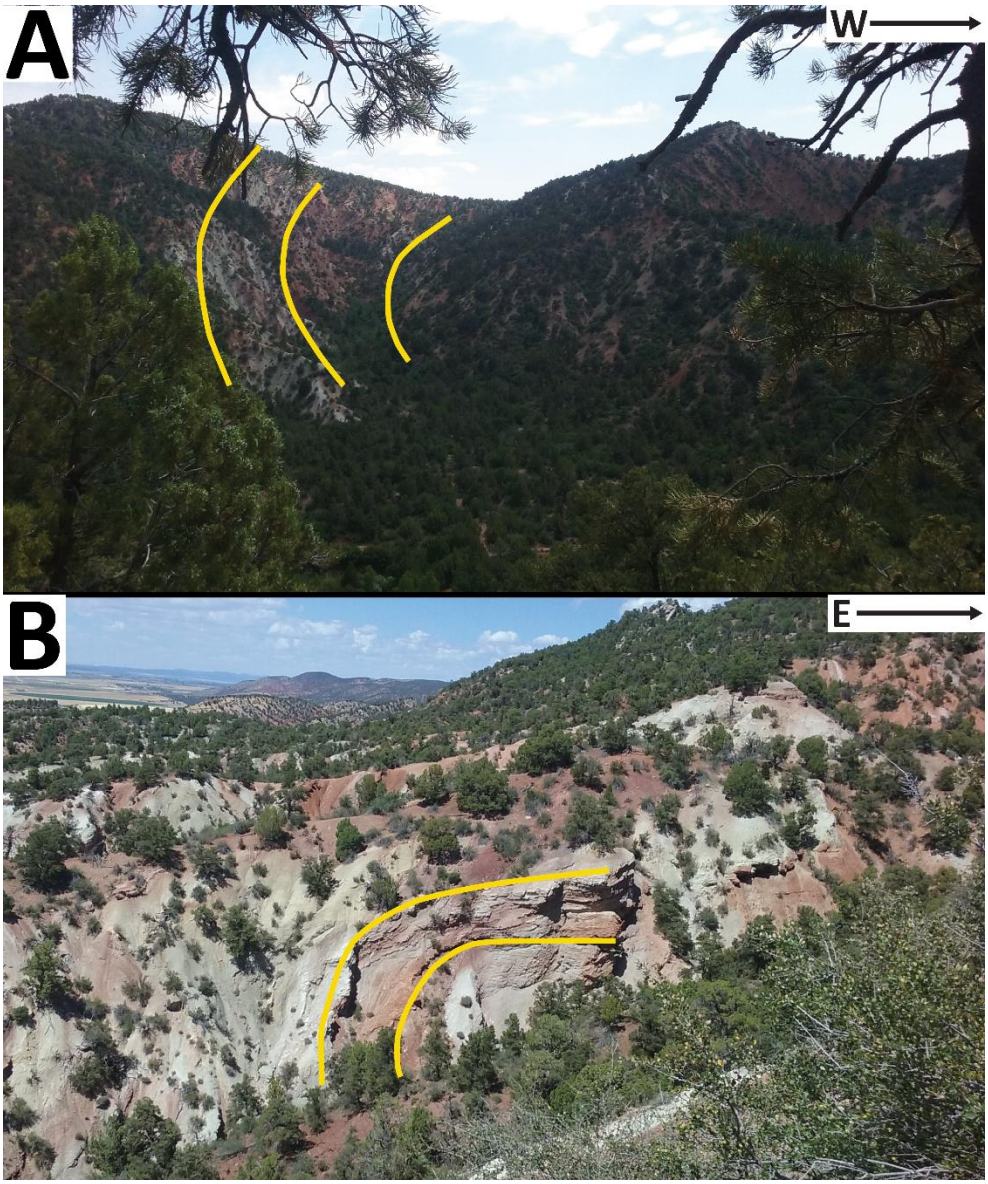

Figure 3.7. Folding of gypsum in the Shnabkaib Member (TRms). Note variations in layer thickness, especially in (A). The folding of gypsum layers is thought to locally thicken these units considerably.

The Jurassic Moenave Formation (JTRm) is represented by the Dinosaur Canyon Member (JTRm) which is a slope former punctuated by ledges of interbedded white to red sandstone layers and deep to orange red siltstone. Its approximate thickness is 90 to 150 m (Figure 3.1, Table 4.1). From the discordance of the Dinosaur Canyon Member

(JTRm) with the Springdale Member (Jks) within Spring Creek (Figure 3.8) and to the south (Figure 3.9), the upper contact of the Dinosaur Canyon Member (JTRm) with the Springdale Member (Jks) is inferred to be a thrust fault that persists along strike. Within Spring Creek, massive white to red sandstone of the Dinosaur Canyon Member (JTRm) can be seen truncating purple sandstones of the Jurassic Springdale Member (Jks) along a thrust contact (Figure 3.8). The dip of the fault plane at the truncation was 63° W. In this location several thrust faults can be seen in both the Dinosaur Canyon (JTRm) and Springdale (Jks) Members (Figure 3.2, Figure 3.9). These closely spaced thrusts are interpreted to represent a duplex structure. In addition, this fault zone is interpreted to represent the along strike correlative to the thrusts of the Taylor Creek thrust fault system mapped south of Spring Creek in Kolob Canyon (Biek, 2007).

Figure 3.8. Truncation of Dinosaur Canyon (JTRm) against Springdale (Jks). The fault is inferred based on a stark contrast in bedding dips at the contact.

Figure 3.9. Dinosaur Canyon Member (JTRm)-Springdale Member (Jks) imbrications. Looking south of Spring Creek, a "T" indicates truncation in the ridges. Some imbrication is also apparent here.

The prominent ledge forming Jurassic Springdale Member (Jks) consists of purple, cross bedded sandstone with interspersed white sand grains. Its approximate thickness is 30-45 m (Figure 3.1, Table 4.1). Within the map area, both the lower and upper contacts of the Springdale Formation are mapped as west dipping faults and the unit is overturned (Figure 3.2). Along the line of section, the Springdale Member (Jks) is overturned 81° W. The upper thrust fault contact is well exposed in Kanarra Creek along Traverse 3 (Appendix D). This contact is represented by a sharp change in lithology from thick bedded, competent sandstone (Jurassic Springdale Member (Jks)) to slope-forming dark red siltstone and mudstone (Jurassic Kayenta Upper Unit, Figure 3.1). Here the Springdale Member (Jks) displays an east verging fold along the thrust contact with the

Jurassic Kayenta Formation (Jku) consistent with overall east directed tectonic transport during thrusting (Figure 3.10).

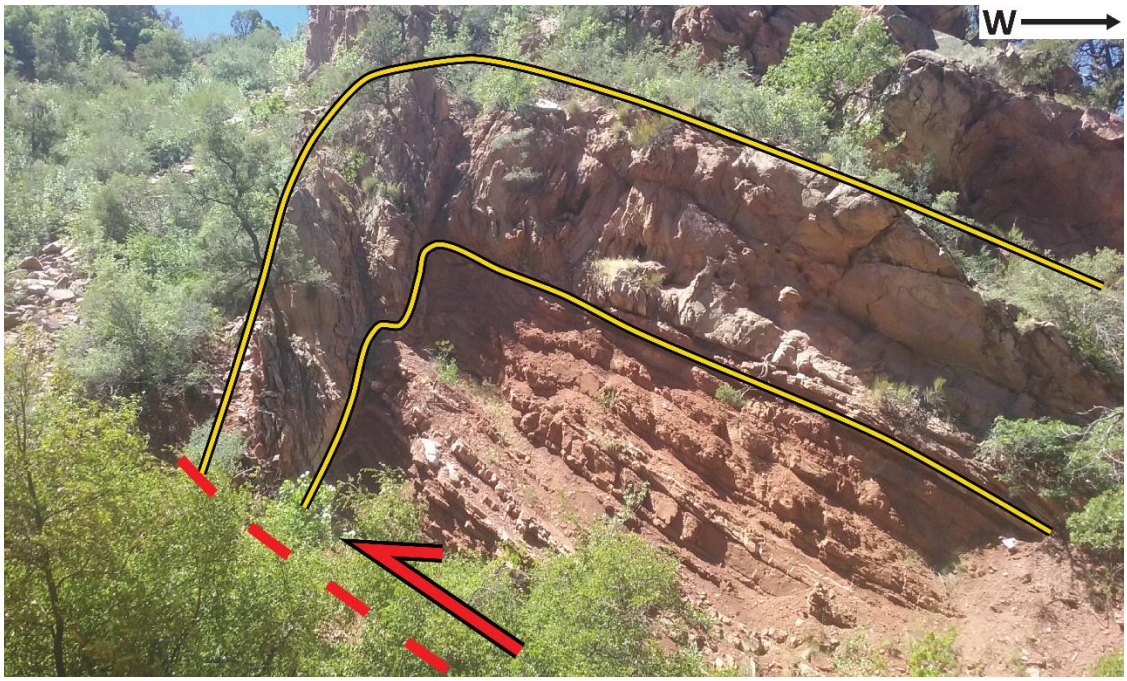

Figure 3.10 .Fault propagation fold in the Springdale Member (Jks). This fold indicates presence of a nearby fault (the red dashed line).

The slope forming Jurassic Kayenta Upper Unit consists of interbedded red siltstone and mudstone. Its approximate thickness is 215 - 240 m. Some lighter colored sandstone beds crop out as short (7 to 9 m tall) flatirons in Spring Creek. The steeply dipping, overturned (79° W) sand bodies are discordant with the bedding of the Jurassic Navajo Sandstone (Jn) (74° E). Based upon this discordance a backthrust is mapped within the Kayenta Formation (Jku) in the Spring Creek area (Figure 3.2). Along strike to the north, this fault changes vergence. It is observed along the Red Rock Trail in the

Jurassic Navajo Formation as a west-dipping reverse fault, suggesting this fault is folded. In Spring Creek, the upper contact of the Kayenta Formation (Jku) with the overlying Jurassic Navajo Sandstone (Jn) is depositional.

The Jurassic Navajo Sandstone (Jn) forms a reddish orange sandstone cliff with large (2 to 3 m tall) cross beds. It is approximately 550 to 600 m thick (Figure 3.1, Table 4.1). Locally heavily fractured with slickensides and deformation bands, the unit dips 74° E near the contact. It quickly returns to horizontal about 0.5 km to the east, within the Spring Creek slot canyon. To the north, it becomes vertical and overturned (Figure 3.11).

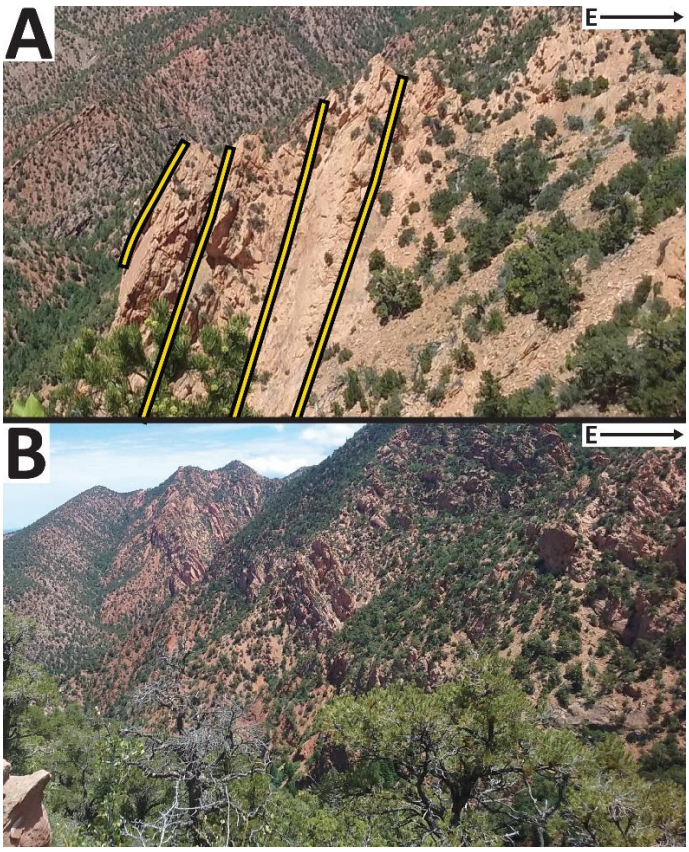

Figure 3.11. Vertical to overturned Jurassic Navajo Sandstone (Jn). A) Approximate location of bedding in yellow. Note steep dip to west (overturned). B) Fractured Jurassic Navajo Sandstone (Jn) with apparent bedding planes that are vertical and overturned.

3.2.2. Faults: Kanarra Thrust and Taylor Creek Thrust. Within the map area, contacts of several competent units against incompetent units (e.g., Virgin Limestone (TRmv), Shinarump Conglomerate (TRcs), and Springdale (Jks) Members) are mapped as major thrusts that persist along strike (Figure 3.2). Beginning in the northern side of Spring Creek, a steeply inclined, overturned (85° W) section of the Triassic Virgin Limestone Member (TRmv) is thrusted over and cuts out the Middle Red Member (TRmm) – this thrust, because of its prominence, is referred to as the Kanarra thrust fault. To the north, the Kanarra thrust fault defines the upper contact of the Virgin Limestone Member (TRmv). Following the ridges of the Virgin Limestone Member (TRmv), the Kanarra thrust fault cuts up section in at least two locations along lateral ramps. At the thrust contact near Traverse 2 (Appendix D), it places folded, overturned Triassic Virgin Limestone above overturned and folded Triassic Middle Red (Figure 3.12). South of Spring Creek, the Kanarra thrust fault dies out in the Middle Red Member (TRmm). However, based upon the cross-section continues as a blind thrust in the subsurface (Figure 3.4). It accounts for the discordance between the Triassic Virgin Limestone Member (TRmv) (65° E, upright) and the Shinarump Conglomerate Member (TRcs) (43° W, overturned). From slickensides (149, 31° W) mapped at the surface and truncation of the Petrified Forest Member (TRcu), a splay of the Kanarra thrust is interpreted to extend through and displace the Shinarump Member.

The Taylor Creek thrust system crops out south of spring Creek in Kolob Canyon, where it can be seen duplicating the Springdale Member (Jks) of the Jurassic Kayenta Formation (Jku) (Kurie, 1966). Biek (2007) mapped it as a zone of at least three east dipping imbricate thrust faults, recognizing this system as “backthrusts”. The Taylor

Creek thrust system has been shown to persist north along strike into Spring Creek (e.g., Kurie, 1966).

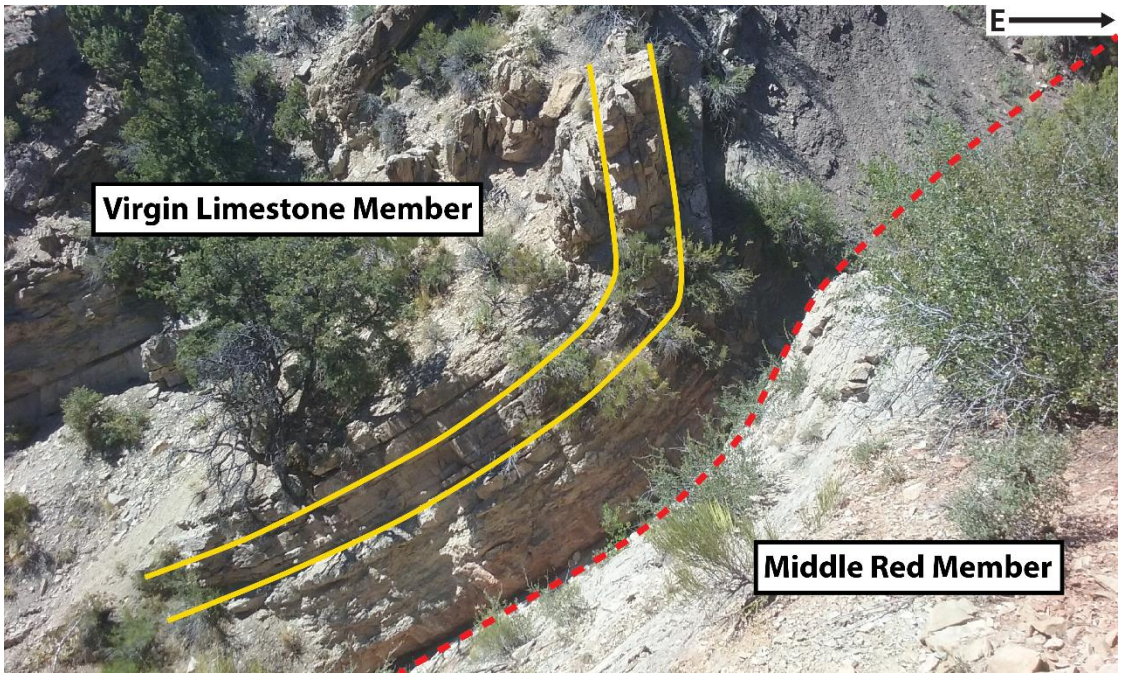

Figure 3.12. Folded Triassic Virgin Limestone Member (TRmv). The limestone beds are folded into a recumbent anticline (older towards the core) and the folding indicates the presence of a nearby thrust fault (approximate contact dashed in red).

Kurie (1966) interprets this fault system to represent the fault that is responsible for formation of the Kanarra Fold. It is unclear from Biek (2007) if the Taylor Creek thrust system is recognized in Spring Creek. In this study it is correlated to folded thrusts in the Dinosaur Canyon and Springdale Member (Jks)s (Figure 3.2; 3.4).

To the east of the Taylor Creek backthrusts, a previously unrecognized "backthrust" is mapped within the Jurassic Kayenta Formation (Jku) (Figure 3.2; 3.4).

Along strike to the north, this backthrust is also folded by the advancing Kanarra fold and changes sense of displacement from an east dipping backthrust to a west dipping thrust that cross-cuts steeply dipping to overturned Jurassic Navajo Sandstone (Jn). The folded backthrust splays in the cross-section have an apparent normal displacement when overturned.

3.2.3. Faults: Minor Thrusts and Lateral Ramps. Minor thrusts observed in the field include those associated with small duplexes within the Kanarra fold (Figure 3.5). These duplexes occur in both the Kaibab Formation (Pkf, Pkh) (Figure 3.5) and the Moenave Formation (JTRm) (Figure 3.8; Figure 3.9). A collection of these duplexes could be partly responsible for overthickening of stratigraphic units as shown in the geologic cross-section (Figure 3.4).

Transfer zones, also known as tear faults or lateral ramps (e.g., Butler, 1982), have a strike-slip component and allow thrust faults to achieve differential displacement along strike (Davis et al., 2012). Several linear, east-west trending faults with apparent strike-slip separation are mapped within Spring Creek (Figure 3.2). They exhibit an apparent strike-slip separation, but without seeing kinematic indicators on the fault face, the separation exhibited by these faults is compatible with either strike-slip or normal slip. From their general orientation and spatial relationship with the Sevier thrust faults, the author interprets these faults to represent lateral ramps rather than being related to younger Basin and Range extensional tectonics.

3.2.4. Post-Sevier Structural Features. Previous workers have interpreted several normal faults in the area, especially at transfer zones (Averitt, 1967; Biek and Hayden, 2013). The only normal fault the author mapped in this area is the Hurricane Fault. It faults out the west limb of the Kanarra fold and is several tens of millions of

years younger than the Kanarra fold (Averitt, 1962; Biek, 2007; Lund, 2007). Thus, it was not depicted with displacement in the cross-section (Figure 3.4) and is there only to show its current position and approximate orientation (80° W, from Averitt, 1962).

The author recognizes the existence of landslides and terraces in the Navajo cliffs which record part of the history of the Hurricane Fault. The focus of this study was the structural geology of the area, not surficial deposits, so several younger landslides and terraces which could be associated with faulting were not mapped. Approximate landslide locations are outlined below (Figure 3.13).

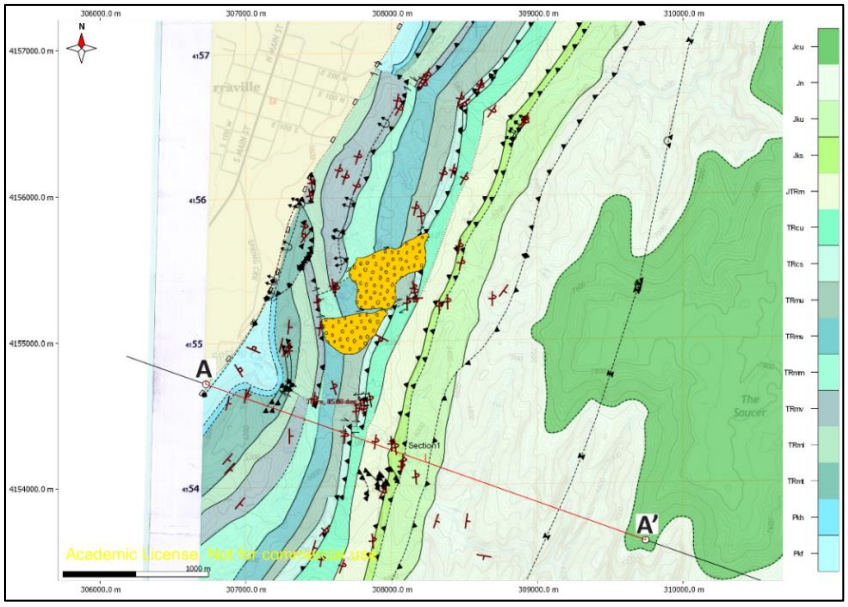

Figure 3.13. Approximate locations of unmapped landslides.

3.3. STRUCTURAL DOMAINS

The field area was divided into structural domains along the line of section (Figure 3.2; Figure 3.4). Traverse 1 in Spring Creek can be split into three structural

domains based on changes in structural attitude and the location of major faults. Domain I consists of upright, tilted beds of alternating limestone and red mudstone from the Permian Kaibab Formation (Pkf, Pkh) to the Triassic Virgin Limestone Member (TRmv). Domain II contains the first major fault seen in the south side of Spring Creek, in the Shinarump Conglomerate Member (TRcs), and overturned beds. A series of overturned, folded thrusts preceding the Jurassic Navajo Sandstone (Jn) make up the eastern part of Domain II. A detailed discussion of important stops in each structural domain can be found in Appendix D.

4. DISCUSSION

4.1. VARIATION IN STRATIGRAPHIC THICKNESS

Differences in the stratigraphic thickness of units cropping out along the Spring Creek traverse as determined from the geologic cross-section (Figure 3.4) and those reported in the literature are presented in Table 4.1 along with a comparison of thickness variation in the hanging wall and footwall limbs of the Kanarra fault propagation fold. Based upon geometric constraints in constructing "balanced" cross-sections of fault propagation folds**,** all units in the forelimb (e.g., hanging wall see Figure 3.4) are expected to undergo uniform thickening (Jamison, 1987). In contrast, stratigraphic units involved in the Kanarra fold exhibit variable thickening depending on the lithology of the stratigraphic layer and its spatial relationship within the fold and to major thrusts (Table 4.1; Figure 3.4). Jamison (1987) also postulates that the constant thickness assumption for area balancing may be more appropriate in regional cross-sections than for individual folds such as the Kanarra fold. Field evidence indicates that the assumption of constant volume, or area, in line-balancing the geologic cross-section along Spring Creek is unlikely to be met. Potential causes of variation in measured and reported stratigraphic thicknesses (e.g., tectonic thickening) are discussed in the following sections.

4.1.1. Tectonic Thickening. The dashed line inside the Fossil Mountain Member (Figure 3.4) reflects the typical lower contact of the unit (Biek and Hayden, 2013). Within the Spring Creek traverse the Fossil Mountain Member (Pkf) is almost twice as thick. Similarly, the Timpoweap Member (TRmt)is almost four times thicker than normal (Table 4.1). Overthickening of these limestone units may reflect the presence of minor parasitic folds and duplex structures that are too small to be represented on a

1:10000 scale geologic map but which are commonly observed in the field (Figure 3.5). Similarly, the presence of duplex structures associated with the Taylor Creek fault system in the Jurassic Moenave can account for the increased thickness of this unit within the cross-section (Figure 3.4, Table 4.1).

4.1.2. Ductile Flow and Folding. Intense folding has been observed in the incompetent units, especially the Triassic Middle Red (TRmm) and Shnabkaib (TRms) Members. The gypsum stringers prevalent throughout these units are commonly folded which will increase the overall layer thickness in response to shortening (Figure 3.6). Additionally, the intrinsically thinner incompetent mudstone units (e.g., Lower Red Member (TRml), Petrified Forest Member (TRcu)) located stratigraphically between more competent units may deform in a ductile manner in response to compression which could explain apparent thinning of units like the Triassic Lower Red Member (TRml) (Figure 3.1, Table 4.1).

4.1.3. Contact Positioning. Location of gradational contacts between the Middle Red Member and the Shnabkaib Member (TRms) based upon the first reappearance of a "thick" gypsum layer is equivocal at best, and the variation in thickness represented by the unit contacts may be partly due to their positioning in the field or lack of along strike stratigraphic continuity of these gypsum layers. For this reason, their combined thickness may be more appropriate to consider when checking for constant thickness. Bringing the minimum stratigraphic thickness for these units into the cross-section, their combined thickness changes from 240m to 230m across the fault. This difference is plausible considering Averitt (1962) also reports thinning of these units from deformation.

Table 4.1. Unit thickness changes from the footwall to the hanging wall.

Unit	Published t (m)	Footwall t(m)	Hanging wall t(m)	% Change from Footwall
Jn	550-600	601	550	-8.49
Jku	215-240	230	241	4.78
Jks	30-45	45	46	2.22
JTRm	90-150	136	147	8.09
TRcu	90-120	129	92	-28.68
TRcs	45-60	66	62	-6.06
TRmu	60-75	73	76	4.11
TRms	120-150	120	144	20.00
TRmm	120-150	119	89	-25.21
TRmv	45-60	62	97	56.45
TRml	75	75	66	-12.00
TRmt	37	37	156	321.62
Pkh	30	30	62	106.67
Pkf	60+	60	111	85.00

4.1.4. Anomalous Thickness Changes. While honoring mapped contacts in the cross-section (Figure 3.4), the thicknesses of some units change inexplicably. The Triassic Virgin Limestone Member (TRmv) thickens by 56% across the fault (Table 4.1). Rare undulation and folding was noted in this unit, but these features are considerably less common than those observed in the Permian limestones that crop out in Spring Creek (e.g., Figure 3.5). Future work will examine the potential for duplication of this unit by thrust faulting along shale interbeds.

Thinning in some incompetent units is also observed in the geologic cross-section (Figure 3.4). For example, the Lower Red Member (TRml) is slightly thinner than normal (66 m instead of 75 m, Table 4.1). No obvious tectonic reason for this difference at the

section line was documented in the field. However, locally this unit has been overthrusted by a klippe of the Timpoweap Member (TRmt) just north of Spring Creek, suggesting slip along this contact may be present.

4.2. STYLES OF DEFORMATION

4.2.1. Fault Propagation Folding. The Kanarra fold is interpreted to have formed as a "fault propagation fold" (see Suppe and Medwedeff, 1990). This is consistent with previous interpretations and Sevier tectonic style (Armstrong, 1968; Averitt, 1962; Grant et al., 1994; Willis, 1999). However, the specific fault responsible for the formation of this fault propagation fold is subject to debate. For example, in the past the thrust near the Kayenta – Navajo contact has been speculated as forming the Kanarra fold prior to breaking through the overturned limb as a "rollover break-thrust" (Noweir, 1990; Grant et al., 1994; Fielding, 1994). In contrast, the thrust fault responsible for creating the Kanarra fold can be identified in the geologic cross-section based upon its spatial association with the Kanarra fold and has been named the "Kanarra thrust" (Figure 3.4). The location of the tip of this blind thrust is constrained in the cross-section by the discordance in dips between the upright Triassic Virgin Limestone Member (TRmv) and the overturned Triassic Shinarump Conglomerate Member (TRcs). The Kanarra thrust crops out as the thrust fault that displaces overturned Triassic Virgin Limestone Member (TRmv) on top of the overturned Triassic Middle Red Member (TRmm) (Figure 3.2). The Kanarra thrust can be seen in the north side of Spring Creek where it cuts-out the Middle Red Member (TRmm) (Figure 3.2).

Within this same cross-section, the evolution and modification of backthrusts during folding can be seen. Thrust faults associated with the Taylor Creek fault system

are interpreted to have been folded and overturned in the foot wall limb of the advancing Kanarra fault propagation fold. This change in geometry results in these initially west-directed thrust being reactivated as east-directed thrusting in concordance with the main Kanarra thrust. Deactivation of the Taylor Creek thrust faults as backthrusts results in the initiation of a new back-thrust further to the east - the thrust fault within the Kayenta Formation (Jku) (Figure 3.4). Thus, this fault cannot be responsible for producing the Kanarra fault propagation fold as previously suggested (see Kurie, 1966; Noweir, 1990; Noweir and Grant, 1995).

In cross-section, displacement along the Kanarra thrust gradually decreases towards the fault tip (Figure 4.1). Displacement along the fault increases then decreases towards the tip as deformation is transferred to folding. The decline in displacement is characteristic of fault propagation folds (see Figure 30 in Dahlstrom, 1970). In cross-section the Kanarra thrust breaks through the overturned limb of the Kanarra fault propagation fold (Figure 3.4). This style is similar to the subcategory of fault-propagation folds termed “high-angle breakthrough” (Suppe and Medwedeff, 1990). Suppe and Medwedeff (1990) suggest this type of fold develops because stratigraphic layers in front of the advancing fault tip are unable to tightly fold. In Spring Creek, tectonically overthickened, competent Permian, Lower Triassic, and Lower Jurassic units and a strong buttressing effect from the thick, highly competent Jurassic Navajo Sandstone (Jn) may have inhibited tight folding, leading to this fault propagation fold geometry (Figure 3.4).

4.2.2. Fold Geometry. Variations in fold geometry, specifically fold tightness and degree of overturning, occur primarily in the footwall syncline (Figure 3.4; Figure 4.3). Units proximal to the fault are upright deeper in the cross-section (e.g., the Permian

Fossil Mountain Member (Pkf), Figure 3.4), but become overturned at shallower structural levels (e.g., the Triassic Middle Red Member (TRmm), Figure 3.4). Fold tightness varies upsection along the syncline fold axis from open to tight, then open again in the Jurassic Navajo Sandstone (Jn) (Figure 3.4; Figure 4.2).

The degree of overturning and fold tightness vary sympathetically along the fault. This may be attributed to several factors including drag along the Kanarra thrust fault, backthrusts in the footwall, ductile flow in the incompetent units, the presence of thick, competent units, and the folding mechanism (fault propagation). However, the abrupt change in fold tightness from the Dinosaur Canyon Member (JTRm) to the Jurassic Navajo Sandstone (Jn) coincides with the folded Taylor Creek faults. The transition from structural domain I of the eastward advancing Kanarra thrust and fault propagation fold to structural domain II the initially west directed backthrusts may reflect a the large difference in the competency contrast between the relatively thick (~215-240 m) incompetent interbedded mudstones and siltstones of the Jurassic Kayenta and the overlying thick (~600 m) competent Jurassic Navajo Sandstone (Jn).

4.3. KANARRA TRIANGLE ZONE

4.3.1. Essential Elements of Triangle Zones. Triangle zones require three essential elements and an essential process to form and develop (Figure 4.3; Jones, 1982; Price, 1986). The essential elements include: 1) a system of thrusts and folds, 2) a floor thrust into which the duplex thrusts merge, and 3) a bounding roof thrust with backthrust sense of displacement. The crucial, defining process, which perpetuates further development, is called “tectonic wedging” (Jones 1982; Price 1986). Tectonic wedging is

the process by which the duplex beneath the roof thrust thickens and propagates. Tectonic wedging is required for triangle zone to develop further.

4.3.2. The Kanarra Triangle Zone. The geologic map and cross-section of the Spring Creek area contain structures consistent with the essential elements needed to form a triangle zone (Figure 3.2; Figure 3.4; Figure 4.3). The Kanarra fault propagation fold and associated Kanara thrust along with its paired syncline represent element 1 – a system of thrust faults and folds. The Kanarra thrust fault, with east-directed tectonic transport, represents the most likely candidate for element 2 - the floor thrust. The Taylor Creek fault zone and the thrust in the Jurassic Kayenta Formation (Jku) represent element 3 – a system of backthrusts with a sense of west directed tectonic transport

The structural style within the Spring Creek area, as seen in the geologic map pattern and cross-section resemble elements of the type triangle zone at Turner Valley (Jones, 1982). The overall structural architecture of the thrust-fold system in Spring Creek could be characterized as a "nascent" triangle zone - at the beginning stages of formation. However, at the present structural level exposed a bounding roof thrust has yet to be identified. It is possible that it has been removed by erosion, but more likely the geometry of the Kanarra fault and associated fault propagation fold inhibited the development of the Taylor Creek thrust fault zone into a bounding roof fault geometry and therefore further development of the "Kanarra Triangle Zone". Mature triangle zones (all key elements present) do exist in the Utah Sevier thrust belt (e.g., Chester, 1996; Decelles and Coogan, 2006; DeCelles and Mitra, 1995). This begs the question as to why the Kanarra Triangle Zone was abandoned prior to reaching full maturity.

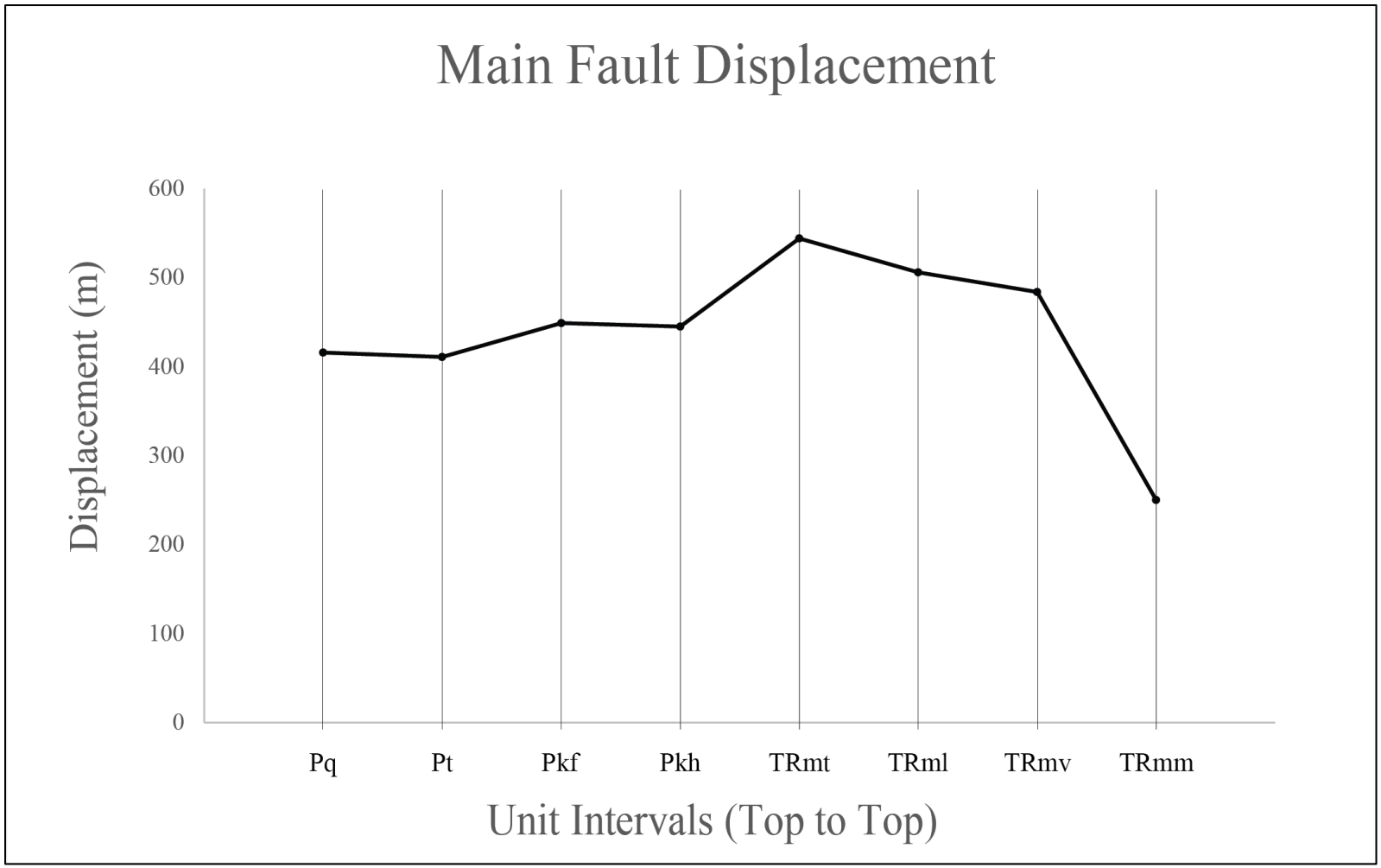

Figure 4.1. Fault displacement values along the main fault. Displacement was measured from unit top to unit top. Note the sharp decrease in displacement after the Timpoweap Member (TRmt) and trend towards zero after the Virgin Limestone Member (TRmv). See Figure 3.1 for unit abbreviations.

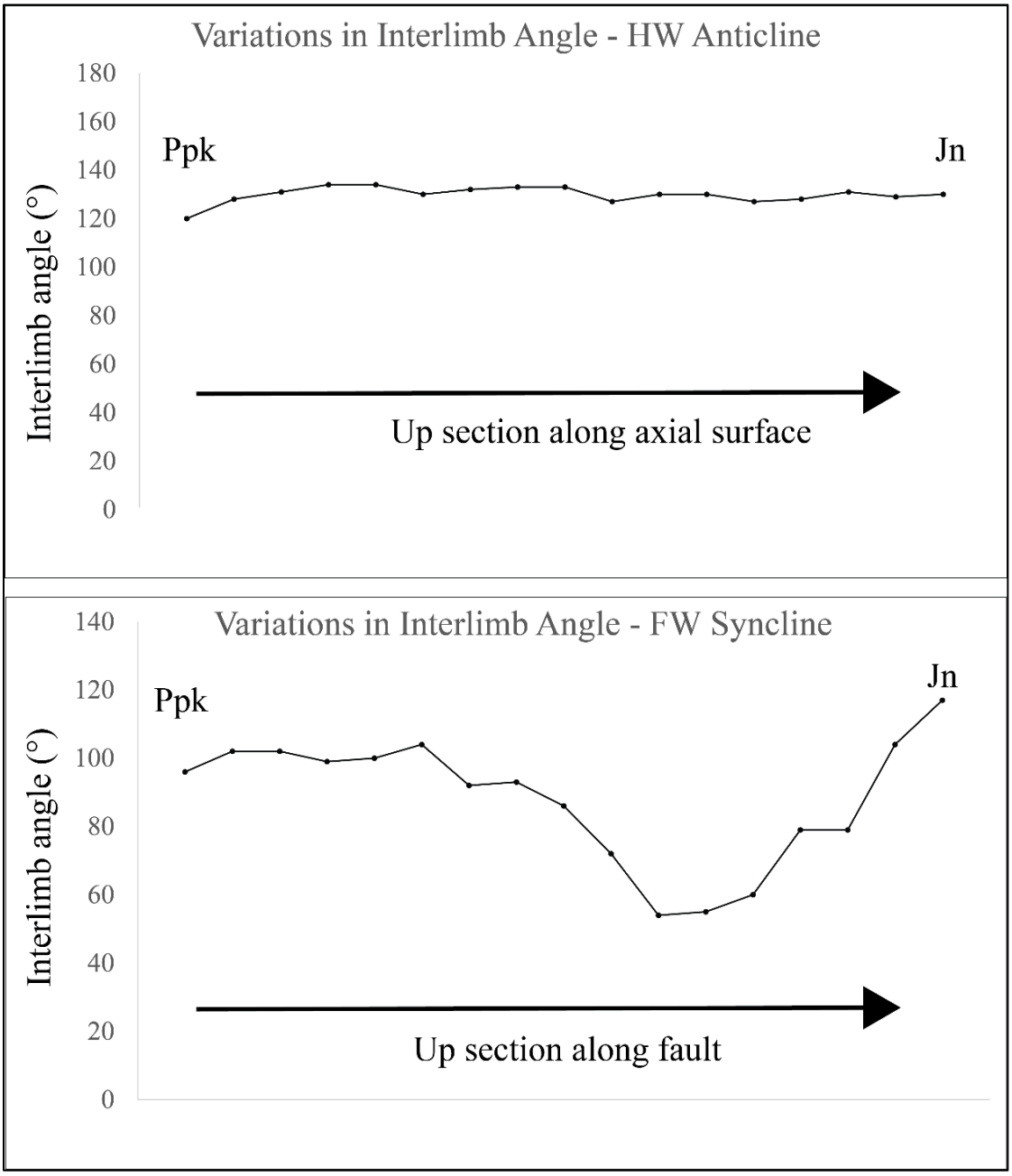

Figure 4.2. Changes in fold tightness. Note how changes in fold tightness (related to overturning) along the Kanarra thrust fault plane occur primarily in the footwall, with little variation in the hanging wall.

4.3.3. Termination of the Kanarra Triangle Zone. Despite exhibiting several essential structural elements, the nascent Kanarra Triangle Zone was abandoned prior to reaching full development. This appears to reflect the absence of a well-developed duplex associated with Kanara fold and thrust system (Figure 3.4). Without the formation of a growing duplex, the process tectonic-wedging mechanism responsible for passively uplifting the roof sequence did not occur during deformation in this area. This is largely interpreted to reflect the geometry of the Kanarra thrust fault and the accompanying Kanarra fault propagation fold.

The breadth of triangle zone models include fault bend folding proximal to the leading edge of the fold and thrust belt (Banks and Warburton, 1986; Charlesworth and Gagnon, 1985; Jones, 1982; Mitra, 1992; Price, 1986). A prerequisite for the development of a fault-bend requires the floor thrust to have a "ramp-flat" geometry, where the dip on the advancing thrust fault ramp flattens out along a low angle detachment - typically within an incompetent unit (Suppe, 1983). The "force-fold" that forms in the advancing hanging wall is a "fault-bend" fold. Fault bend folds differs significantly in geometry from that of a "fault propagation" fold in that the fore-limb of the fault remains upright, typically with a shallower dip (Suppe, 1983; Suppe and Medwedeff, 1990). As the thrust sheet advances, multiple fault bend folds can develop to produce an imbricated duplex structure (Figure 4.3). In a triangle zone, the formation of this duplex structure represents the "tectonic wedge" (Price, 1986). Transport of the growing duplex, as well as the geometry of the fault bend fold forelimb, drives the tectonic wedging process. As the tip of the advancing tectonic wedge (i.e., duplex) approaches the back-thrust, rocks in the hanging wall of the backthrust (i.e., roof thrust)

are passively uplifted and the triangle zone grows (Price, 1986; Tanner et al., 2010; see Figure 4.3).

The absence of tectonic wedging (i.e., formation of a significant duplex structure) may be the primary reason the nascent Kanarra triangle zone did not mature. The geometry, dip angle, and displacement along the Kanarra thrust are appropriate for forming a fault-propagation fold, with a steeply dipping overturned forelimb, rather than a fault-bend fold (Figure 3.4). This reflects that the Kanarra thrust fault retains a steep dip along a thrust ramp rather than eventually flattening along a low angle detachment in one of the incompetent units at a higher structural level in the stratigraphic section. Termination and abandonment of the Kanarra Triangle Zone in the early stages of development also reflects inability of the Taylor Creek thrust faults to develop into the roof–thrust of the triangle zone. South of Spring Creek, along strike, the Kanarra fold is mapped as a broad, shallow anticline that has undergone significantly less shortening than in Spring Creek (Biek, 2007; see Figure 4.4).

Here the Taylor Creek thrust faults are mapped in Jurassic Moenave Formation (JTRm) and the Springdale Member (Jks). These early formed back-thrust faults are folded and overturned in Spring Creek as result of the growth of the Kanara fault propagation fold (Figure 3.4). During this process, rotation of these faults to vertical caused the Taylor Creek thrust system to lock up by rotation out of a favorable orientation for failure. The offsets in competent units cut by the backthrusts were preserved when the faults locked up (gray arrows represent former slip directions, Figure 3.4). Locking of the Taylor Creek thrust system resulted in formation of a new backthrust

in the Jurassic Kayenta Formation (Jku) (Figure 3.2; Figure 3.4), which was also subsequently overturned.

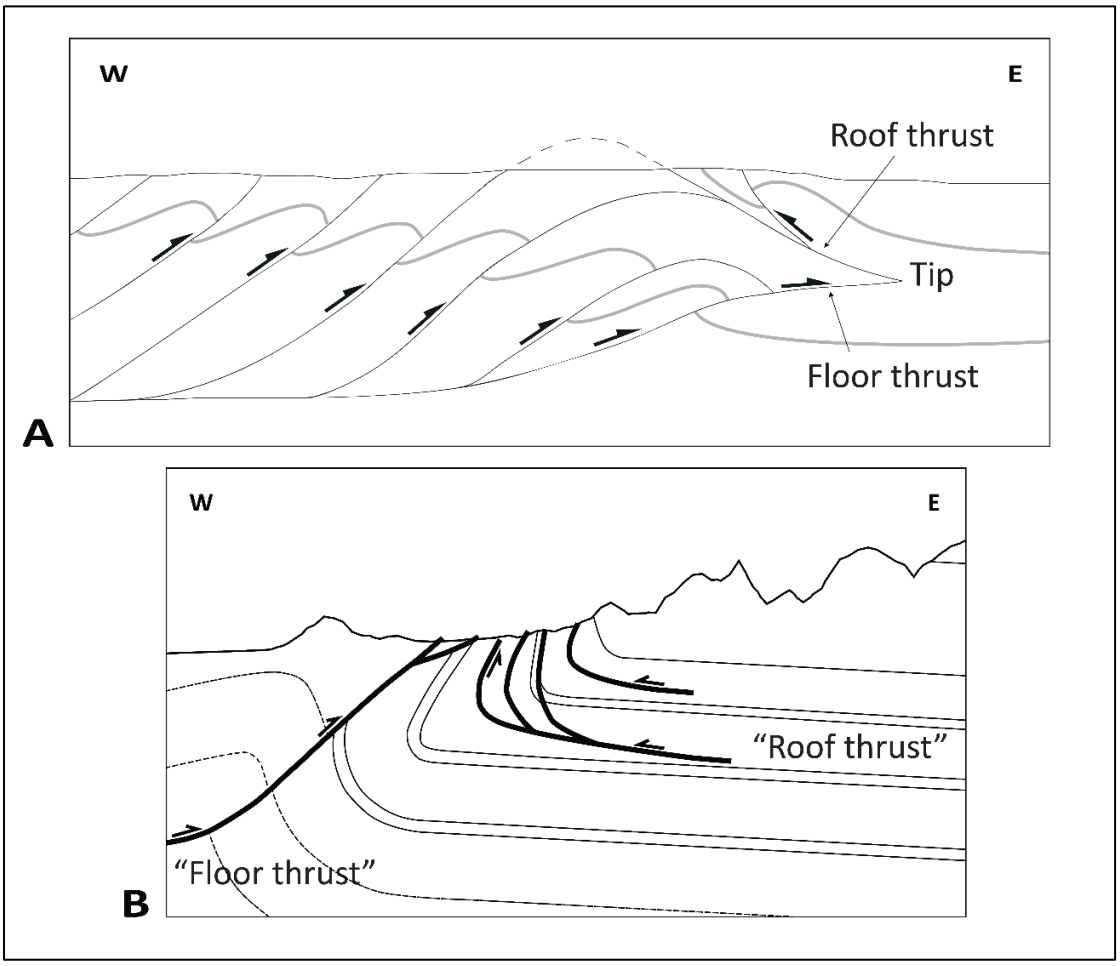

Figure 4.3. Essential structural elements. A) Idealized triangle zone. Material propagating tectonically is forced between the floor and roof thrust (tectonic wedging). Modified from Jones (1982). B) Schematic cross-section of the Kanarra Fold in Spring Creek for comparison.

Continued rotation of these former back-thrusts during shortening may have resulted in their reactivation as east directed reverse faults, ending their potential for

forming the roof-thrust to the Kanarra Triangle Zone (Figure 3.4). Abandonment of the nascent Kanarra Triangle Zone is postulated to have occurred when the advancing Kanarra thrust fault merges with the rotated former back-thrusts to extend the length of the ramp to the Kanarra thrust up section through the Jurassic Navajo Sandstone (Jn). Overturned Jurassic Navajo Sandstone (Jn) and evidence for faulting in this unit (deformation bands, fracturing, and slickensided talus) north of Spring Creek, along the Red Rock Trail (Traverse 2) demonstrates the plausibility of this outcome. Searching for kinematic indicators showing slip direction and cross cutting relationships to test these ideas will be an objective for future work along Traverse 2.

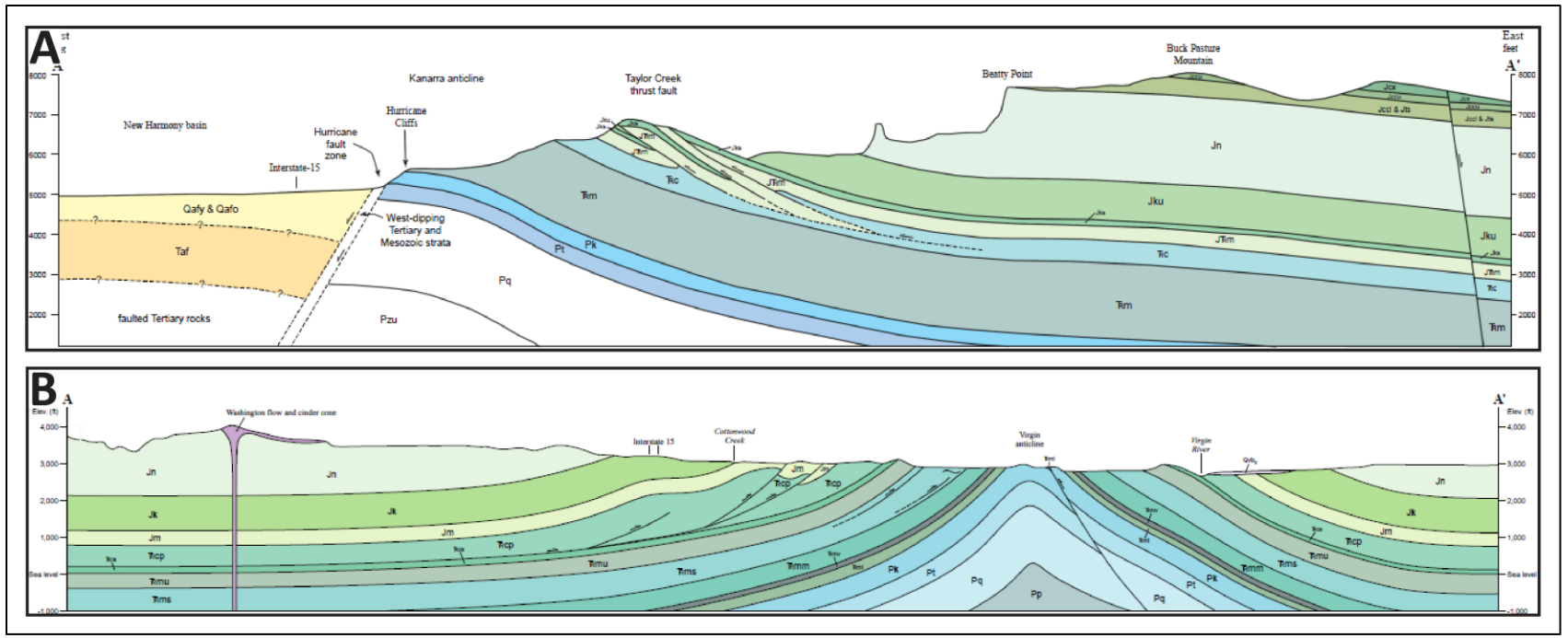

Figure 4.4. Cross sections showing early imbrication. A) Cross-section across the Kanarra fold, from Biek (2007). Note the west-verging (backthrust) imbrication of the Moenave Formation (JTRm) (light green). B) Cross-section across the Virgin anticline from Biek (2003), which coincides with the Kanarra fold south along strike. Note the east-verging imbrication in the Petrified Forest Member (TRcu). These cross-sections show how easily the Lower Jurassic and Upper Triassic units deform at relatively early shortening stages.

5. CONCLUSIONS

Geologic map patterns and field relationships observed from field mapping between June 16th to July 7th, 2016 in the Spring Creek drainage and vicinity indicate the Kanarra fold is a fault propagation fold. The geologic cross-section constructed for Spring Creek reveals the presence of a steeply west dipping (~40^{o}) blind thrust beneath this fold – the Kanarra thrust. The Kanarra thrust crops out to the north as the fault contact along overturned west dipping Virgin Limestone Member (TRmv) and the Middle Red Member (TRmm) of the Triassic Moenkopi Formation. Movement along this thrust fault during the Sevier Orogeny produced the Kanarra fault propagation fold and accompanying syncline. Displacement along the Kanarra fault and growth of the Kanarra fold resulted in folding and rotation of the early formed east-dipping Taylor Creek thrust system, a collection of several imbricate backthrusts, to overturned west-dipping reverse faults. This rotation led to the development of a new backthrust located near and crossing the Jurassic Kayenta and Navajo Sandstone (Jn) contacts. Continued shortening to the north result in rotation and overturning of this backthrust in a similar manner to the Taylor Creek thrust faults.

Within Spring Creek the basic structural elements for a Triangle Zone are present. The Kanarra fault propagation fold and associated Kanara thrust along with its paired syncline represent element 1 – a system of thrust faults and folds. The Kanarra thrust fault, with east-directed tectonic transport, represents the most likely candidate for element 2 - the floor thrust. The Taylor Creek fault zone and the thrust in the Jurassic Kayenta Formation (Jku) represent element 3 – a system of backthrusts with a sense of west directed tectonic transport. However, the nascent Kanarra triangle zone was

abandoned early in its development due to the geometry of the Kanarra thrust maintaining a steep ramp rather than connecting to a “flat” floor thrust up-section. This geometry preserved the overturned limb of the fault propagation fold and inhibited the development of a significant duplex structure. The lack of a duplex structure prevented advancement of the tectonic wedge beneath the back-thrust(s) and the formation of a roof-thrust. In addition, growth of the steeply dipping overturned forelimb of the Kanarra fold resulted in folding and rotation of the early formed backthrusts (the Taylor Creek thrust system) into an orientation favorable for extending the Kanarra thrust ramp through merging of these two fault systems. This crucial process of extending the ramp of the Kanarra thrust fault lead to the abandonment of the Kanarra triangle zone as this thrust fault continued to cut-up section through the Jurassic Navajo Sandstone (Jn). This suggests triangle zones are less likely to fully develop in association with fault-propagation folds in comparison to fault bend folds.

APPENDIX A.

ROCK DESCRIPTIONS

Stratigraphy and Rock Descriptions

The overall thickness of the exposed section is approximately 1.8 km thick and comprises units of Permian to Early Jurassic age (Biek and Hayden, 2013). There is some minor stratigraphic thickness variation in several of the incompetent mudstone units (Averitt, 1962). The transition from Triassic to Jurassic constitutes a major change in general depositional environment from shallow marine limestones to continental clastics and evaporites. Major unconformities occur between the Permian and Triassic (Hintze, 1988), the Early to Late Triassic, and the Late Triassic to Early Jurassic (Hintze, 2005). Permian units that do not outcrop in the field area but are in the cross section include the Pakoon Dolomite (PPk, approximate thickness 214 m), the Queantoweap Sandstone (Pq, approximate thickness 405 m), and the Toroweap Formation (Pt, approximate thickness 146 m) (Hintze, 1988). Descriptions of exposed units are from Biek and Hayden (2013) (Figure 3.1) and field notes.

The Permian Kaibab Limestone is split into the Fossil Mountain Member (Pkf) and Harrisburg Member (Pkh). The Fossil Mountain Member (Pkf) is a ledge former distinguished by bands of black chert, large chert nodules, and abundant large crinoids near the base of the exposure in the field. Approximate thickness of this unit is greater than 60 m. The Harrisburg Member (Pkh) is a difficult to differentiate, slope forming unit on top of tall cliffs of the lower unit.

The several lithologically distinct units of the Triassic Moenkopi Formation exhibit a repetitive distribution of carbonates and siliciclastic/evaporitic red beds. Exposures of the limestone Timpoweap Member (TRmt) are often weathered yellow. Some beds unmistakably contain abundant brachiopods and gastropods, and thin, fine-

grained yellow beds are interbedded with massive, thick beds of cherty limestone. Gastropods are a distinguishing fossil.

The Lower Red Member (TRml) is an incompetent red mudstone that contains small amounts of gypsum and is approximately 75 m thick, easily mistakable for other similar units in repeated sections.

Often consisting of thin fins of limestone, the Virgin Limestone Member (TRmv) has a distinct gray color and the presence of small, circular and star shaped crinoids help distinguish it from Timpoweap Limestone, which contains no crinoids. It is approximately 45-60 m thick.

The double gypsum layers of the Middle Red Member (TRmm) that occur right after the Virgin Limestone Member (TRmv) were a useful visual check in the field against the other red mudstone units. The upper contact with the Shnabkaib Member (TRms) is gradational and often chosen by the next thick gypsum layer. Approximate thickness is 120 to 150 m.

Thick gypsum layers alternating with red mudstone give the Shnabkaib Member (TRms) a characteristic “bacon striped” appearance that is unmistakable, though the lower boundary is difficult to place. In the field, these gypsum layers were extensively folded. Approximate thickness is 120 to 150 m.

The Upper Red Member (TRmu) is characterized by dark red siltstone interbedded with thin to thick sand bodies. Presence of gypsum stringers was used in the field helped to distinguish this unit from the Moenave Formation (JTRm) in highly disturbed sections. Crossbedding is present in the sandstone layers. Approximate thickness is 60-75 m.

The Shinarump Conglomerate Member (TRcs) of the Triassic Chinle Formation is a yellowish to white coarse sandstone and pebbly conglomerate with abundant cross beds, containing petrified wood in some locations. Approximate thickness is 30-60 m.

Gray-green to purple, the incompetent Upper Chinle typically presents with mass wasting, badland topography, and abundant mud cracks. A thin purplish-white sandstone unit is common throughout the field area near the lower contact. Approximate thickness is 90-120 m.

The Jurassic Moenave Formation (JTRm) consists of deep red to orange red interbedded siltstone and white sandstone layers that are sometimes stained red. The colored layers often exhibit green to white reduction spots. Approximate thickness is 90-150 m.

The Springdale Member (Jks) of the Kayenta Formation (Jku) is a purplish, thick bedded sandstone with abundant cross-bedding and was often found with interspersed, small white grains. Approximate thickness is 30-45 m.

The Upper Kayenta Formation (Jku) consists of red mudstone and siltstone with some sandstone beds. Approximate thickness is 240 m.

Towering orange-red cliffs and huge cross-beds typify the Navajo Sandstone (Jn). Locally heavily fractured with slickensides and deformation bands. Approximate thickness is 550-600 m.

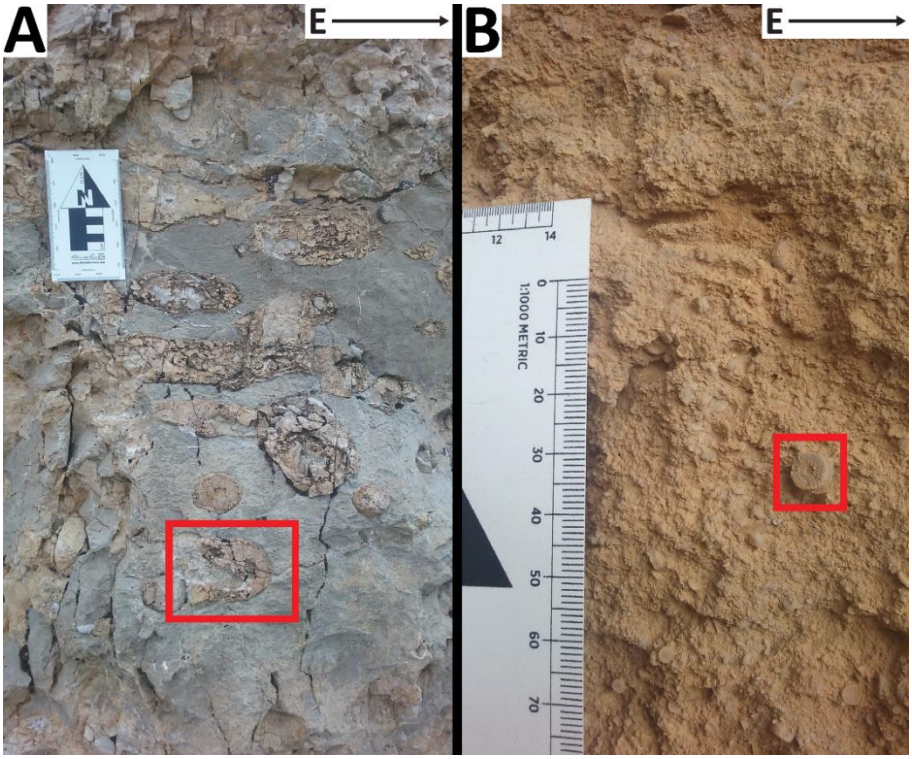

Figure A.1. Chert nodules and crinoids. These fossils are helpful in distinguishing the Permian Kaibab Formation (Pkf, Pkh).

Figure A.2. Field example of the Triassic Moenkopi Formation near Kanarraville.

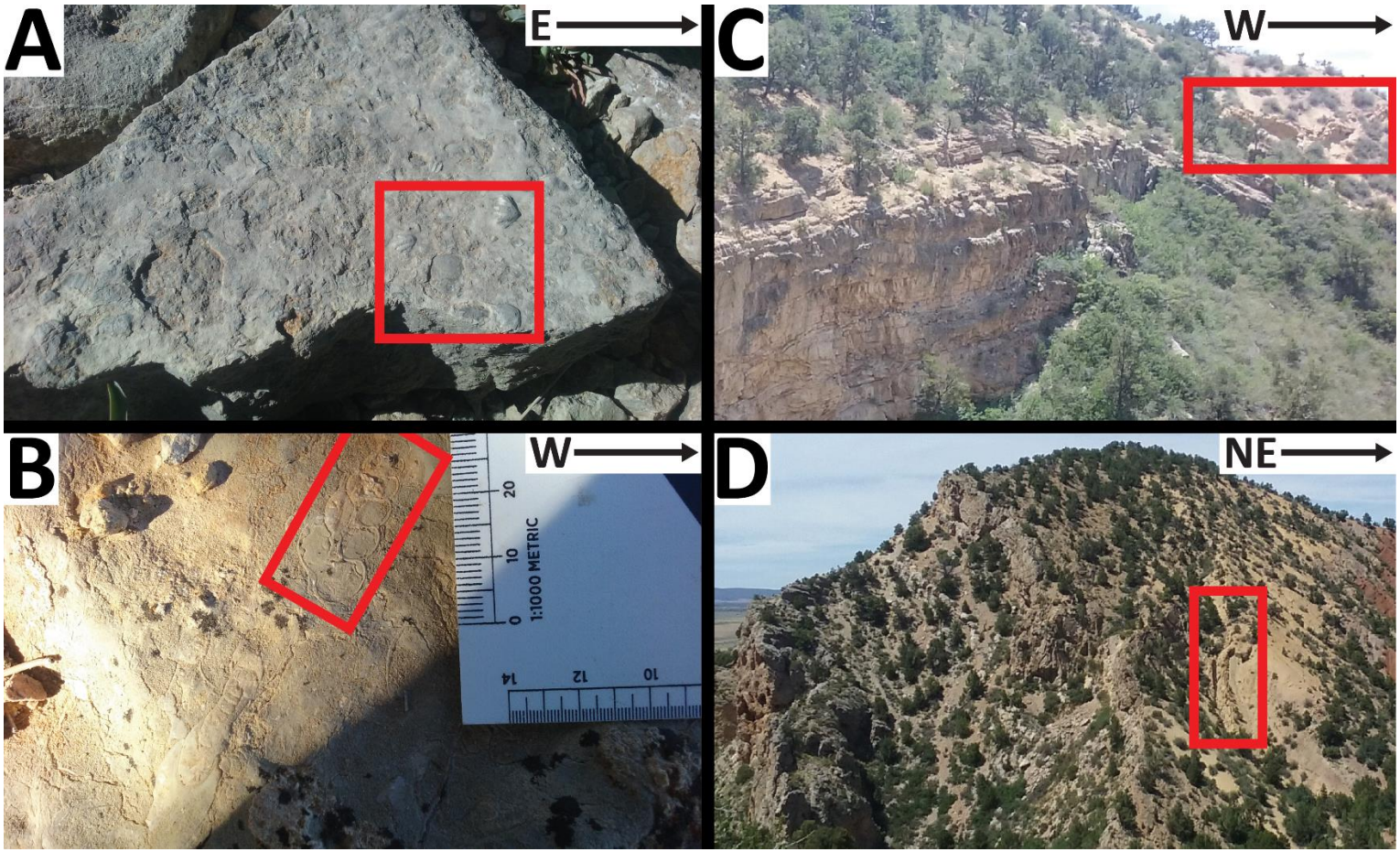

Figure A.3. Distinguishing features of the Triassic Timpoweap Member. A) Brachiopod fossils which are present in the Timpoweap Member. Few of these were found in the Kaibab or Virgin Limestone, though the literature states they are present. B) This blob-like line is actually a high-spired gastropod, diagnostic fossil of the Timpoweap Member (TRmt) (no other limestone units in the Triassic Moenkopi Formation have been found to contain gastropods). C, D) Thin, fissile, yellow beds typical of the Timpoweap Member, which appear to readily deform due to high competence contrast.

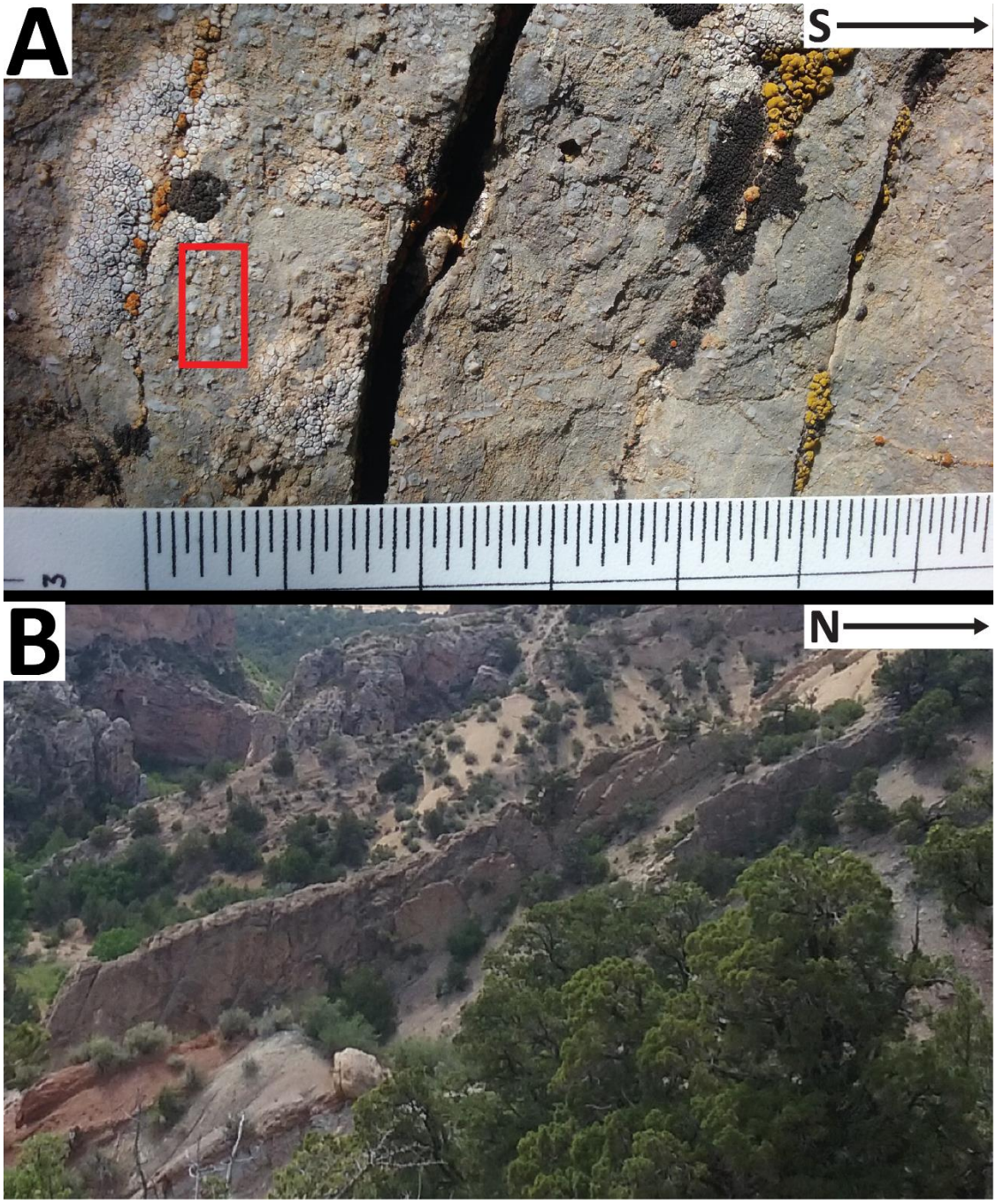

Figure A.4. Distinguishing features of the Virgin Limestone Member (TRmv). A) Patch of small, circular and five-sided crinoids in gray Virgin Limestone Member (TRmv). Ruler scale in cm. B) Center: outcrop of thin fins of Virgin Limestone Member (TRmv) (here overturned west). Note small patch of red mudstone before the first Shnabkaib gypsum layer, indicating the Triassic Middle Red Member (TRmm) has been cut out by faulting.

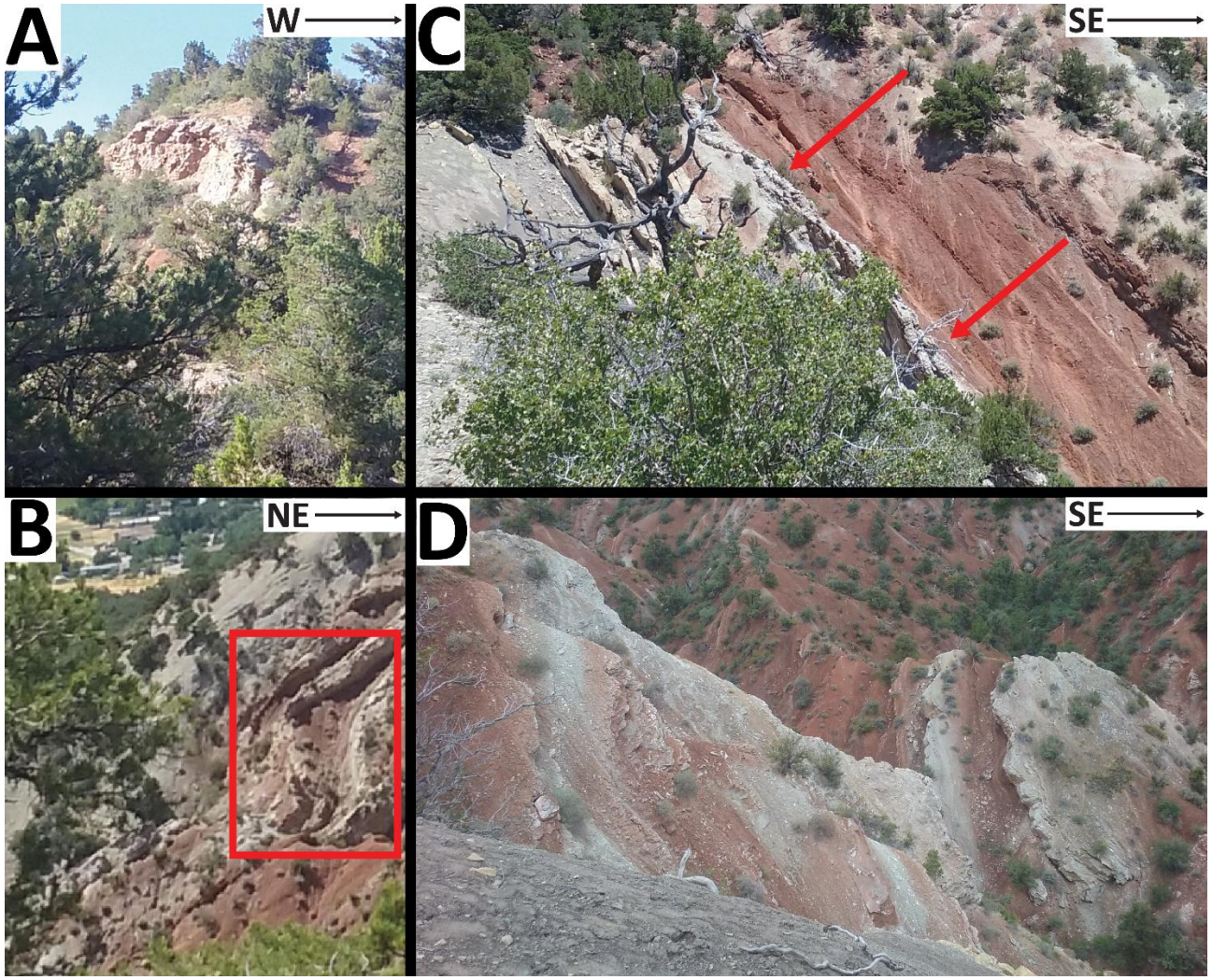

Figure A.5. Examples of thick, double-layered gypsum at the base of the Middle Red Member (TRmm). The same double layer is depicted from different viewpoints in B (inside the square) and D. Arrows point to first gypsum layer in C.

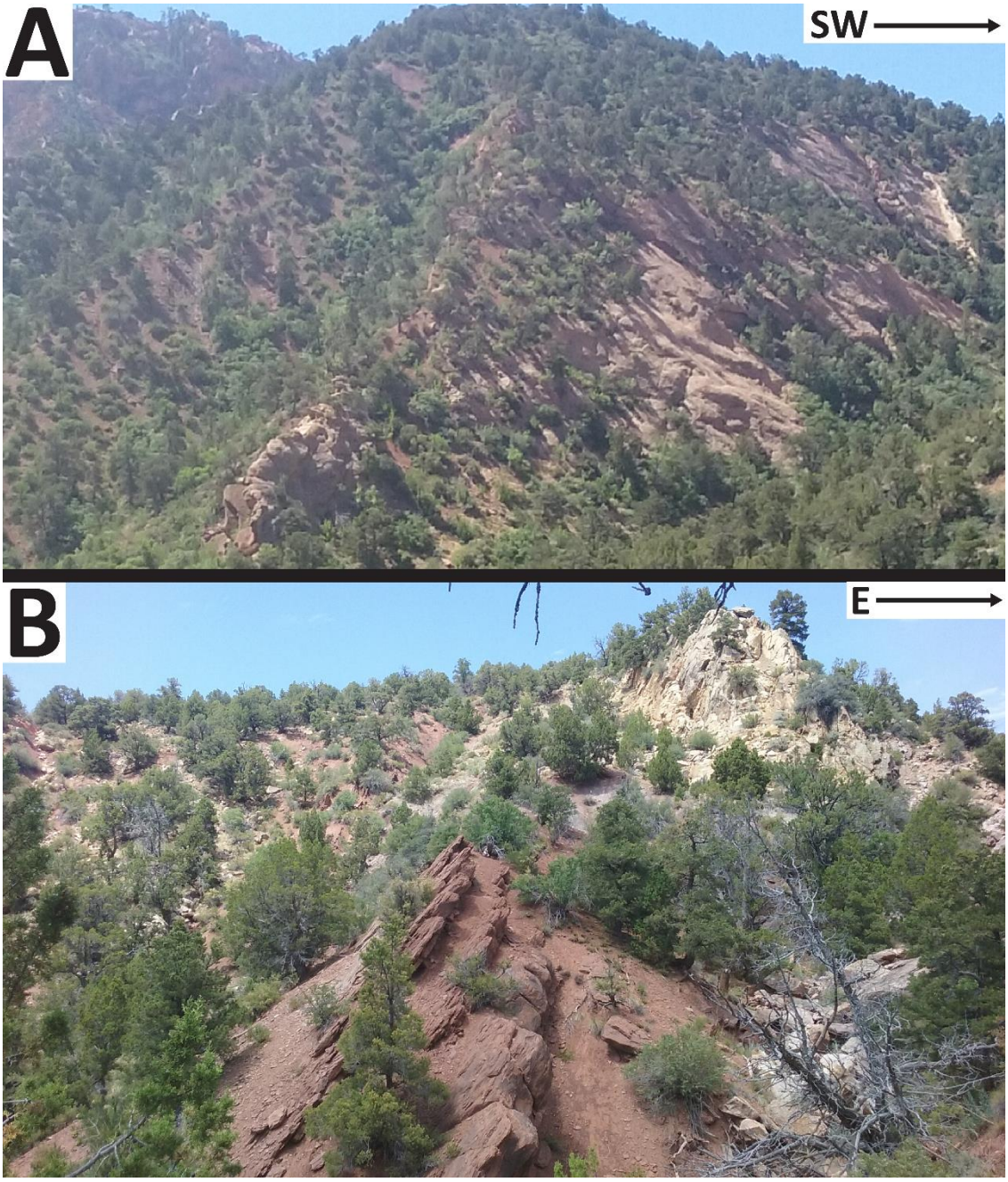

Figure A.6. Upper Red Member (TRmu) with dark red interbedded siltstone and sandstone. Softer layers form strike valleys (A) and sand bodies not continuous over large distances.

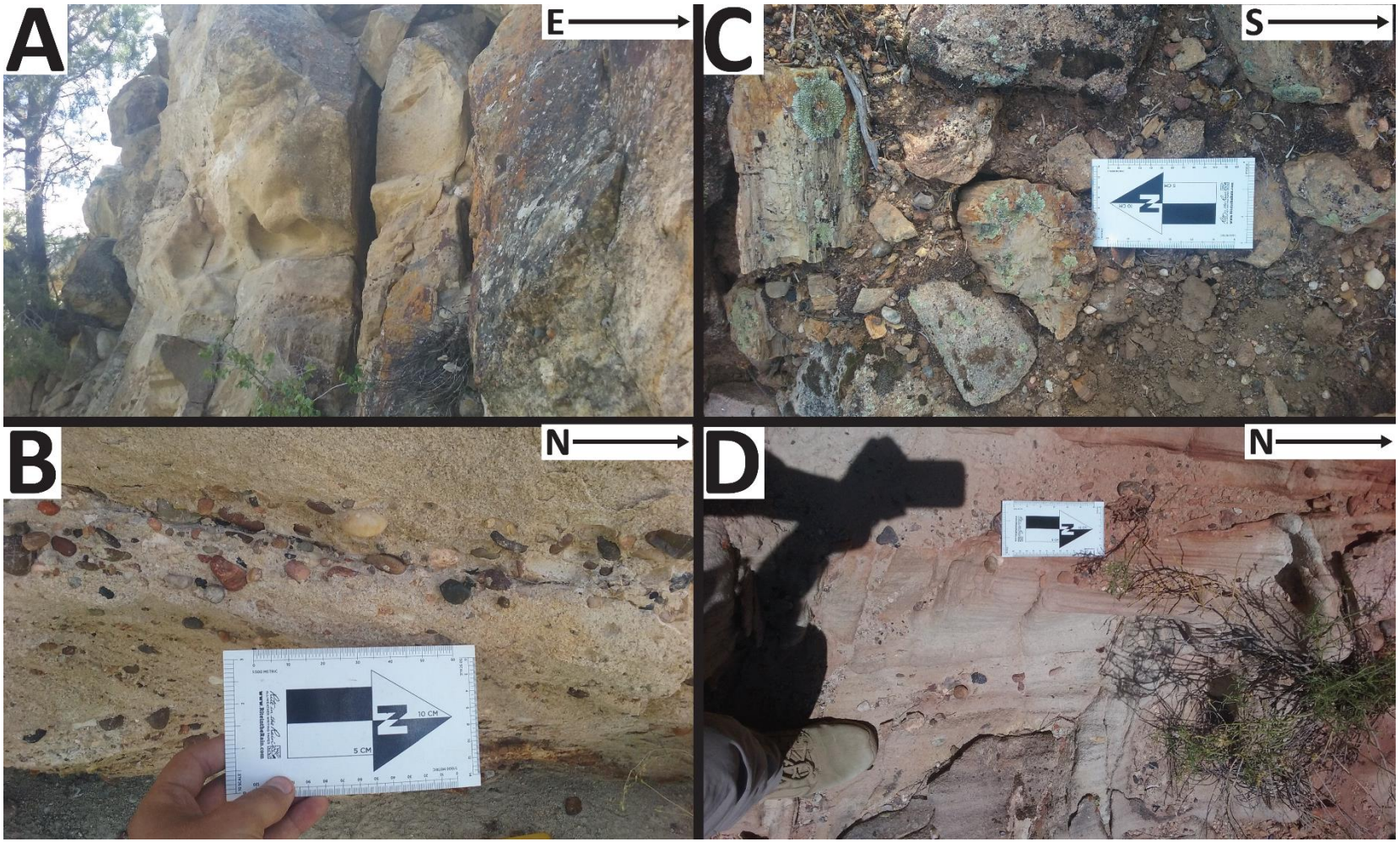

Figure A.7. Characteristics of the Shinarump Conglomerate Member (TRcs). Thick, yellow sandstone bed with thin basal conglomerate layer. B) Conglomerate layer at a different field location - note multicolored pebbles. C) Petrified wood in the Shinarump Member. D) Cross bedding in a west-dipping outcrop displaying top to east (overturned).

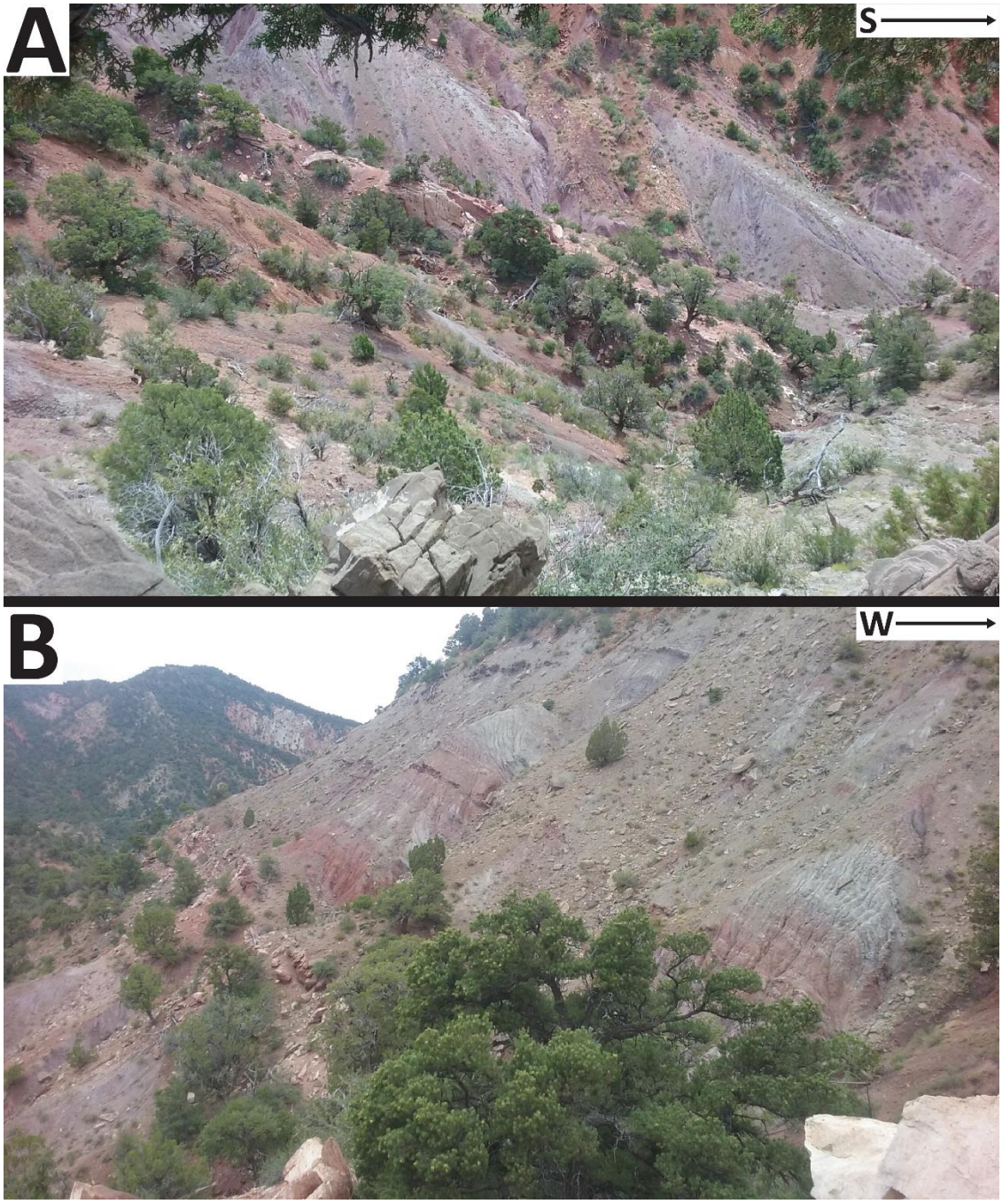

Figure A.8. Examples of the Petrified Forest Member (TRcu). Note the gray-green to purple color, badland topography, and mass wasting.

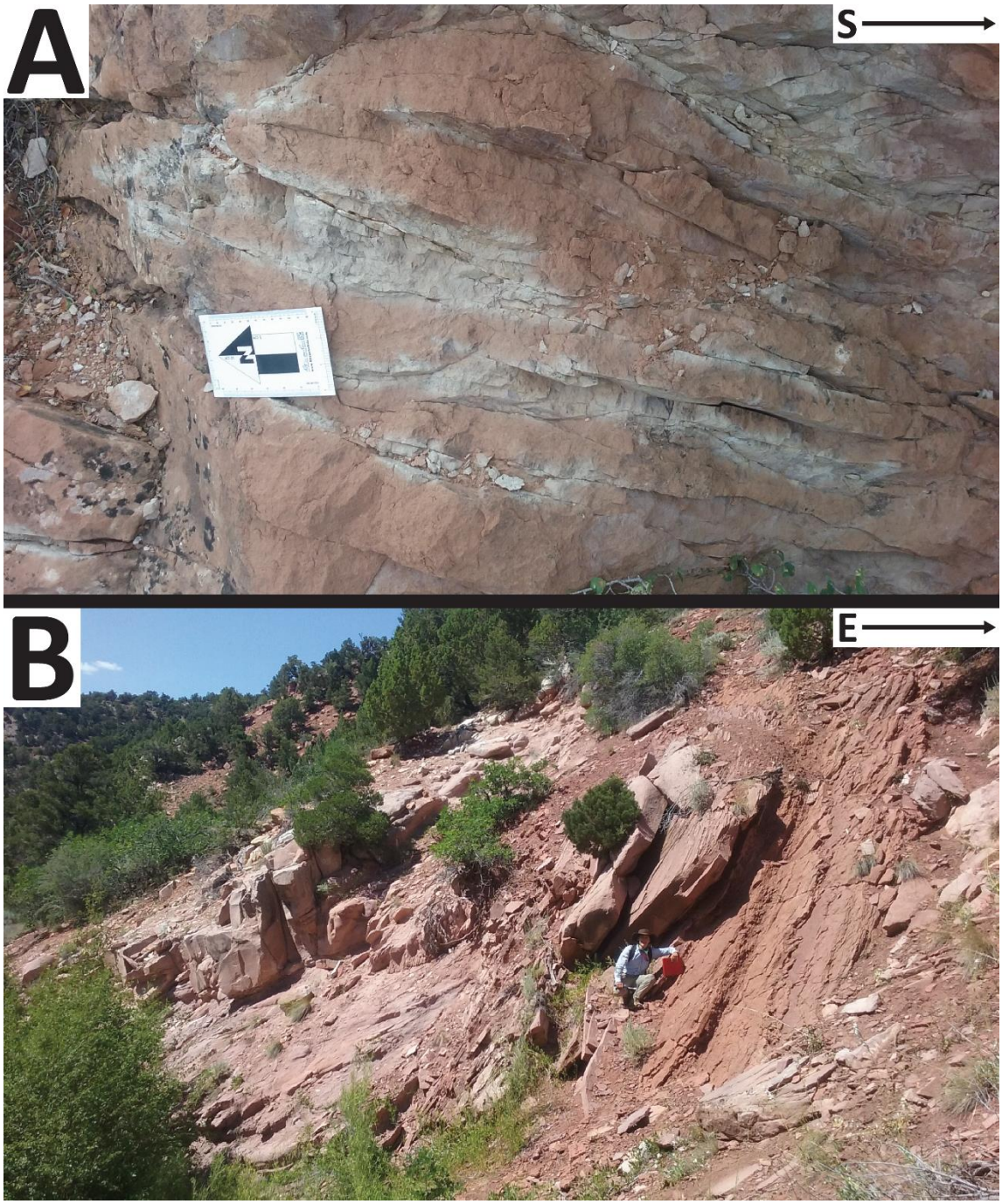

Figure A.9. Examples of the Jurassic Dinosaur Canyon Member (JTRm). A) Outcrop example of red sandstone bleached white in some spots. B) Fine-grained orange-red outcropping on top of Jurassic Springdale Member (Jks).

Figure A.10. Cross-beds in the Jurassic Springdale Member (Jks). A) Large cross beds in a west-dipping outcrop of the Springdale Member (Jks) showing top to east (overturned). Close inspection shows small white sand grains interspersed throughout a purple-colored sandstone.

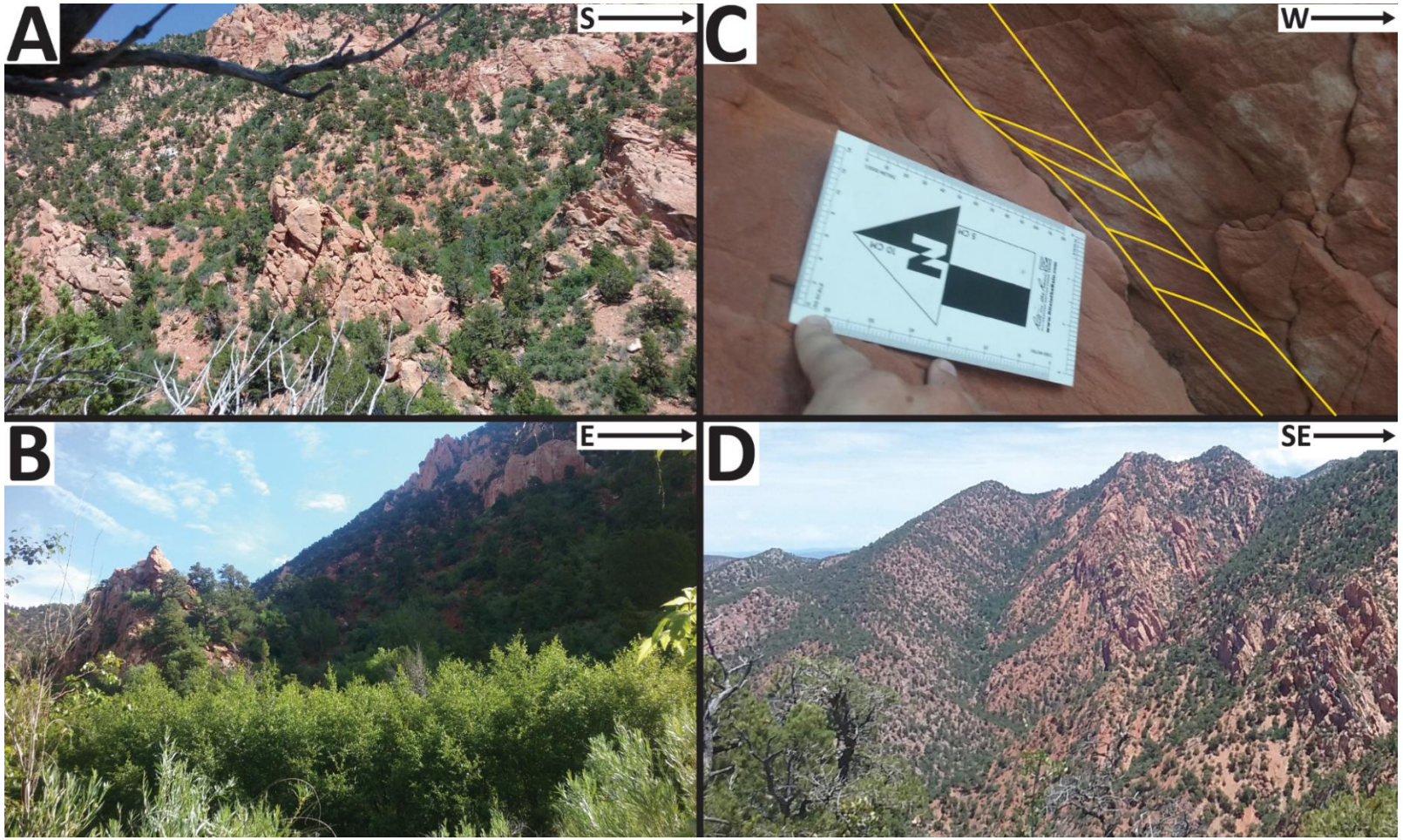

Figure A.11. Jurassic Kayenta Formation (Jku). A, B) West-dipping triangular fins of sandstone surrounded by red mudstone in the Kayenta Formation (Jku). C) Tiny crossbeds in one fin with top to east (overturned). Note also the scouring on top surface. D) Strike valley in the red, finegrained Kayenta Formation (Jku). Note attitude of the Navajo Sandstone (Jn) to the east (approaching vertical to overturned).

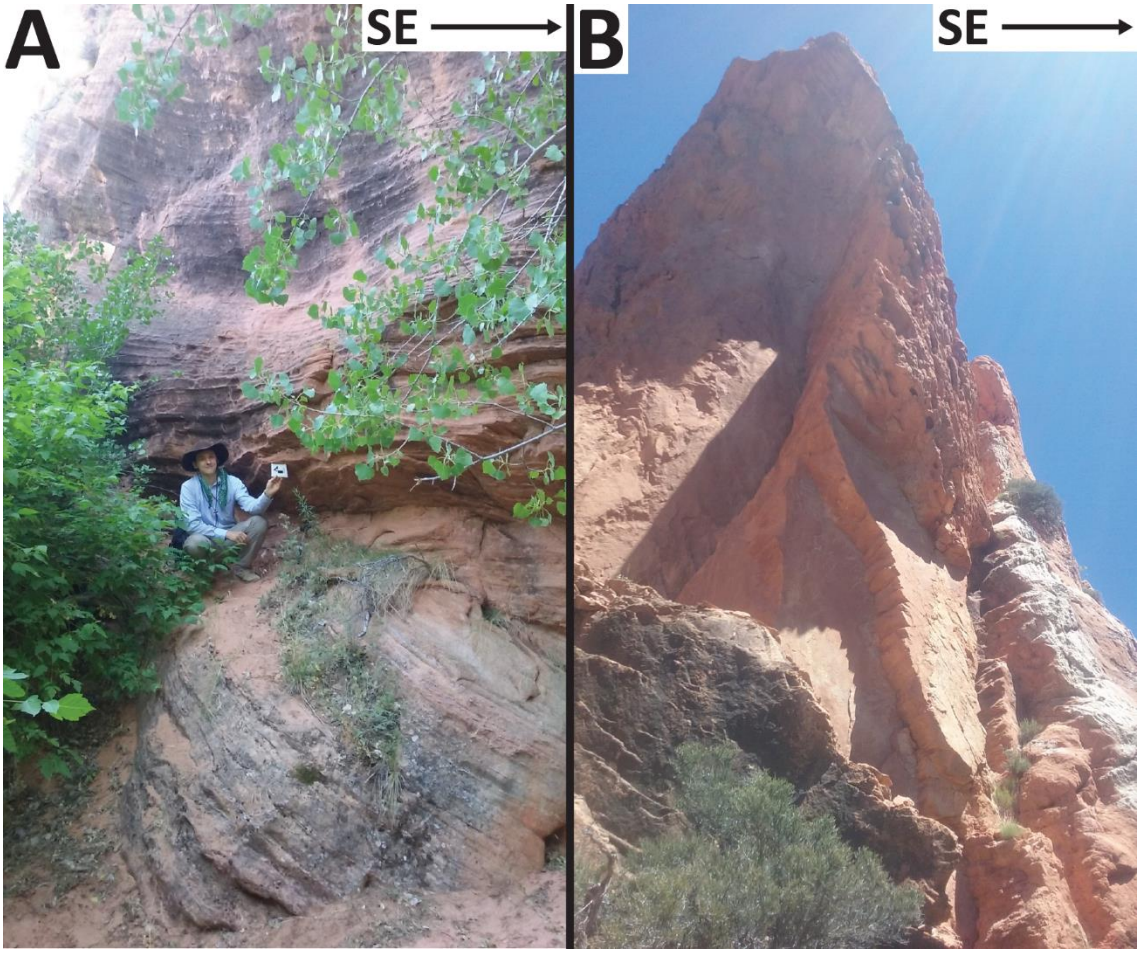

Figure A.12. Jurassic Navajo Sandstone (Jn). A) Giant cross beds in the Jurassic Navajo Sandstone (Jn) - author for scale. Note cross-cutting relationships between the cross-bed sets show the top is up. B) Towering, fractured cliff of Jurassic Navajo Sandstone (Jn).

APPENDIX B.

FIELD WORK OPPORTUNITIES SUMMER 2017

Future Work

This study demonstrates the feasibility and necessity of more field work in the area to constrain the processes involved in the development of the Kanarra fold. It is a structurally important area in the context of triangle zone evolution, but receives little attention as such. Future work will focus on refining the observations and data from this study in order to build multiple balanced cross-sections to integrate into a restorable 3D model of the area with 3DMove™. This model will yield insight into the processes that occurred during folding. Steps toward achieving this end goal will include refining the map pattern and data acquisition pattern with a predetermined plan for success.

Priorities for future field work:

1) Walk out contacts: Important contacts (especially competent unit boundaries and faults) need to be more carefully constrained by walking them out where possible. This will involve using GPS to pinpoint contact boundaries at certain intervals. A good interval to balance speed and precision might be every 200 m.
2) Constrain contact orientations: Dips along competent contacts need to be sampled more frequently and as close to the contact as possible. This can be accomplished by using a smartphone app like FieldMove Clino™ to quickly and accurately measure orientations, simultaneously plotting them on the map. This would eliminate a step and increase efficiency. The compass can be used as a check against odd values. This point can be accomplished simultaneously with (1).
3) Check for evidence of fault planes: This follows (2). If chattermarks and slickensides (potential kinematic indicators) show up on float in a certain unit, a fault needs to be confirmed. Float and in-place chattermarks and slickensides need

to be visually documented. In-place fault planes and kinematic indicators must also be measured. Multiple samples of the orientations of in-place kinematic indicators will be necessary to confirm whether they are from flexural slip or faulting. Several thrusts in the incompetent Petrified Forest Member (TRcu) have been mapped to the south. Also, mappable faults could show up in the gypsum layers of units like the Shnabkaib Member (TRms). The badland topography of these units may need to be endured to search for these potential faults and lower the uncertainty in problem areas.

4) Carefully identify and record important visual data: More sketches could be made of important structural relationships, especially slickensides or truncations of layers. Most importantly, photos taken cannot be frivolous or too general, especially if it means missing the important details at stops. Some photos from last summer left out details at important. The more photos of important structural relationships the better.
5) Avoid scarps: In the case of very steeply inclined strata, the scarp was actually easier and safer to climb (e.g., Springdale, which was smooth on the dip slope). Climbing scarps in general was a waste of time and energy that happened when mapping at least one other unit, the southern Shinarump ridge. Focus on getting to the dip slope; climb down to measure if necessary.

Target areas in the next field season:

1) Spring Creek - duplex hill in the Moenave Formation (JTRm): Not enough time was spent here to constrain fault planes, kinematic indicators, and attitudes. One or even two whole days could be spent on this hill alone, maybe split with the Shinarump hogback to the west.
2) Spring Creek - southern Shinarump hogback, Upper Red, and Shnabkaib: This area was underexplored and it could be beneficial to gather more data here. Shinarump becomes upright uphill and to the south and the transition should be more closely measured. Also, there are multiple slickenside planes that could be targeted. The Upper Red Member (TRmu) has sandstone bodies that were largely ignored and it would be beneficial to revisit, document, and measure these. There may be a surprise in this unit missed last summer, especially along the cross-section line. The southern Shnabkaib saddle was not reached last summer and may be helpful to explore, especially since the main fault has been interpreted as blindly deforming this unit. If it is there, it could exposed and emergent.
3) Spring Creek - Harrisburg Member (Pkh) contacts: The contacts for this unit may be easier to locate than it appeared, and it could help to constrain the cross-section to locate these contacts more precisely. The slope where this unit is thought to be was very steep, but with more experience in this terrain it may be possible to safely navigate along it. This is lower priority because even the published map dashes out this contact, it could be a time sink, and there are safety issues associated with this target.

4) Spring Creek-Red Rock Trail Transition - Middle Red, Virgin, Shnabkaib, Upper Red, and Shinarump: The badland topography here was a barrier to exploration. First priority will be visiting the Virgin Limestone Member (TRmv) to walk out the contact where it truncates, then walk up the dip slope to the saddle with Middle Red and attempt to identify the contacts. Another priority will be the search for faults and documenting the folding in the gypsum layers.
5) Red Rock Trail - Upper Red Member (TRmu)**:** This unit is important in discerning Area 4 and adding to contact orientation data.
6) Red Rock Trail - Springdale Member (Jks): This unit needs to be checked for fault surfaces, duplication, and contact-checked north to south. Especially important is the transition to the Upper Kayenta Formation (Jku), where Kanarra Creek forks, close to the fold outcrop (Stop 19-6).
7) Red Rock Trail - Timpoweap Member: A lot of time was spent in this area last summer, and it may be good to revisit to further refine the map pattern. There is a good deal of uncertainty here that could be cleared up with more time spent. The biggest target will be finding a tear fault plane or transfer zone that could explain the offset and discordance in dip with the rest of the unit to the south.
8) Kanarra Creek - Murie Creek: Further constrain contacts to the north and extend the map northwards. Map to Murie Creek (additional ~2 km^2). Spending time on the northern Timpoweap Member (TRmt)exposure in Kanarra Creek will be helpful, especially in confirming the Harrisburg Member (Pkh) contacts. The fault that duplicates Shinarump will be especially important to document in more detail, including finding the fault surfaces and measuring kinematic indicators.

APPENDIX C.

CROSS-SECTION CONSTRUCTION

Cross-section Construction

The cross-section evolved from 32 different attempts. Important assumptions related to the field area include the presence of certain structures and thickening mechanisms:

1) The Hurricane fault borders the system to the west and approximates the Kanarra fold axis (Averitt, 1962; Biek, 2007).
2) Thrust faults and backthrusts are a common and known structure in the area
3) The primary thickening mechanism in competent units (especially in the limestones) is backthrusting.
4) The primary thickening mechanism in the mudstone units is folding of gypsum layers.
5) The Kanarra fold is a fault propagation fold (Biek, 2007; Fielding, 1994; Grant et al., 1994).
6) The steep limb of the fault propagation fold is expected to experience some thickening (Jamison, 1987; Mitra, 1990; Suppe and Medwedeff, 1990).
7) Wherever possible, constant thickness is assumed.

These assumptions have allowed the construction of what the author believes is an admissible, unbalanced cross-section (Elliott, 1983). More field data is required to constrain the structure and produce balanced cross-sections throughout the field area. Example cross-sections showing various stages of interpretation are below.

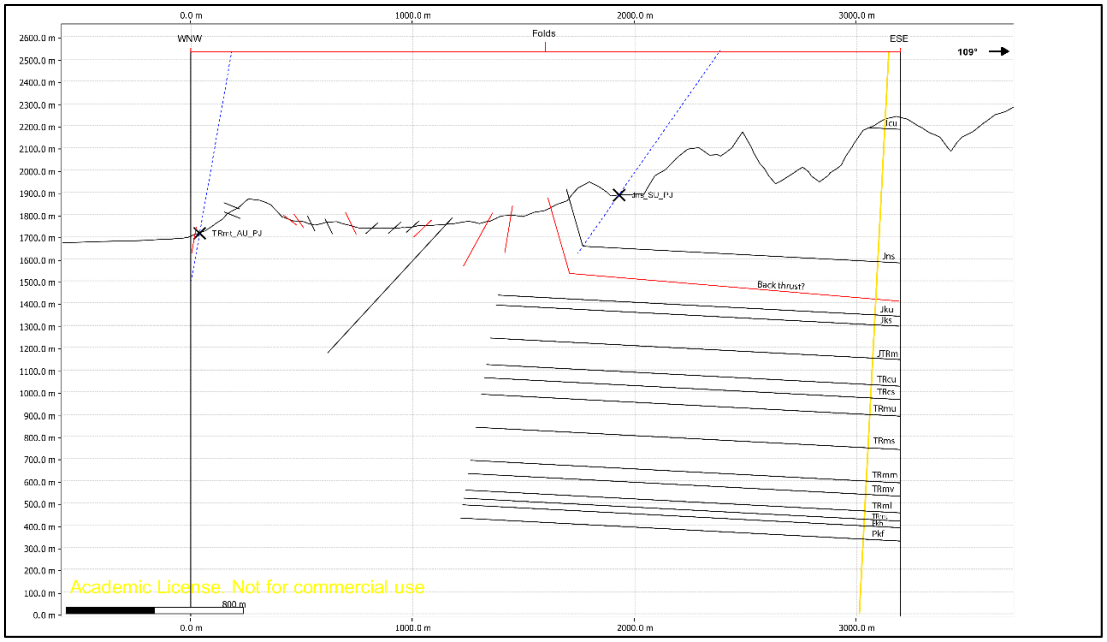

Figure C.1. Initial input of contacts. The layercake geology beneath the Carmel Formation was projected down, using known thicknesses from Biek and Hayden (2013).

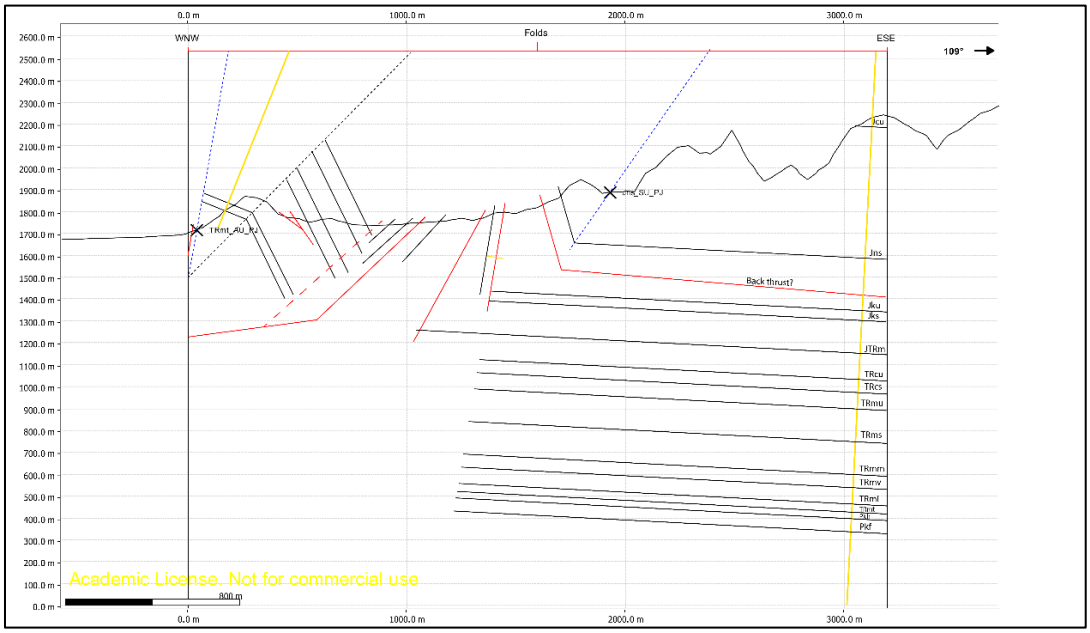

Figure C.2. Initial problems with projecting units down. This occurred due to discordance between upright and overturned attitudes. Fault inferred from map pattern north of Spring Creek and discordance of dips. This figure reflects the first attempt to project Timpoweap (TRmt) overthrusting north of Spring Creek into the section.

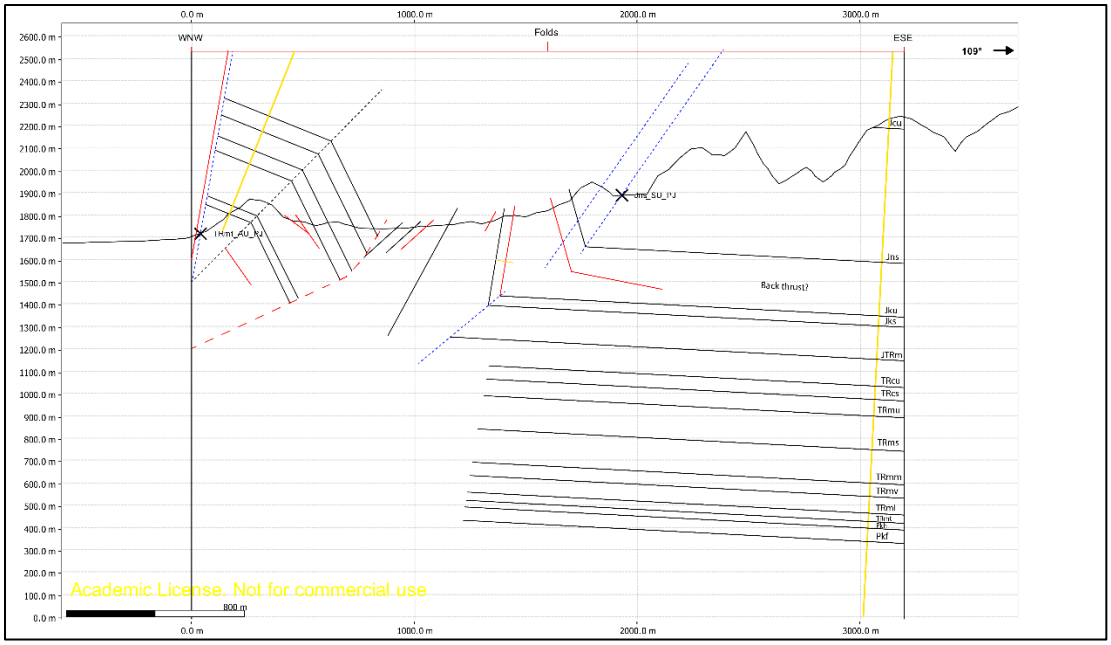

Figure C.3. Map pattern projection and fault placement. Projection of map pattern with Virgin Limestone Member (TRmv) overthrusting north of Spring Creek into the section. Fault Main fault placed in the Shnabkaib Member (TRms), before the overturned units, to account for discordance in dips between the Virgin Limestone Member (TRmv) and the Shnabkaib Member (TRms).

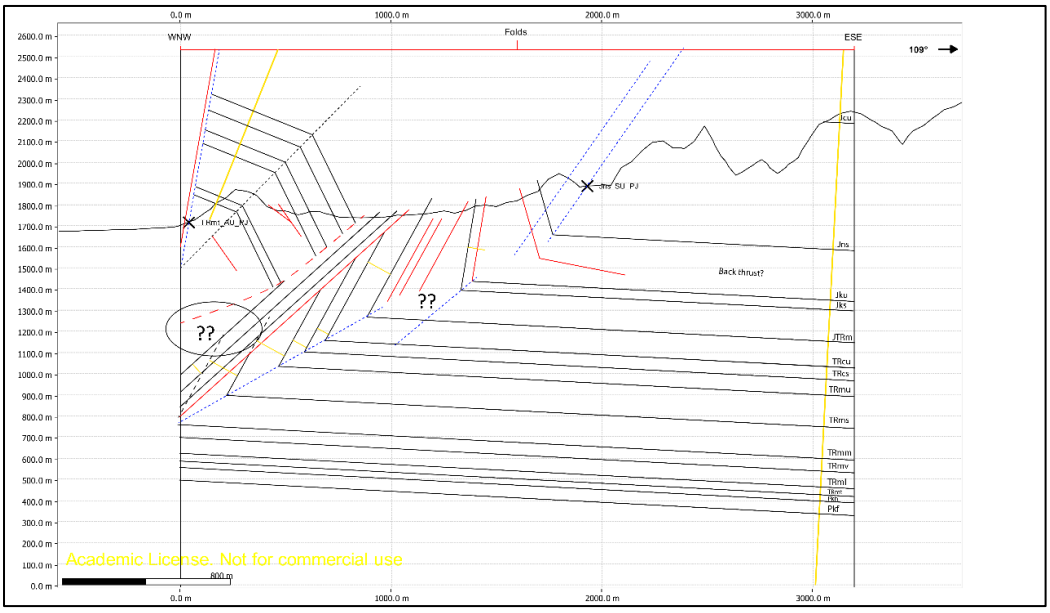

Figure C.4. Space and faulting problems. Maintaining constant thickness and constant dip (the cause of the angular appearance, e.g., Suppe and Medwedeff, 1990).

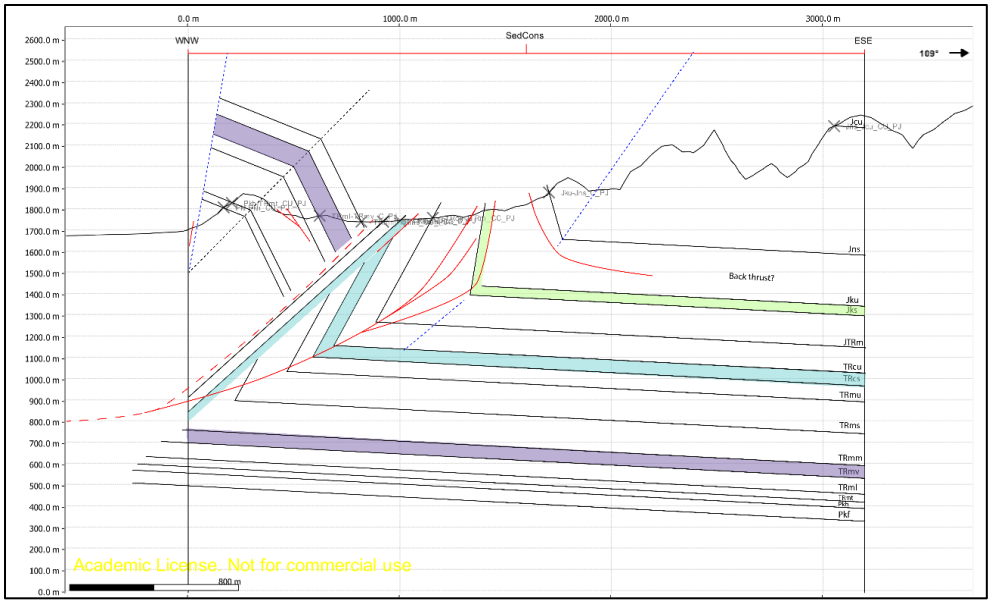

Figure C.5. First iteration with curvature. Note the attempt to place the main fault further west, as part of an imbricate fan in the Moenave Formation (JTRm) - this was deemed unlikely based on surface control

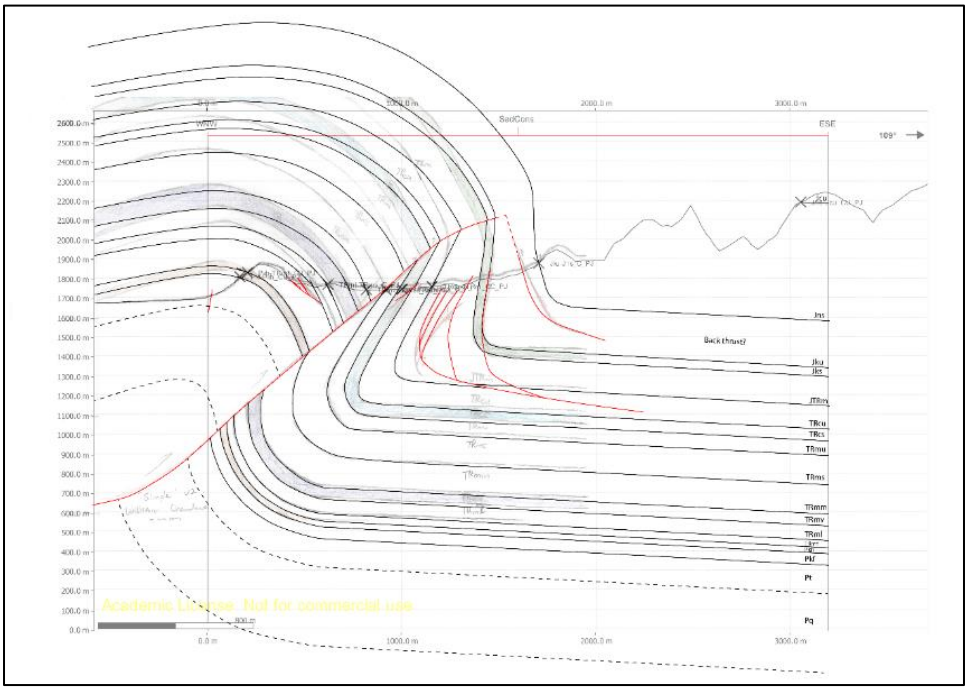

Figure C.6. Discarding constant dip assumption. Matching contacts and faults to hand-drawn, curved cross-section. In the future, can be transferred to Move and restored to check for validity (e.g., Bekkers, 2011; Schootstra, 2012).

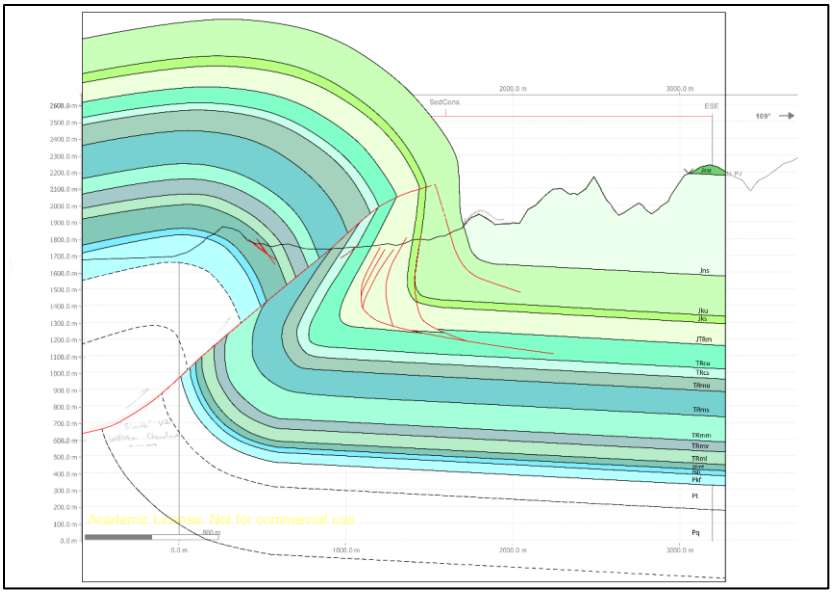

Figure C.7. Main fault cutting through the Triassic Shinarump Conglomerate Member (TRcs). Revisit of similar, previous idea (Figure C.5). To explain offset caused by the Triassic Shnabkaib Member (TRms) and the Triassic Upper Red Member (TRmu) being overthickened, an attempt is made to connect the backthrust and main thrust without folding. This is thought to be a less likely interpretation.

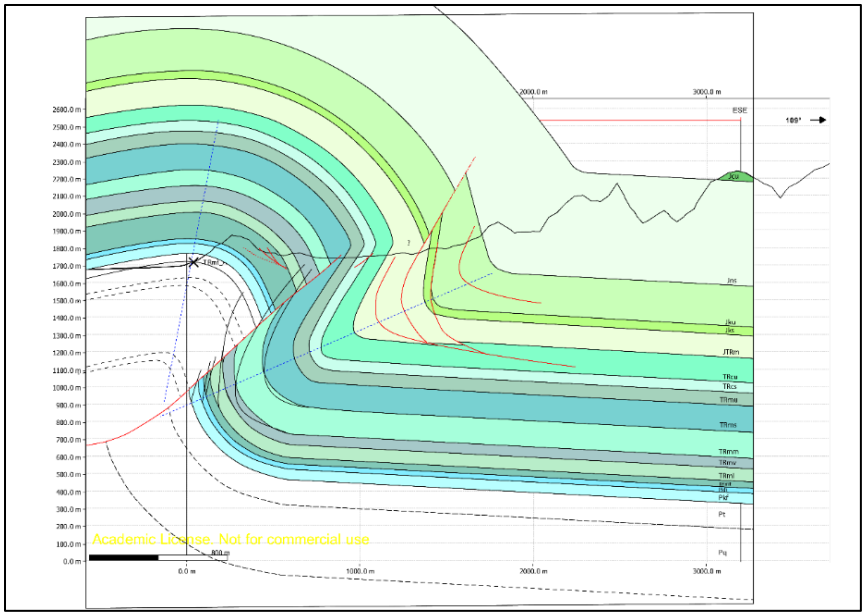

Figure C.8. Projection of Taylor Creek backthrust system upwards. Apparent normal sense is due to overturning of the backthrust. Fewer faults are interpreted to be required to produce the overthickening in the Moenave.

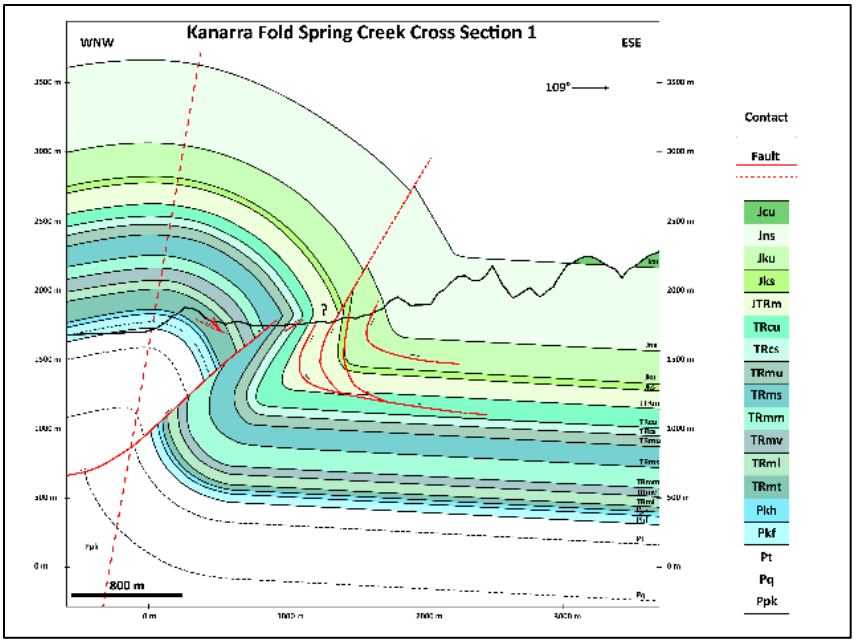

Figure C.9. Refinement of the Cross-section C.8. Part of the Taylor Creek backthrust system is projected up further, through the Jurassic Navajo Sandstone (Jn), reflecting what appears to happen further north along the Red Rock Trail (Traverse 2, Appendix D).

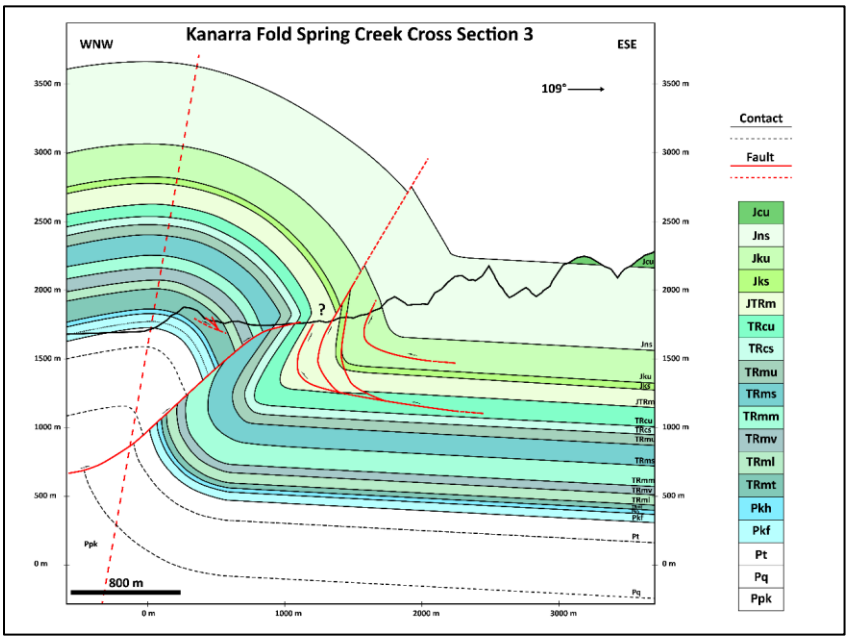

Figure C.10. Attempt to place a flat in the fault. This is to account for faulting of the Shinarump Conglomerate Member (TRcs). The ideas was discarded because no detachment for the flat can be explained.

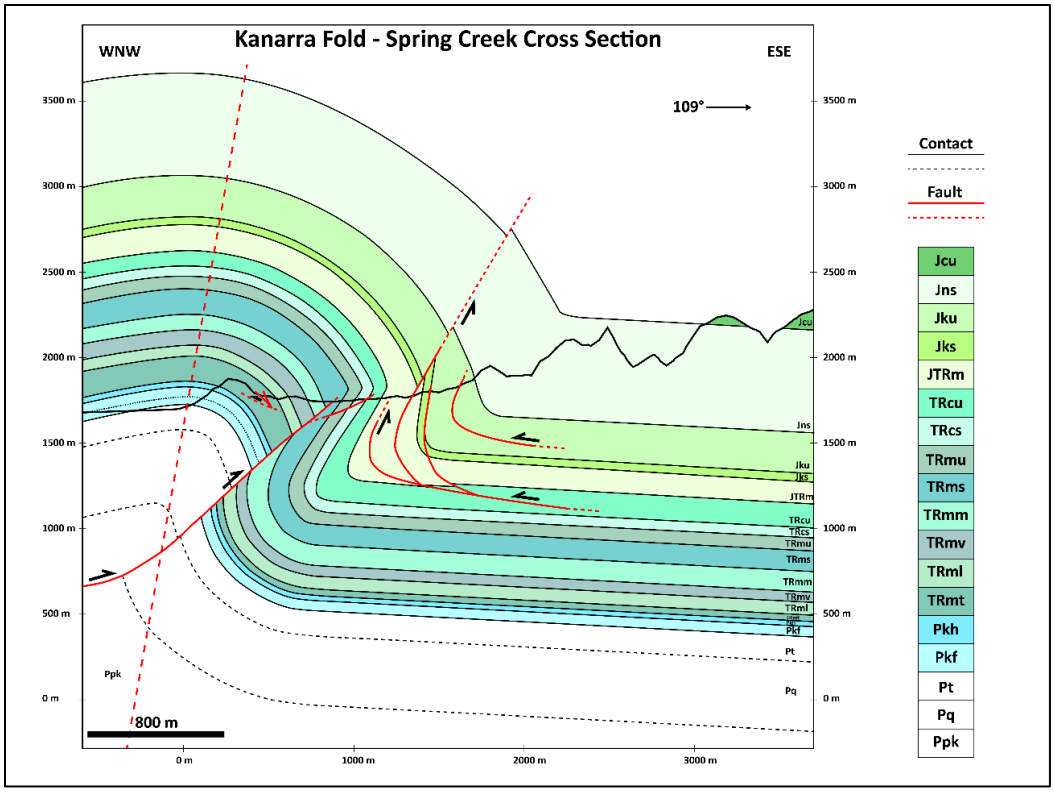

Figure C.11. Final cross-section. The Middle Red and Shnabkaib Member (TRms)s were thinned in the footwall to the minimum thickness reported by Biek and Hayden (2013) to account for the thickness change of the units across the fault from contacts placed in the field.

APPENDIX D.

FIELD STOPS AND DATA ACQUIRED

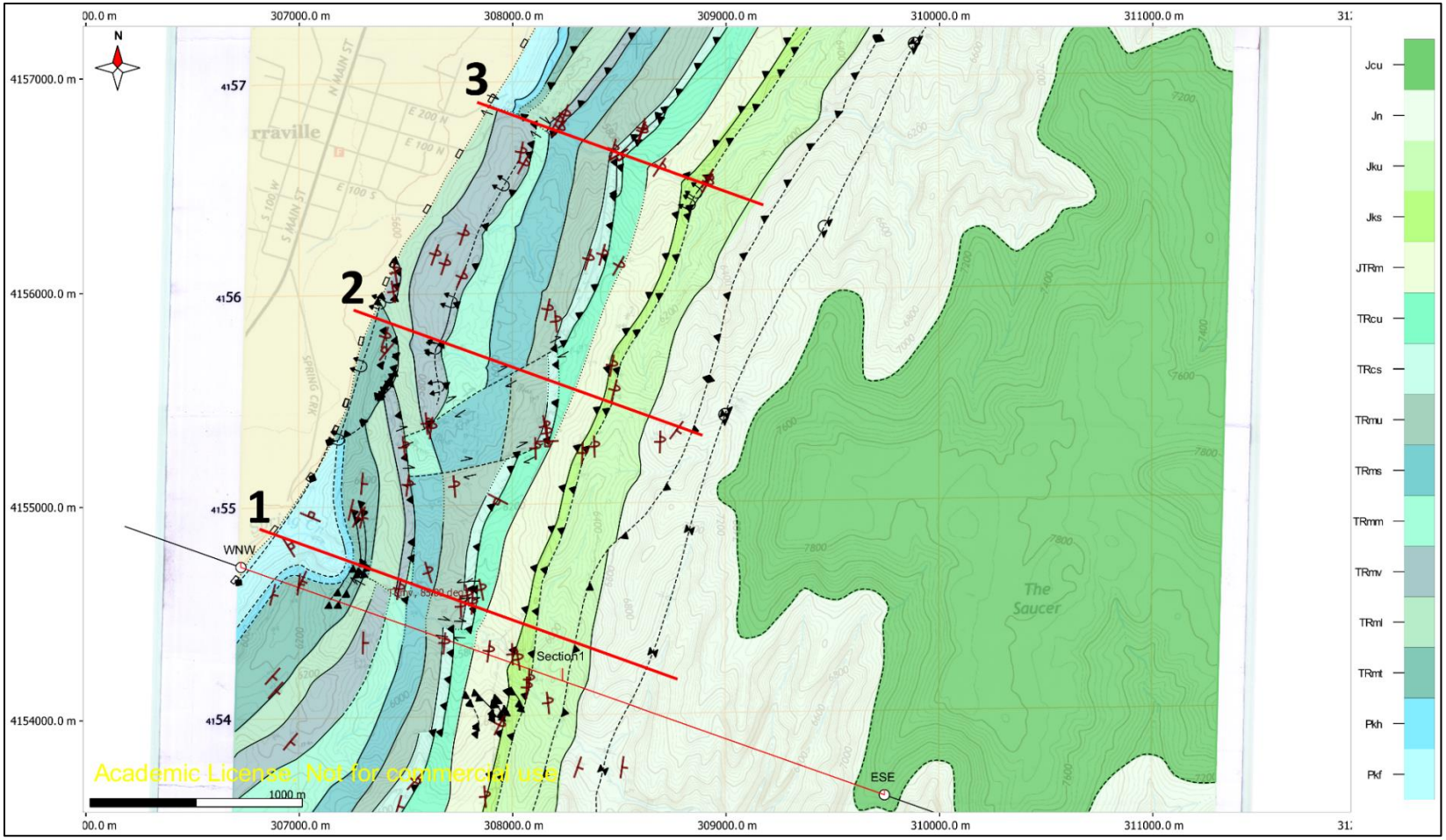

Figure D.1. Field mapping traverses. Traverse 1 runs through Spring Creek; Traverse 2 cuts across the Red Rock Trail; Traverse 3 runs through Kanarra Creek.

Domain I Field Stops

Stop 1. The first units encountered along Traverse 1 (Figure D.1) are towering cliffs of Permian Kaibab and Triassic Timpoweap Limestone. Both limestones are intensely folded and faulted. In Spring Creek, faulting in these units is dominantly towards the hinterland (backthrusts). A series of folds along a backthrust fault plane can be observed in the Kaibab at the base of the cliffs, looking to the south (Figure 3.5).

Stop 2. The Timpoweap Member (TRmt)in Spring Creek contains two major backthrusts that have left behind massive, isolated, folded ridges (Figure D.2). These ridges are highly fractured, and bedding is nearly unrecognizable. A fold on the western ridge verges west (Figure D.3).

Figure D.2. Isolated ridges of TRmt. A) Looking south, note folding of eastern ridge. B) Break and apparent upward offset on ridge of TRmt, looking north. Bedding contacts are solid yellow; red dashed contacts are inferred backthrust locations. Black line denotes topographic surface.

Figure D.3. Apparent fault propagation fold, Triassic Timpoweap Member. On western ridge (Figure D.2, above), verging west, indicative of west-directed faulting nearby.

Throughout the field area, one can find friable, limey, yellow mud layers in the Timpoweap with low amplitude, high frequency folds which are a highly visible indication of compression (Figure D.4). One of these folds can be seen from the creek bed, just before crossing the Timpoweap contact. Slickensides and a possible fault plane were found just above this fold, closer to the top of the hill. Chatter marks indicated a westward sense of motion, and conjugate fractures appeared to indicate a compressional stress field (Figure D.5). From the surface, the over-thickened units in Stop 1 and 2 appear to have acted as a rigid buttress that pressed and squeezed the thinner, less competent layers against an even thicker, more rigid buttress to the east (the Jurassic Navajo Sandstone (Jn)).

Stop 3. The next competent unit, the Virgin Limestone Member (TRmv) of the Triassic Moenkopi Formation, caps the top of a hill in the south. Dipping steeply to the east closer towards the creek bed, the limestone beds flatten southwards to gently dipping east along the hilltop. This is the last competent unit to be upright and dipping east. Ripples in the limestone at the top of the hill suggest the top is to the east. Looking north across the creek, this same unit is overturned steeply to the west and shifted further east. In doing so, it appears to have cut out a significant portion of the Triassic Middle Red Member (TRmm) (Figure A.4).

Domain II Field Stops

Stop 4. The Shinarump Conglomerate Member (TRcs) lies further east. The prevalence of slickensides in this unit is a possible sign of faulting, but they do not have a uniform orientation and no uniform, obvious fault plane was found in Traverse 1. A potential fault plane in this unit outcrops northwards along Traverse 2 (Figure D.7). .Tear faulting in several areas splits outcropping ridges apart, and abundant slickensides and fractures give it a jumbled appearance. Looking south of Spring Creek, a tear fault can be inferred by a break in the outcrop that shifts one block further east. About half a kilometer south up the hill, the ridge breaks again and forms a wall steeply inclined west.

Stop 5. Further upsection along the creek, an important structural relationship between the Jurassic Moenave Formation (JTRm) and the Springdale Member (Jks) is apparent to the north. A thick white layer of Moenave sandstone appears to truncate steeper dipping Springdale sandstone. Hidden in the scrub towards the creek center, close to the contact, this relationship is much easier to see and measure. Truncation of beds at this stop indicates the presence of a fault between the units.

Figure D.4. Folded layer of thin, fissile limestone in the Triassic Timpoweap Member. Proximal to a possible backthrust plane.

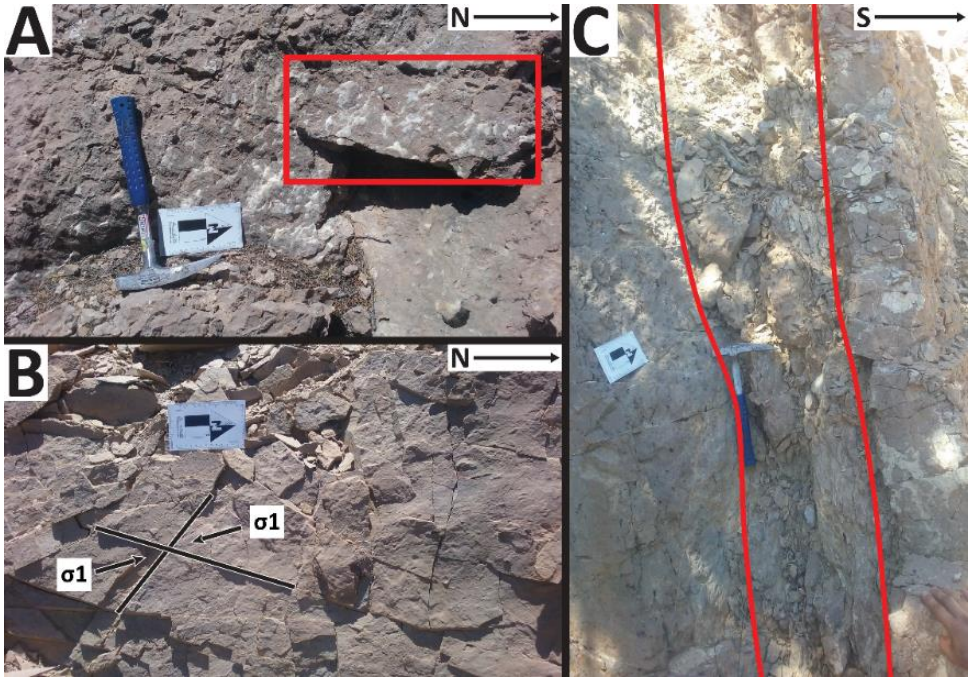

Figure D.5. Potential backthrust plane proximal to folded shaley limestone layer. A) Chattermarks above the fold which are smooth to the west. B) Conjugate fractures with max principal stress orientation approximately horizontal (one possibly overprinting vertical). C) Potential zone of brecciation near chattermarks.

Figure D.6. Ripple marks on block of upright Triassic Virgin Limestone Member (TRmv). The crests show this is the upper surface of the bedding plane, which dips east (upright). However, the heavily disturbed nature of the top of the ridge suggests this piece may not be representative (not in place).

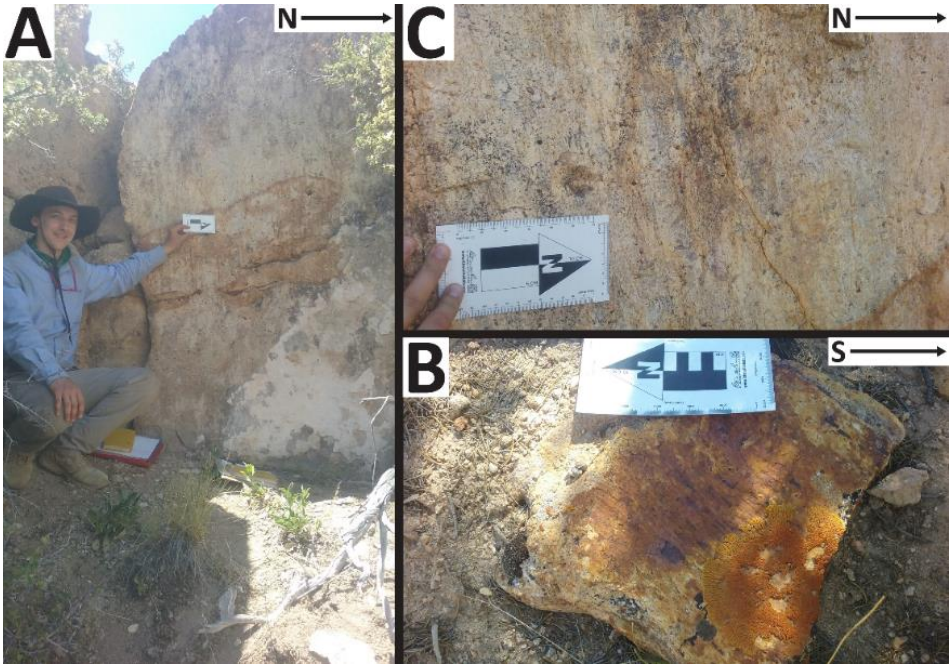

Figure D.7. Slickensides with slickenlines, Triassic Shinarump Conglomerate Member (TRcs). A,C) Polished, smooth surfaces at an outcrop of the Shinarump Conglomerate Member (TRcs) with slickenlines. B) Float from the Triassic Shinarump Conglomerate Member (TRcs) with smooth slickenside containing slickenlines stained by iron oxide weathering.

Stop 6. Just past the Springdale Member (Jks) in the Kayenta Formation (Jku), a large fin of sandstone crops out to the north. This represents the last overturned unit before reaching the Jurassic Navajo Sandstone (Jn). It is obvious from afar that the beds dip west, and upon close inspection crossbedding shows the body is overturned. Because the next unit is upright, something must happen between them to explain the discordant bedding, so a fault is inferred here (see Appendix A, Figure A.11).

Domain III Field Stop

Stop 7. Upon exiting the Kayenta Formation (Jku) upsection, the transition to the Jurassic Navajo Sandstone (Jn) is sudden. Towering, heavily fractured cliffs appear sharply inclined to the east and quickly return to horizontal. The thickness and high degree of competence of this unit are demonstrated by the intensity of brittle deformation and the sharp flexure upwards from horizontal. The axis of a broad syncline is inferred at the transition from steeply inclined to horizontal, which is readily seen here (Figure D.1). Further north, there is evidence of this unit overturning (Figure 3.11).

Table D.1. Stops with planar measurement data. Bdg is bedding; SS is slickenside.

Stop	Fmn	UTM Zone	Northing (mN)	Easting (mE)	Strike (###)	Dip (##)	Dip Dir.	OT? (1/0)	Type
2-2	TRmv	12	4,154,618.00	307,469.00	190	85	W	1	Bdg
3-3	TRmv	12	4,156,138.00	307,683.00	198	56	W	1	Bdg
3-5	TRmv	12	4,156,076.00	307,761.00	198	78	W	1	Bdg
3-5	TRmv	12	4,156,076.00	307,761.00	201	70	W	1	Bdg
3-5	TRmv	12	4,156,076.00	307,761.00	215	74	W	1	Bdg
3-5	TRmv	12	4,156,076.00	307,761.00	202	82	W	1	Bdg
3-5	TRmv	12	4,156,076.00	307,761.00	041	75	E	0	Bdg
3-7	JTRm	12	4,155,872.00	308,205.00	175	45	W	1	Bdg
3-7	JTRm	12	4,155,872.00	308,205.00	185	40	W	1	Bdg
3-7	JTRm	12	4,155,872.00	308,205.00	167	48	W	1	Bdg
3-8	TRcs	12	4,155,779.00	308,223.00	008	46	E	0	Bdg
3-9	Jks	12	4,155,664.00	308,472.00	196	47	W	1	Bdg
3-9	Jks	12	4,155,664.00	308,472.00	196	51	W	1	Bdg
3-9	Jks	12	4,155,664.00	308,472.00	190	60	W	1	Bdg
3-10	Jku	12	4,155,550.00	308,478.00	192	71	W	1	Bdg
3-10	Jku	12	4,155,550.00	308,478.00	185	65	W	1	Bdg
3-11	Jn	12	4,155,363.00	308,770.00	035	83	E	0	Bdg
3-11	Jn	12	4,155,363.00	308,770.00	039	50	E	0	Bdg
3-13	Jks	12	4,155,255.00	308,329.00	182	46	W	1	Bdg
5-3	Pkf	12	4,154,955.00	307,054.00	288	74	N	----	Frac
5-3	Pkf	12	4,154,955.00	307,054.00	301	85	N	----	Frac
5-3	Pkf	12	4,154,955.00	307,054.00	290	85	N	----	Frac

Stop	Fmn	UTM Zone	Northing (mN)	Easting (mE)	Strike (###)	Dip (##)	Dip Dir.	OT? (1/0)	Type
5-5	Pkf	12	4,154,813.00	306,953.00	328	53	N	----	Frac
5-5	Pkf	12	4,154,813.00	306,953.00	290	71	N	----	Frac
5-8	TRmt	12	4,154,702.00	307,308.00	199	76	W	1	Bdg
5-8	TRmt	12	4,154,702.00	307,308.00	205	54	W	1	Bdg
5-8	TRmt	12	4,154,702.00	307,308.00	012	71	E	0	Bdg
5-8	TRmt	12	4,154,702.00	307,308.00	199	60	W	1	Bdg
5-9	TRmt	12	4,154,733.00	307,315.00	011	69	E	0	Bdg
5-9	TRmt	12	4,154,733.00	307,315.00	014	47	E	0	Bdg
5-10	TRmv	12	4,154,613.00	307,465.00	191	85	W	1	Bdg
6-3	TRcs	12	4,154,550.00	307,812.00	183	41	W	1	Bdg
6-3	TRcs	12	4,154,550.00	307,812.00	358	77	E	----	SS
6-3	TRcs	12	4,154,550.00	307,812.00	355	31	E	----	SS
6-3	TRcs	12	4,154,550.00	307,812.00	003	36	E	----	SS
6-3	TRcs	12	4,154,550.00	307,812.00	006	31	E	----	SS
6-3	TRcs	12	4,154,550.00	307,812.00	112	86	S	----	SS
6-5	TRcs	12	4,154,587.00	307,790.00	165	80	W	1	Bdg
6-5	TRcs	12	4,154,587.00	307,790.00	174	70	W	1	Bdg
6-6	TRcu	12	4,154,615.00	307,855.00	169	89	W	1	Bdg
6-6	TRcu	12	4,154,615.00	307,855.00	170	87	W	1	Bdg
6-7	TRmu	12	4,154,535.00	307,759.00	180	40	W	1	Bdg
6-7	TRmu	12	4,154,535.00	307,759.00	180	54	W	1	Bdg
6-7	TRmu	12	4,154,535.00	307,759.00	175	48	W	1	Bdg
6-10	TRmu	12	4,154,696.00	307,607.00	163	48	W	1	Bdg

Stop	Fmn	UTM Zone	Northing (mN)	Easting (mE)	Strike (###)	Dip (##)	Dip Dir.	OT? (1/0)	Type
7-3	JTRm	12	4,154,326.00	307,890.00	187	48	W	1	Bdg
7-4	Jn	12	4,153,545.00	308,636.00	107	13	S	0	Bdg
7-4	Jn	12	4,153,545.00	308,636.00	092	23	S	0	Bdg
7-5	Jn	12	4,153,618.00	308,515.00	006	37	E	0	Bdg
7-5	Jn	12	4,153,618.00	308,515.00	006	25	E	0	Bdg
7-5	Jn	12	4,153,618.00	308,515.00	011	34	E	0	Bdg
7-7	Jn	12	4,153,784.00	308,307.00	019	74	E	0	Bdg
7-8	Jks	12	4,154,156.00	308,068.00	182	72	W	1	Bdg
7-9	Jks	12	4,154,193.00	308,079.00	182	81	W	1	Bdg
7-10	JTRm	12	4,154,312.00	308,001.00	179	63	W	1	Bdg
7-10	JTRm	12	4,154,312.00	308,001.00	177	63	W	1	Bdg
7-11	Jks	12	4,154,288.00	308,028.00	171	72	W	1	Bdg
8-2	TRmv	12	4,156,100.00	307,452.00	199	46	W	1	Bdg
8-2	TRmv	12	4,156,100.00	307,452.00	200	37	W	1	Bdg
8-2	TRmv	12	4,156,100.00	307,452.00	216	70	W	1	Bdg
8-2	TRmv	12	4,156,100.00	307,452.00	212	52	W	1	Bdg
8-3	TRmv	12	4,156,011.00	307,443.00	174	36	W	1	Bdg
8-3	TRmv	12	4,156,011.00	307,443.00	194	36	W	1	Bdg
8-3	TRmv	12	4,156,011.00	307,443.00	189	24	W	1	Bdg
8-3	TRmv	12	4,156,011.00	307,443.00	196	42	W	1	Bdg
8-3	TRmv	12	4,156,011.00	307,443.00	119	32	W	1	Bdg
8-3	TRmv	12	4,156,011.00	307,443.00	181	38	W	1	Bdg
8-3	TRmv	12	4,156,011.00	307,443.00	180	89	W	1	Bdg

Stop	Fmn	UTM Zone	Northing (mN)	Easting (mE)	Strike (###)	Dip (##)	Dip Dir.	OT? (1/0)	Type
8-3	TRmv	12	4,156,011.00	307,443.00	180	90	V	1	Bdg
8-5	TRmt	12	4,155,797.00	307,403.00	185	66	W	1	Bdg
8-5	TRmt	12	4,155,797.00	307,403.00	176	79	W	1	Bdg
8-5	TRmt	12	4,155,797.00	307,403.00	179	81	W	1	Bdg
8-5	TRmt	12	4,155,797.00	307,403.00	180	65	W	1	Bdg
8-5	TRmt	12	4,155,797.00	307,403.00	168	74	W	1	Bdg
8-5	TRmt	12	4,155,797.00	307,403.00	332	51	E	0	Bdg
8-5	TRmt	12	4,155,797.00	307,403.00	330	51	E	0	Bdg
8-5	TRmt	12	4,155,797.00	307,403.00	319	70	E	0	Bdg
8-5	TRmt	12	4,155,797.00	307,403.00	331	42	E	0	Bdg
8-5	TRmt	12	4,155,797.00	307,403.00	333	49	E	0	Bdg
8-5	TRmt	12	4,155,797.00	307,403.00	316	64	E	0	Bdg
8-6	TRmt	12	4,155,730.00	307,411.00	213	39	W	----	SS
8-6	TRmt	12	4,155,730.00	307,411.00	228	46	W	----	SS
8-6	TRmt	12	4,155,730.00	307,411.00	220	57	W	----	SS
8-8	TRmt	12	4,155,590.00	307,405.00	058	57	SE	0	Bdg
8-8	TRmt	12	4,155,590.00	307,405.00	060	76	SE	0	Bdg
8-8	TRmt	12	4,155,590.00	307,405.00	307	48	NE	0	Bdg
8-8	TRmt	12	4,155,590.00	307,405.00	310	46	NE	0	Bdg
8-8	TRmt	12	4,155,590.00	307,405.00	054	55	SE	0	Bdg
8-8	TRmt	12	4,155,590.00	307,405.00	059	67	SE	0	Bdg
8-8	TRmt	12	4,155,590.00	307,405.00	235	87	SE	0	Bdg
8-8	TRmt	12	4,155,590.00	307,405.00	338	55	NE	0	Bdg
8-8	TRmt	12	4,155,590.00	307,405.00	320	62	NE	0	Bdg

Stop	Fmn	UTM Zone	Northing (mN)	Easting (mE)	Strike (###)	Dip (##)	Dip Dir.	OT? (1/0)	Type
8-8	TRmt	12	4,155,590.00	307,405.00	343	63	NE	0	Bdg
8-8	TRmt	12	4,155,590.00	307,405.00	305	45	N	0	Bdg
8-8	TRmt	12	4,155,590.00	307,405.00	035	64	SE	0	Bdg
8-8	TRmt	12	4,155,590.00	307,405.00	063	65	SE	0	Bdg
8-9a	TRmv	12	4,155,521.00	307,429.00	353	49	E	0	Bdg
8-9a	TRmv	12	4,155,521.00	307,429.00	000	80	E	0	Bdg
8-9b	TRmv	12	4,155,501.00	307,433.00	359	69	E	0	Bdg
8-10	TRml	12	4,155,511.00	307,403.00	328	54	E	0	Bdg
8-10	TRml	12	4,155,511.00	307,403.00	323	62	E	0	Bdg
8-10	TRml	12	4,155,511.00	307,403.00	161	60	W	1	Bdg
8-11	TRmv	12	4,155,401.00	307,433.00	352	65	E	0	Bdg
8-11	TRmv	12	4,155,401.00	307,433.00	031	31	E	0	Bdg
8-12	TRmv	12	4,155,377.00	307,424.00	083	46	S	----	SS
8-12	TRmv	12	4,155,377.00	307,424.00	078	43	S	----	SS
8-12	TRmv	12	4,155,377.00	307,424.00	195	22	W	----	SS
9-3	TRmv	12	4,155,283.00	307,493.00	161	42	W	1	Bdg
9-3	TRmv	12	4,155,283.00	307,493.00	173	35	W	1	Bdg
9-5	TRmt	12	4,155,112.00	307,296.00	006	65	E	0	Bdg
9-5	TRmt	12	4,155,112.00	307,296.00	006	72	E	0	Bdg
9-5	TRmt	12	4,155,112.00	307,296.00	001	68	E	0	Bdg
9-5	TRmt	12	4,155,112.00	307,296.00	002	74	E	0	Bdg
9-5	TRmt	12	4,155,112.00	307,296.00	005	68	E	0	Bdg
9-5	TRmt	12	4,155,112.00	307,296.00	007	59	E	0	Bdg

Stop	Fmn	UTM Zone	Northing (mN)	Easting (mE)	Strike (###)	Dip (##)	Dip Dir.	OT? (1/0)	Type
9-5	TRmt	12	4,155,112.00	307,296.00	005	57	E	0	Bdg
9-5	TRmt	12	4,155,112.00	307,296.00	015	52	E	0	Bdg
9-5	TRmt	12	4,155,112.00	307,296.00	002	34	E	0	Bdg
9-5	TRmt	12	4,155,112.00	307,296.00	000	46	E	0	Bdg
9-5a	TRmt	12	4,155,109.00	307,282.00	012	35	E	0	Bdg
9-6	TRmt	12	4,154,989.00	307,244.00	011	49	E	0	Bdg
9-6	TRmt	12	4,154,989.00	307,244.00	012	46	E	0	Bdg
9-6	TRmt	12	4,154,989.00	307,244.00	018	54	E	0	Bdg
9-8	TRmt	12	4,154,955.00	307,276.00	023	36	E	0	Bdg
9-8	TRmt	12	4,154,955.00	307,276.00	028	37	E	0	Bdg
9-8	TRmt	12	4,154,955.00	307,276.00	010	55	E	----	SS
9-8	TRmt	12	4,154,955.00	307,276.00	061	33	SE	----	SS
9-8	TRmt	12	4,154,955.00	307,276.00	047	44	SE	----	SS
9-9	TRmt	12	4,154,993.00	307,284.00	020	56	E	----	SS
9-9	TRmt	12	4,154,993.00	307,284.00	351	38	E	----	SS
9-9	TRmt	12	4,154,993.00	307,284.00	138	49	W	----	SS
9-10	TRmt	12	4,154,954.00	307,298.00	113	64	S	----	SS
9-10	TRmt	12	4,154,954.00	307,298.00	009	53	E	0	Bdg
9-10	TRmt	12	4,154,954.00	307,298.00	009	57	E	0	Bdg
9-10	TRmt	12	4,154,954.00	307,298.00	020	50	E	0	Bdg
9-10	TRmt	12	4,154,954.00	307,298.00	015	60	E	0	Bdg
10-1a	TRmt	12	4,155,797.00	307,403.00	096	48	S	----	Frac
10-1a	TRmt	12	4,155,797.00	307,403.00	173	56	E	----	Frac

Stop	Fmn	UTM Zone	Northing (mN)	Easting (mE)	Strike (###)	Dip (##)	Dip Dir.	OT? (1/0)	Type
10-1a	TRmt	12	4,155,797.00	307,403.00	001	37	E	----	Frac
10-1a	TRmt	12	4,155,797.00	307,403.00	296	30	E	----	SS
10-1a	TRmt	12	4,155,797.00	307,403.00	198	52	W	1	Bdg
10-1a	TRmt	12	4,155,797.00	307,403.00	015	14	E	----	Frac
10-1a	TRmt	12	4,155,797.00	307,403.00	022	22	E	----	Frac
10-1a	TRmt	12	4,155,797.00	307,403.00	339	24	E	----	Frac
10-3	TRmv	12	4,155,315.00	307,419.00	049	84	E	----	Frac
10-3	TRmv	12	4,155,315.00	307,419.00	049	79	E	----	Frac
10-3	TRmv	12	4,155,315.00	307,419.00	018	83	E	----	Frac
10-3	TRmv	12	4,155,315.00	307,419.00	158	54	SW	1	Bdg
10-3	TRmv	12	4,155,315.00	307,419.00	143	36	SW	1	Bdg
10-3	TRmv	12	4,155,315.00	307,419.00	332	75	E	0	Bdg
10-4	TRmv	12	4,155,104.00	307,510.00	004	37	E	0	Bdg
10-4	TRmv	12	4,155,104.00	307,510.00	003	35	E	0	Bdg
10-4	TRmv	12	4,155,104.00	307,510.00	014	30	E	0	Bdg
11-4	TRcs	12	4,155,040.00	307,934.00	117	29	S	----	SS
11-4	TRcs	12	4,155,040.00	307,934.00	118	71	S	----	SS
11-4	TRcs	12	4,155,040.00	307,934.00	118	27	S	----	SS
11-4	TRcs	12	4,155,040.00	307,934.00	224	09	N	----	SS
11-4	TRcs	12	4,155,040.00	307,934.00	146	27	W	----	SS
11-4	TRcs	12	4,155,040.00	307,934.00	126	39	S	----	SS
11-4	TRcs	12	4,155,040.00	307,934.00	155	48	W	----	SS

Stop	Fmn	UTM Zone	Northing (mN)	Easting (mE)	Strike (###)	Dip (##)	Dip Dir.	OT? (1/0)	Type
11-4	TRcs	12	4,155,040.00	307,934.00	----	----	----	----	----
11-4	TRcs	12	4,155,040.00	307,934.00	123	24	S	----	SS
11-4	TRcs	12	4,155,040.00	307,934.00	148	27	SW	----	SS
11-4	TRcs	12	4,155,040.00	307,934.00	143	20	S	----	SS
11-4	TRcs	12	4,155,040.00	307,934.00	111	27	S	----	SS
11-4	TRcs	12	4,155,040.00	307,934.00	255	19	S	----	SS
11-6a	TRcs	12	4,155,311.00	308,165.00	088	21	E	----	SS
11-6a	TRcs	12	4,155,311.00	308,165.00	147	43	SW	----	SS
11-7	TRcu	12	4,155,277.00	308,109.00	179	55	W	1	Bdg
11-7	TRcu	12	4,155,277.00	308,109.00	024	57	E	----	SS
11-7	TRcu	12	4,155,277.00	308,109.00	044	16	E	----	SS
11-7	TRcu	12	4,155,277.00	308,109.00	359	30	E	----	SS
11-7	TRcu	12	4,155,277.00	308,109.00	000	34	E	----	SS
11-8	Jks	12	4,155,263.00	308,374.00	147	28	SW	1	Bdg
11-8a	Jks	12	4,155,286.00	308,385.00	178	57	W	1	Bdg
11-9	TRmu	12	4,155,099.00	307,729.00	175	27	W	1	Bdg
11-9	TRmu	12	4,155,099.00	307,729.00	195	29	W	1	Bdg
12-5	TRcs	12	4,153,717.00	307,542.00	222	69	W	1	Bdg
12-5	TRcs	12	4,153,717.00	307,542.00	120	27	W	----	SS
12-5	TRcs	12	4,153,717.00	307,542.00	244	54	E	----	SS
12-5	TRcs	12	4,153,717.00	307,542.00	----	----	----	----	----
12-5a	TRcs	12	4,153,685.00	307,489.00	006	21	E	0	Bdg

Stop	Fmn	UTM Zone	Northing (mN)	Easting (mE)	Strike (###)	Dip (##)	Dip Dir.	OT? (1/0)	Type
12-5a	TRcs	12	4,153,685.00	307,489.00	355	26	E	0	Bdg
12-7	TRcs	12	4,153,621.00	307,466.00	017	32	E	0	Bdg
12-8	TRcu	12	4,153,519.00	307,521.00	190	70	W	1	Bdg
12-8a	JTRm	12	4,153,474.00	307,662.00	199	55	W	1	Bdg
12-8a	JTRm	12	4,153,474.00	307,662.00	198	63	W	1	Bdg
12-9a	JTRm	12	4,153,646.00	307,873.00	176	30	W	1	Bdg
12-9a	JTRm	12	4,153,646.00	307,873.00	182	19	W	1	Bdg
12-10	JTRm	12	4,153,981.00	307,940.00	207	40	W	1	Bdg
12-10	JTRm	12	4,153,981.00	307,940.00	207	36	W	1	Bdg
12-10	JTRm	12	4,153,981.00	307,940.00	187	32	W	1	Bdg
13-2	TRmt	12	4,154,143.00	306,891.00	042	38	E	0	Bdg
13-2	TRmt	12	4,154,143.00	306,891.00	041	34	E	0	Bdg
13-2a	TRmt	12	4,154,209.00	306,877.00	047	14	E	0	Bdg
13-2a	TRmt	12	4,154,209.00	306,877.00	050	25	E	0	Bdg
13-2a	TRmt	12	4,154,209.00	306,877.00	028	21	E	0	Bdg
13-3	TRmt	12	4,154,591.00	306,986.00	012	18	E	0	Bdg
13-3	TRmt	12	4,154,591.00	306,986.00	015	25	E	0	Bdg
13-3	TRmt	12	4,154,591.00	306,986.00	042	80	E	----	Frac
13-3	TRmt	12	4,154,591.00	306,986.00	274	68	N	----	Frac
13-3	TRmt	12	4,154,591.00	306,986.00	256	82	N	----	Frac
13-3	TRmt	12	4,154,591.00	306,986.00	134	68	S	----	Frac
13-4	TRmt	12	4,154,656.00	307,014.00	023	23	E	0	Bdg

Stop	Fmn	UTM Zone	Northing (mN)	Easting (mE)	Strike (###)	Dip (##)	Dip Dir.	OT? (1/0)	Type
13-4	TRmt	12	4,154,656.00	307,014.00	357	30	E	0	Bdg
13-4	TRmt	12	4,154,656.00	307,014.00	025	14	E	0	Bdg
13-4a	TRmt	12	4,154,640.00	307,000.00	204	82	W	----	Frac
13-4a	TRmt	12	4,154,640.00	307,000.00	038	76	E	----	Frac
13-4a	TRmt	12	4,154,640.00	307,000.00	048	46	E	----	Frac
13-4a	TRmt	12	4,154,640.00	307,000.00	067	54	E	----	Frac
13-4a	TRmt	12	4,154,640.00	307,000.00	022	72	E	----	Frac
13-4a	TRmt	12	4,154,640.00	307,000.00	030	14	E	0	Bdg
13-4a	TRmt	12	4,154,640.00	307,000.00	057	10	E	0	Bdg
13-4a	TRmt	12	4,154,640.00	307,000.00	007	23	E	0	Bdg
13-4a	TRmt	12	4,154,640.00	307,000.00	005	25	E	0	Bdg
13-4a	TRmt	12	4,154,640.00	307,000.00	020	23	E	0	Bdg
13-4a	TRmt	12	4,154,640.00	307,000.00	355	27	E	0	Bdg
13-4a	TRmt	12	4,154,640.00	307,000.00	021	16	E	0	Bdg
13-4b	TRmt	12	4,154,652.00	307,026.00	244	72	W	----	Frac
13-5	TRmt	12	4,154,404.00	306,887.00	095	43	S	0	Bdg
13-5	TRmt	12	4,154,404.00	306,887.00	104	35	S	0	Bdg
13-5	TRmt	12	4,154,404.00	306,887.00	085	25	S	0	Bdg
13-5	TRmt	12	4,154,404.00	306,887.00	056	30	S	0	Bdg
13-5a	TRmt	12	4,154,213.00	306,875.00	036	30	E	0	Bdg
13-5a	TRmt	12	4,154,213.00	306,875.00	056	20	E	0	Bdg
13-5a	TRmt	12	4,154,213.00	306,875.00	040	45	E	0	Bdg

Stop	Fmn	UTM Zone	Northing (mN)	Easting (mE)	Strike (###)	Dip (##)	Dip Dir.	OT? (1/0)	Type
13-5a	TRmt	12	4,154,213.00	306,875.00	031	33	E	0	Bdg
13-6	TRmv	12	4,153,904.00	306,961.00	040	32	E	0	Bdg
14-4	Jku	12	4,154,084.00	308,168.00	178	79	W	1	Bdg
14-4	Jku	12	4,154,084.00	308,168.00	170	72	W	1	Bdg
14-5a	Pkf	12	4,154,971.00	307,040.00	005	45	E	0	Bdg
14-5a	Pkf	12	4,154,971.00	307,040.00	013	45	E	0	Bdg
14-5a	Pkf	12	4,154,971.00	307,040.00	023	75	E	0	Bdg
14-5a	Pkf	12	4,154,971.00	307,040.00	017	64	E	0	Bdg
14-5a	Pkf	12	4,154,971.00	307,040.00	179	66	W	1	Bdg
14-5a	Pkf	12	4,154,971.00	307,040.00	030	84	E	0	Bdg
14-5a	Pkf	12	4,154,971.00	307,040.00	224	57	W	1	Bdg
14-5a	Pkf	12	4,154,971.00	307,040.00	194	54	W	1	Bdg
14-5a	Pkf	12	4,154,971.00	307,040.00	347	51	E	0	Bdg
14-5a	Pkf	12	4,154,971.00	307,040.00	346	62	E	0	Bdg
14-5a	Pkf	12	4,154,971.00	307,040.00	004	64	E	0	Bdg
14-6	TRmv	12	4,156,183.00	307,638.00	199	47	W	1	Bdg
14-6	TRmv	12	4,156,183.00	307,638.00	036	76	E	0	Bdg
14-6	TRmv	12	4,156,183.00	307,638.00	046	63	E	0	Bdg
14-6	TRmv	12	4,156,183.00	307,638.00	010	40	E	0	Bdg
14-7	TRmv	12	4,156,122.00	307,765.00	050	06	E	0	Bdg
14-7	TRmv	12	4,156,122.00	307,765.00	041	86	E	0	Bdg
14-7	TRmv	12	4,156,122.00	307,765.00	209	76	W	1	Bdg

Stop	Fmn	UTM Zone	Northing (mN)	Easting (mE)	Strike (###)	Dip (##)	Dip Dir.	OT? (1/0)	Type
14-7	TRmv	12	4,156,122.00	307,765.00	216	78	W	1	Bdg
14-7	TRmv	12	4,156,122.00	307,765.00	216	76	W	1	Bdg
15-2	TRmv	12	4,156,277.00	307,770.00	200	33	W	1	Bdg
15-2	TRmv	12	4,156,277.00	307,770.00	195	33	W	1	Bdg
15-2	TRmv	12	4,156,277.00	307,770.00	199	26	W	1	Bdg
15-3	TRmv	12	4,156,192.00	307,685.00	194	86	W	1	Bdg
15-3	TRmv	12	4,156,192.00	307,685.00	355	90	V	0	Bdg
15-3	TRmv	12	4,156,192.00	307,685.00	254	13	NW	1	Bdg
15-3	TRmv	12	4,156,192.00	307,685.00	258	05	NW	1	Bdg
15-3	TRmv	12	4,156,192.00	307,685.00	250	21	NW	1	Bdg
15-3	TRmv	12	4,156,192.00	307,685.00	261	19	NW	1	Bdg
15-3	TRmv	12	4,156,192.00	307,685.00	212	39	NW	1	Bdg
15-3	TRmv	12	4,156,192.00	307,685.00	222	34	NW	1	Bdg
15-3	TRmv	12	4,156,192.00	307,685.00	198	42	NW	1	Bdg
15-4a	TRmv	12	4,155,866.00	307,691.00	281	31	N	0	Bdg
15-4a	TRmv	12	4,155,866.00	307,691.00	269	40	N	0	Bdg
15-4a	TRmv	12	4,155,866.00	307,691.00	338	25	NE	0	Bdg
15-5	TRms	12	4,155,927.00	308,165.00	192	39	W	1	Bdg
15-6	JTRm	12	4,155,876.00	308,203.00	169	60	W	1	Bdg
15-7a	JTRm	12	4,155,707.00	308,305.00	178	67	W	1	Bdg
15-7a	JTRm	12	4,155,707.00	308,305.00	185	70	W	1	Bdg
15-7a	JTRm	12	4,155,707.00	308,305.00	186	65	W	1	Bdg

Stop	Fmn	UTM Zone	Northing (mN)	Easting (mE)	Strike (###)	Dip (##)	Dip Dir.	OT? (1/0)	Type
15-8	Jks	12	4,155,665.00	308,467.00	192	48	W	1	Bdg
15-8	Jks	12	4,155,665.00	308,467.00	190	71	W	1	Bdg
15-10	TRcs	12	4,156,184.00	308,422.00	051	33	E	----	SS
15-10	TRcs	12	4,156,184.00	308,422.00	210	90	V	----	SS
15-10	TRcs	12	4,156,184.00	308,422.00	038	88	E	----	SS
15-10	TRcs	12	4,156,184.00	308,422.00	038	88	E	----	SS
15-10	TRcs	12	4,156,184.00	308,422.00	049	88	E	----	SS
15-10	TRcs	12	4,156,184.00	308,422.00	049	88	E	----	SS
15-10	TRcs	12	4,156,184.00	308,422.00	228	86	W	----	SS
15-10	TRcs	12	4,156,184.00	308,422.00	228	86	W	----	SS
15-10	TRcs	12	4,156,184.00	308,422.00	188	25	W	1	Bdg
15-10	TRcs	12	4,156,184.00	308,422.00	192	33	W	1	Bdg
15-10	TRcs	12	4,156,184.00	308,422.00	200	40	W	1	Bdg
15-10	TRcs	12	4,156,184.00	308,422.00	200	42	W	1	Bdg
15-10	TRcs	12	4,156,184.00	308,422.00	048	38	E	----	SS
15-10	TRcs	12	4,156,184.00	308,422.00	048	38	E	----	SS
16-3a	TRcs	12	4,156,131.00	308,498.00	210	48	W	1	Bdg
16-5	TRcs	12	4,156,161.00	308,356.00	197	54	W	1	Bdg
16-5	TRcs	12	4,156,161.00	308,356.00	070	20	S	----	SS
16-5	TRcs	12	4,156,161.00	308,356.00	124	21	S	----	SS
16-7	TRcu	12	4,155,425.00	308,180.00	172	68	W	1	Bdg
16-7	TRcu	12	4,155,425.00	308,180.00	174	69	W	1	Bdg

Stop	Fmn	UTM Zone	Northing (mN)	Easting (mE)	Strike (###)	Dip (##)	Dip Dir.	OT? (1/0)	Type
16-8	TRcs	12	4,155,381.00	308,154.00	170	56	W	1	Bdg
16-8	TRcs	12	4,155,381.00	308,154.00	068	80	S	----	SS
16-8	TRcs	12	4,155,381.00	308,154.00	247	76	N	----	SS
16-8a	TRcs	12	4,155,349.00	308,163.00	174	78	W	1	Bdg
16-8a	TRcs	12	4,155,349.00	308,163.00	004	24	E	----	SS
16-8a	TRcs	12	4,155,349.00	308,163.00	280	23	N	----	SS
16-8a	TRcs	12	4,155,349.00	308,163.00	292	36	N	----	SS
16-8a	TRcs	12	4,155,349.00	308,163.00	346	19	E	----	SS
17-3	Jn	12	4,155,308.00	308,693.00	189	66	W	----	SS
17-3	Jn	12	4,155,308.00	308,693.00	170	51	W	----	SS
17-3	Jn	12	4,155,308.00	308,693.00	185	63	W	----	SS
18-2	TRmv	12	4,156,776.00	308,219.00	216	53	W	1	Bdg
18-2	TRmv	12	4,156,776.00	308,219.00	228	48	W	1	Bdg
18-2a	TRmv	12	4,156,812.00	308,212.00	211	45	W	1	Bdg
18-2a	TRmv	12	4,156,812.00	308,212.00	210	44	W	1	Bdg
18-3	TRcu	12	4,156,593.00	308,690.00	213	68	W	1	Bdg
18-3	TRcu	12	4,156,593.00	308,690.00	214	64	W	1	Bdg
18-5	Jks	12	4,156,542.00	308,916.00	218	60	W	1	Bdg
18-5	Jks	12	4,156,542.00	308,916.00	207	54	W	1	Bdg
18-5	Jks	12	4,156,542.00	308,916.00	211	70	W	1	Bdg
18-9	TRmu	12	4,156,676.00	308,472.00	205	47	W	1	Bdg
18-9	TRmu	12	4,156,676.00	308,472.00	197	40	W	1	Bdg

Stop	Fmn	UTM Zone	Northing (mN)	Easting (mE)	Strike (###)	Dip (##)	Dip Dir.	OT? (1/0)	Type
18-9	TRmu	12	4,156,676.00	308,472.00	187	33	W	1	Bdg
19-4	TRmv	12	4,156,838.00	308,245.00	204	48	W	1	Bdg
19-4	TRmv	12	4,156,838.00	308,245.00	195	50	W	1	Bdg
19-4	TRmv	12	4,156,838.00	308,245.00	021	71	E	----	Frac
19-4	TRmv	12	4,156,838.00	308,245.00	025	72	E	----	Frac
19-4	TRmv	12	4,156,838.00	308,245.00	096	29	S	----	Frac
19-5	TRmv	12	4,156,662.00	308,041.00	194	37	W	1	Bdg
19-5	TRmv	12	4,156,662.00	308,041.00	188	38	W	1	Bdg
19-5a	TRmv	12	4,156,607.00	308,052.00	210	22	W	1	Bdg
19-6	Jks	12	4,156,518.00	308,915.00	221	50	W	1	Bdg
19-6	Jks	12	4,156,518.00	308,915.00	212	44	W	1	Bdg
19-6	Jks	12	4,156,518.00	308,915.00	209	39	W	1	Bdg
19-6	Jks	12	4,156,518.00	308,915.00	037	76	E	0	Bdg
19-7	TRcs	12	4,156,668.00	308,521.00	200	32	W	----	SS
19-7	TRcs	12	4,156,668.00	308,521.00	207	35	W	----	SS
19-7a	TRcs	12	4,156,758.00	308,621.00	200	42	W	1	Bdg
19-7a	TRcs	12	4,156,758.00	308,621.00	187	32	W	----	SS
19-7a	TRcs	12	4,156,758.00	308,621.00	176	32	W	----	SS
19-7b	TRcs	12	4,156,773.00	308,608.00	197	65	W	1	Bdg
20-3	TRmv	12	4,155,742.00	307,665.00	192	60	W	1	Bdg
20-3	TRmv	12	4,155,742.00	307,665.00	195	48	W	1	Bdg
20-3	TRmv	12	4,155,742.00	307,665.00	196	45	W	1	Bdg

Stop	Fmn	UTM Zone	Northing (mN)	Easting (mE)	Strike (###)	Dip (##)	Dip Dir.	OT? (1/0)	Type
20-3	TRmv	12	4,155,742.00	307,665.00	191	40	W	1	Bdg
20-3	TRmv	12	4,155,742.00	307,665.00	204	42	W	1	Bdg
20-3	TRmv	12	4,155,742.00	307,665.00	188	70	W	1	Bdg
20-3	TRmv	12	4,155,742.00	307,665.00	202	27	W	1	Bdg
20-3	TRmv	12	4,155,742.00	307,665.00	205	36	W	1	Bdg
20-3	TRmv	12	4,155,742.00	307,665.00	200	27	W	1	Bdg
20-3	TRmv	12	4,155,742.00	307,665.00	204	31	W	1	Bdg
20-3	TRmv	12	4,155,742.00	307,665.00	201	18	W	1	Bdg
20-3	TRmv	12	4,155,742.00	307,665.00	200	27	W	1	Bdg
20-3	TRmv	12	4,155,742.00	307,665.00	170	24	W	1	Bdg
20-3	TRmv	12	4,155,742.00	307,665.00	175	22	W	1	Bdg
20-3	TRmv	12	4,155,742.00	307,665.00	219	22	W	1	Bdg
20-3	TRmv	12	4,155,742.00	307,665.00	204	21	W	1	Bdg
20-3	TRmv	12	4,155,742.00	307,665.00	200	27	W	1	Bdg
20-3	TRmv	12	4,155,742.00	307,665.00	178	18	W	1	Bdg
20-3	TRmv	12	4,155,742.00	307,665.00	355	81	E	0	Bdg
20-3	TRmv	12	4,155,742.00	307,665.00	338	75	E	0	Bdg
20-3	TRmv	12	4,155,742.00	307,665.00	345	90	V	0	Bdg
20-5	TRmv	12	4,155,394.00	307,599.00	178	72	W	1	Bdg
20-5	TRmv	12	4,155,394.00	307,599.00	171	75	W	1	Bdg
20-5a	TRmv	12	4,155,373.00	307,620.00	188	78	W	1	Bdg
20-9	TRmt	12	4,154,666.00	307,241.00	191	72	W	1	Bdg

Stop	Fmn	UTM Zone	Northing (mN)	Easting (mE)	Strike (###)	Dip (##)	Dip Dir.	OT? (1/0)	Type
20-9	TRmt	12	4,154,666.00	307,241.00	194	88	W	1	Bdg
20-9	TRmt	12	4,154,666.00	307,241.00	014	85	E	0	Bdg
20-9	TRmt	12	4,154,666.00	307,241.00	011	67	E	0	Bdg
20-9	TRmt	12	4,154,666.00	307,241.00	011	84	E	0	Bdg
20-9	TRmt	12	4,154,666.00	307,241.00	010	86	E	0	Bdg
20-9	TRmt	12	4,154,666.00	307,241.00	009	65	E	0	Bdg
20-9	TRmt	12	4,154,666.00	307,241.00	017	52	E	0	Bdg
20-9	TRmt	12	4,154,666.00	307,241.00	013	69	E	0	Bdg
20-9	TRmt	12	4,154,666.00	307,241.00	019	68	E	0	Bdg
20-9	TRmt	12	4,154,666.00	307,241.00	018	70	E	0	Bdg
20-9	TRmt	12	4,154,666.00	307,241.00	010	67	E	0	Bdg
20-9	TRmt	12	4,154,666.00	307,241.00	019	90	V	0	Bdg
20-9	TRmt	12	4,154,666.00	307,241.00	190	62	W	1	Bdg
20-9	TRmt	12	4,154,666.00	307,241.00	188	65	W	1	Bdg
20-9	TRmt	12	4,154,666.00	307,241.00	189	69	W	1	Bdg
20-9	TRmt	12	4,154,666.00	307,241.00	190	74	W	1	Bdg
20-9	TRmt	12	4,154,666.00	307,241.00	178	85	W	1	Bdg
20-10	TRmt	12	4,154,730.00	307,295.00	023	66	E	0	Bdg
20-10a	TRmt	12	4,154,780.00	307,291.00	005	49	E	0	Bdg
20-10b	TRmt	12	4,154,840.00	307,269.00	016	80	E	----	SS
20-10b	TRmt	12	4,154,840.00	307,269.00	355	85	E	----	SS
21-1	TRmv	12	4,154,365.00	307,301.00	000	68	E	0	Bdg

Stop	Fmn	UTM Zone	Northing (mN)	Easting (mE)	Strike (###)	Dip (##)	Dip Dir.	OT? (1/0)	Type
21-1	TRmv	12	4,154,365.00	307,301.00	358	70	E	0	Bdg
21-1	TRmv	12	4,154,365.00	307,301.00	008	45	E	0	Bdg
21-1	TRmv	12	4,154,365.00	307,301.00	003	72	E	0	Bdg
21-1	TRmv	12	4,154,365.00	307,301.00	357	72	E	0	Bdg
21-1	TRmv	12	4,154,365.00	307,301.00	200	50	W	1	Bdg
21-1a	TRmv	12	4,154,264.00	307,267.00	005	41	E	0	Bdg
21-1a	TRmv	12	4,154,264.00	307,267.00	026	36	E	1	Bdg
21-2	TRcs	12	4,154,363.00	307,682.00	185	43	W	1	Bdg
21-2	TRmu-TRcs*	12	4,154,363.00	307,682.00	190	42	W	1	Bdg
21-2a	TRmu-TRcs*	12	4,154,312.00	307,695.00	177	66	W	1	Bdg
21-2a	TRmu-TRcs*	12	4,154,312.00	307,695.00	214	54	W	1	Bdg

Table D.2. Stops with slickenline measurements.

Stop	Fmn	UTM Zone	Northing (mN)	Easting (mE)	Trend (###)	Plunge (##)	Type
6-3	TRcs	12	4,154,550.00	307,812.00	118	47	SL
6-3	TRcs	12	4,154,550.00	307,812.00	109	29	SL
6-3	TRcs	12	4,154,550.00	307,812.00	041	53	SL
11-4	TRcs	12	4,155,040.00	307,934.00	289	09	SL
11-4	TRcs	12	4,155,040.00	307,934.00	250	06	SL
11-4	TRcs	12	4,155,040.00	307,934.00	257	27	SL
11-4	TRcs	12	4,155,040.00	307,934.00	265	29	SL

Stop	Fmn	UTM Zone	Northing (mN)	Easting (mE)	Trend (###)	Plunge (##)	Type
11-4	TRcs	12	4,155,040.00	307,934.00	199	25	SL
11-4	TRcs	12	4,155,040.00	307,934.00	265	16	SL
11-4	TRcs	12	4,155,040.00	307,934.00	266	26	SL
11-4	TRcs	12	4,155,040.00	307,934.00	275	11	SL
11-4	TRcs	12	4,155,040.00	307,934.00	264	11	SL
11-4	TRcs	12	4,155,040.00	307,934.00	155	15	SL
11-6a	TRcs	12	4,155,311.00	308,165.00	115	09	SL
11-6a	TRcs	12	4,155,311.00	308,165.00	317	09	SL
11-7	TRcu	12	4,155,277.00	308,109.00	132	16	SL
12-5	TRcs	12	4,153,717.00	307,542.00	157	38	SL
15-10	TRcs	12	4,156,184.00	308,422.00	126	86	SL
15-10	TRcs	12	4,156,184.00	308,422.00	121	89	SL
15-10	TRcs	12	4,156,184.00	308,422.00	139	82	SL
15-10	TRcs	12	4,156,184.00	308,422.00	129	84	SL
15-10	TRcs	12	4,156,184.00	308,422.00	134	90	SL
15-10	TRcs	12	4,156,184.00	308,422.00	137	90	SL
15-10	TRcs	12	4,156,184.00	308,422.00	098	28	SL
15-10	TRcs	12	4,156,184.00	308,422.00	100	30	SL
16-5	TRcs	12	4,156,161.00	308,356.00	128	11	SL
16-5	TRcs	12	4,156,161.00	308,356.00	127	07	SL
16-8	TRcs	12	4,155,381.00	308,154.00	338	72	SL
16-8a	TRcs	12	4,155,349.00	308,163.00	326	22	SL

Stop	Fmn	UTM Zone	Northing (mN)	Easting (mE)	Trend (###)	Plunge (##)	Type
16-8a	TRcs	12	4,155,349.00	308,163.00	090	20	SL
16-8a	TRcs	12	4,155,349.00	308,163.00	296	16	SL
17-3	Jn	12	4,155,308.00	308,693.00	306	63	SL
18-8	TRcs	12	4,156,651.00	308,497.00	120	23	SL
18-8	TRcs	12	4,156,651.00	308,497.00	291	73	SL
19-7	TRcs	12	4,156,668.00	308,521.00	335	24	SL
19-7	TRcs	12	4,156,668.00	308,521.00	294	37	SL
19-7a	TRcs	12	4,156,758.00	308,621.00	294	34	SL
19-7a	TRcs	12	4,156,758.00	308,621.00	281	31	SL

BIBLIOGRAPHY

Armstrong, R. L. (1968). Sevier orogenic belt in Nevada and Utah. *Geological Society of America Bulletin*, *79*(4), 429-458.

Averitt, P. (1962). *Geology and coal resources of the Cedar Mountain quadrangle, Iron County, Utah* (No. 389). US Govt. Print. Off.

Baby, P., Hérail, G., Salinas, R., & Sempere, T. (1992). Geometry and kinematic evolution of passive roof duplexes: Examples from the foreland thrust system of the Subandean belt of Bolivia. *Tectonics*, *11*(3), 523-536.

Bekkers, R. W. G. (2011). 3D Modeling of a foreland fold and thrust basin in the French sub-Alpine chains.

Biek, R. F. (2003). *Geologic Map of the Harrisburg Junction 7.5' Quadrangle, Washington County, Utah [map]*. 1:24,000. Map 191. Washington County, Utah: Utah Geological Survey.

Biek, R. F. (2007). *Geologic Map of the Kolob Arch Quadrangle, Washington and Iron Counties, Utah [map]*. 1:24,000. Map 217. Iron County, Utah: Utah Geological Survey.

Biek, R. F. and Hayden, J. M. (2013). *Interim Geologic Map of the Kanarraville Quadrangle, Iron County, Utah [map]*. 1:24,000. Open-file Report 618. Iron County, Utah: Utah Geological Survey.

Boyer, S. E., & Elliott, D. (1982). Thrust systems. *AAPG Bulletin*, *66*(9), 1196-1230.

Banks, C. J., & Warburton, J. (1986). 'Passive-roof'duplex geometry in the frontal structures of the Kirthar and Sulaiman mountain belts, Pakistan. *Journal of Structural Geology*, *8*(3-4), 229-237.

Charlesworth, H. A., & Gagnon, L. G. (1985). Intercutaneous wedges, the triangle zone and structural thickening of the Mynheer coal seam at Coal Valley in the Rocky Mountain Foothills of central Alberta. *Bulletin of Canadian Petroleum Geology*, *33*(1), 22-30.

Chester, J. S. (1996). Geometry and kinematics of a passive-roof duplex in the interior of the Idaho-Wyoming-northern Utah thrust belt. *Bulletin of Canadian petroleum geology*, *44*(2), 363-374.

Coe, A. L. (Ed.). (2010). *Geological field techniques*. John Wiley & Sons.

Compton, R. R., & Compton, R. R. (1985). *Geology in the Field* (pp. 366-367). New York: Wiley.

Davis, G.H. Reynolds, S.J. and Kluth, C.F., 2012. Structural Geology of Rocks and Regions. 3rd ed. John Wiley and Sons, New York, p 315-316.

Dahlstrom, C. D. (1970). Structural geology in the eastern margin of the Canadian Rocky Mountains. *Bulletin of Canadian Petroleum Geology*, *18*(3), 332-406.

Dahlstrom, C. D. A. (1969). Balanced cross sections. *Canadian Journal of Earth Sciences*, *6*(4), 743-757.

DeCelles, P. G., & Coogan, J. C. (2006). Regional structure and kinematic history of the Sevier fold-and-thrust belt, central Utah. *Geological Society of America Bulletin*, *118*(7-8), 841-864.

DeCelles, P. G., Lawton, T. F., & Mitra, G. (1995). Thrust timing, growth of structural culminations, and synorogenic sedimentation in the type Sevier orogenic belt, western United States. *Geology*, *23*(8), 699-702.

Dubiel, R. F., Ridgley, J. L., Armstrong, A. K., & Holcomb, L. D. (1989). *Depositional environments of the Upper Triassic Chinle Formation in the eastern San Juan Basin and vicinity, New Mexico. Trace fossils and mollusks from the upper member of the Wanakah Formation, Chama Basin, New Mexico; evidence for a lacustrine origin. Stratigraphy, facies, and paleotectonic history of Mississippian rocks in the San Juan Basin of northwestern New Mexico and adjacent areas* (No. 1808-BD).

Dubiel, R. F. (1994). Triassic deposystems, paleogeography, and paleoclimate of the Western Interior. Rocky Mountain Section (SEPM).

Elliott, D. (1983). The construction of balanced cross-sections. Journal of structural geology, 5(2), 101.

Ellis, T. C. (2013). A structural analysis of the El Kasr structure in the western desert of Egypt.

Fielding, L. W. (1994). *Fault-propagation folding, depth to detachment, and variations in folding intensity in the overthrust belt of southwest Utah* (Master's thesis).

Goldstrand, P. M. (1994). Tectonic development of Upper Cretaceous to Eocene strata of southwestern Utah. Geological Society of America Bulletin, 106(1), 145-154.

Grant, S. K., Fielding, L. W., & Noweir, M. A. (1994). Cenozoic Fault Patterns in Southwestern Utah and Their Relationships to Structures of the Sevier Orogeny.

Hintze, L. F. (1993). *Geologic history of Utah* (Vol. 7). Dept. of Geology, Brigham Young University.

Hintze, L. F. (2005). Utah's Spectacular Geology: Provo. *Department of Geology, Brigham Young University*.

Jamison, W. R. (1987). Geometric analysis of fold development in overthrust terranes. *Journal of Structural Geology*, *9*(2), 207-219.

Jamison, W. R. (1996). Mechanical models of triangle zone evolution. *Bulletin of Canadian Petroleum Geology*, *44*(2), 180-194.

Jones, P. B. (1982). Oil and Gas Beneath East-Dipping Underthrust Faults in the Alberta Foothills.

Jones, P. B. (1996). Triangle zone geometry, terminology and kinematics. *Bulletin of Canadian Petroleum Geology*, *44*(2), 139-152.

Kurie, A. E. (1966). Recurrent structural disturbance of Colorado Plateau margin near Zion National Park, Utah. *Geological Society of America Bulletin*, *77*(8), 867-872.

Lawton, T. F., Sprinkel, D. A., Decelles, P. G., Mitra, G., Sussman, A. J., & Weiss, M. P. (1997). Stratigraphy and structure of the Sevier thrust belt and proximal foreland-basin system in central Utah. Brigham Young University Geology Studies, 42(2), 33-67.

Mitra, S. (1990). Fault-propagation folds: geometry, kinematic evolution, and hydrocarbon Traps (1). AAPG Bulletin, 74(6), 921-945.

Mitra, S. (1992). Balanced structural interpretations in fold and thrust belts. *Structural geology of fold and thrust belts*, 53-77.

Morley, C. K. (1986). A classification of thrust fronts. *AAPG Bulletin*, *70*(1), 12-25.

Noweir, M.A. (1990). *Structural analysis of the overthrust belt (OTB) of southwest Utah* (Doctoral dissertation).

Noweir, M. Atef, and Sheldon K. Grant. "Balanced Cross-Section Across The Southern Utah Overthrust Belt (Otb)." (1995).

Price, R. A. (1986). The southeastern Canadian Cordillera: thrust faulting, tectonic wedging, and delamination of the lithosphere. *Journal of Structural Geology*, *8*(3-4), 239-254.

Ramos, V. A. (1989). Andean foothills structures in northern Magallanes Basin, Argentina. *AAPG Bulletin*, *73*(7), 887-903.

Royse, F. (1993). Case of the phantom foredeep: Early Cretaceous in west-central Utah. Geology, 21(2), 133-136.

Schootstra, J. (2012). Step-by-step Three-Dimensional Modeling and Visualization of an area in the southwestern part of France (in the French Subalpine Basin).

Soule, G. S., & Spratt, D. A. (1996). En echelon geometry and two-dimensional model of the triangle zone, Grease Creek Syncline area, Alberta. *Bulletin of Canadian petroleum geology*, *44*(2), 244-257.

Suppe, J. (1983). Geometry and kinematics of fault-bend folding. *American Journal of science*, *283*(7), 684-721.

Suppe, J., & Medwedeff, D. A. (1990). Geometry and kinematics of fault-propagation folding. *Eclogae Geologicae Helvetiae*, *83*(3), 409-454.

Tanner, D. C., Brandes, C., & Leiss, B. (2010). Structure and kinematics of an outcrop-scale fold-cored triangle zone. *AAPG bulletin*, *94*(12), 1799-1809.

Threet, R. L. (1963). Structure of the Colorado Plateau margin near Cedar City, Utah.

Vann, I. R., Graham, R. H., & Hayward, A. B. (1986). The structure of mountain fronts. *Journal of Structural Geology*, *8*(3-4), 215-227.

Willis, G. C. (1999). The Utah thrust system-an overview.

Woodward, N. B., Boyer, S. E., & Suppe, J. (1989). Balanced Geological Cross-sections: An Essential Technique in Geological Research and Exploration; Short Course Presented at the 28th International Geological Congress Washington, DC.

VITA

William Joseph Michael Chandonia received a Bachelor of Science degree in Geology from Georgia State University, where he graduated *magna cum laude* in 2014. In 2015, he joined Dr. John P. Hogan's structural geology research group as a master's student in the Geology and Geophysics Department of Missouri University of Science and Technology. Since August, 2015 he has worked as a structural geology and mineralogy teaching assistant on campus and in summer 2016 was a teaching assistant at field camp. William had interdisciplinary research interests in the areas of structural geology and petroleum geology. More specifically, his research interests included integrating field mapping, analog models, and numerical models to identify geologic structures that could be hydrocarbon traps. In March 2017, he was accepted to the Geology and Geophysics PhD program at Missouri University of Science and Technology. He received his degree of Master of Science in Geology and Geophysics from the Missouri University of Science and Technology in May of 2017.